Università degli Studi di Palermo

AREA RICERCA E TRASFERIMENTO TECNOLOGICO
SETTORE DOTTORATI E CONTRATTI PER LA RICERCA
U.O. DOTTORATI DI RICERCA

PhD Course in Biomedicine, Neurosciences and Advanced Diagnostics
Dipartimento di Biomedicina, Neuroscienze e Diagnostica Avanzata
Settore Scientifico Disciplinare – Biochimica- BIOS-07/A

TARGETING LIPOGENESIS PROMOTES THE SYNERGISTIC EFFECT OF THE SELECTIVE HDAC6 INHIBITOR ITF3756 WITH BORTEZOMIB IN COLON CANCER CELLS

Doctor
Marzia Franzò

Coordinator
Prof. Fabio Bucchieri

Tutor
Prof.ssa Sonia Emanuele

XXXVIII CYCLE - YEAR OF TITLE ACHIEVEMENT 2025/2026

SUMMARY

Introduction

1.0 Colorectal cancer

1.1 Epidemiology

Colorectal cancer (CRC) is the third most diagnosed cancer and the second most common cause of cancer-related deaths worldwide. According to the GLOBOCAN 2018 database, 18.1 million new cases (17.0 million excluding nonmelanoma skin cancer) and 9.6 million cancer deaths (9.5 million excluding nonmelanoma skin cancer) worldwide were estimated. ***Figure 1*** illustrates the distribution of all-cancer incidence and mortality by world areas, shown for both sexes as well as separately for men and women. Asia accounts for nearly 50% of new cancer cases and more than 50% of all cancer deaths, primarily due to increasing urbanization and the adoption of Western dietary habits (Matsuda, Fujimoto, and Igarashi 2025). Europe, despite representing only 9% of the world's population, accounts for 23.4% of incidence and 20.3% of mortality of cancer. Followed by America with 21% of incidence and 14.4% of mortality. In contrast to other regions, cancer mortality in Asia (57.3%) and Africa (7.3%) is higher than cancer incidence (48.4% and 5.8%, respectively) because of the different distribution of cancer types and higher case fatality rates in these regions (Bray et al. 2018).

These geographic differences appear to be attributable to differences in diet, aging, and growth of the population, and levels of socioeconomic development. (Bray et al. 2018).

The average annual overall incidence rate from 2015 to 2019 was 33% higher in males (41.5 per 100,000) compared to females (31.2 per 100,000). However, the sex disparity varies by age at diagnosis and tumor site (Siegel et al. 2023).

The risk of CRC increases significantly after the age of 40, begins to rise sharply between ages 50–55, doubling with each decade, and continues to grow exponentially (Barna et al. 2025).

However, in the last few years CRC incidence rate has decreased and is attributable to changing patterns in risk factors, such as reductions in smoking and increased use of nonsteroidal anti-inflammatory drugs, and the uptake of CRC screening, surveillance, and high-quality treatment among individuals aged 50 years and older (Siegel et al. 2023).

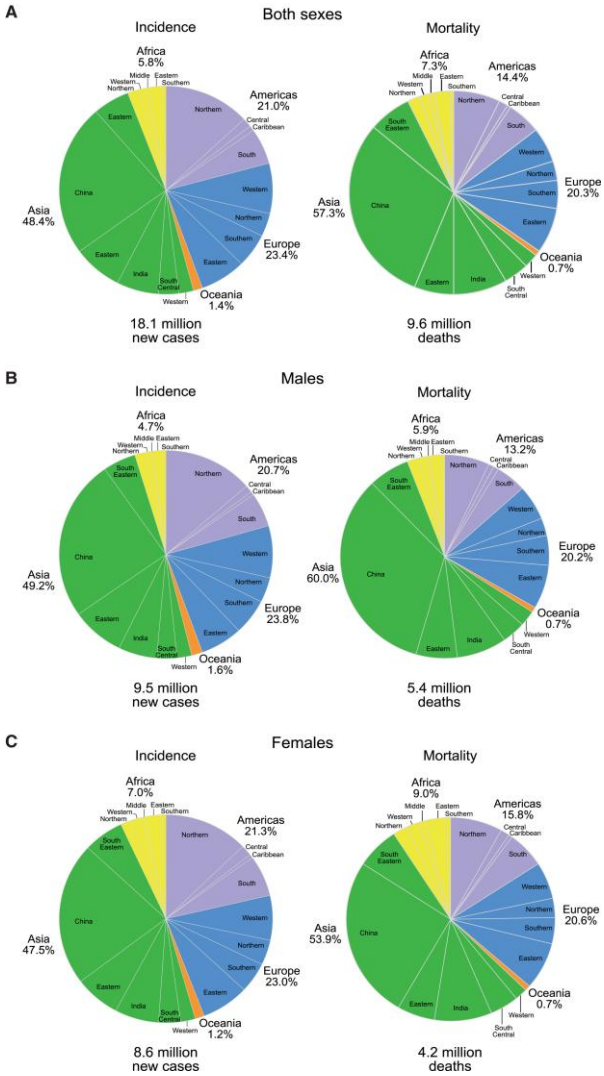

Figure 1. *Distribution of incidence and mortality by World Area in 2018 for (A) Both Sexes, (B) Males, and (C) Females (Bray et al. 2018).*

1.2 Aetiology and risk factors

Colorectal cancer is a disorder that occurs exclusively in the colon or rectum and is caused by the colon's aberrant proliferation of glandular epithelial cells.

Both environmental and genetic factors determine the risk of developing CRC. The genetic, as well as epigenetic, alterations in the DNA interact with various environmental factors, including a diet high in saturated fats and carbohydrates, a sedentary lifestyle, obesity, smoking, or alcohol consumption, to initiate the process of oncogenesis (Ionescu et al. 2023; Hossain et al. 2022). In addition, a history of previous colon polyps, an inflammatory bowel disease such as ulcerative colitis or Crohn's disease, and hereditary conditions such as the Lynch syndrome or Familial Adenomatous Polyposis (FAP) may increase the risk of developing CRC (Aran et al. 2016; Weledji EP 2024). CRC risk factors, including

environmental and genetic factors, may be divided into modifiable and non-modifiable risk factors (***Figure 2***).

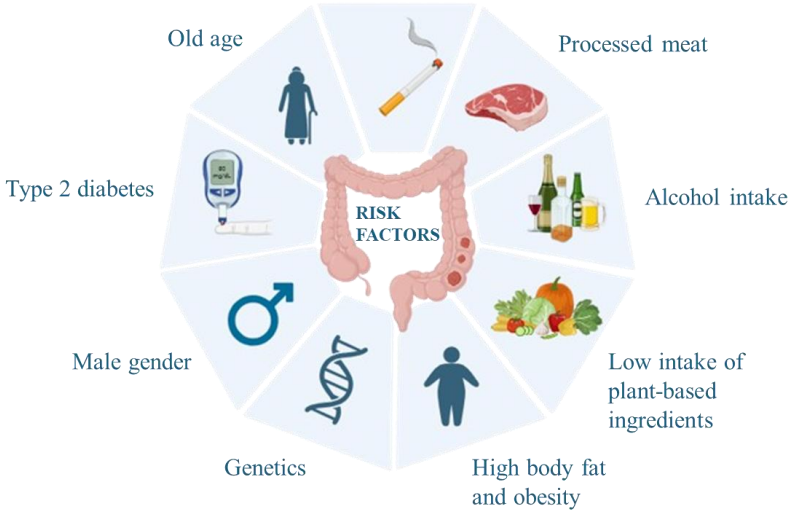

Figure 2. *Modifiable and non-modifiable risk factors of colorectal cancer.*

1.2.1 Non-modifiable risk factors

The main non-modifiable risk factors are:

- ***Sex***: the risk is about 2 times higher in men than in women (Aran et al. 2016). In addition, previous studies have identified sex-based differences in colorectal cancer (CRC) in terms of tumor type, anatomical location, and survival outcomes. The incidence of rectal and sigmoid cancer is higher in men, and that of colonic cancer is higher in women (Weledji EP 2024). The proportion of cases in the caecum and ascending colon is higher in females (17.2% and 9.8%, respectively) than in males (12.2% and 7.3%, respectively), which are harder to detect and diagnose (White et al. 2018).
- ***Age***: advancing age is a major risk factor for CRC incidence. 76% of all colorectal cancer patients are diagnosed between 65 and 85 years old (Weledji EP 2024). However, there has recently been a noteworthy increase in CRC incidence in individuals younger than 50 years old (early-onset CRC patients—EOCRC). Moreover, EOCRC often presents at an advanced stage and is associated with adverse pathological characteristics that increase the risk of premature morbidity and death (Barna et al. 2025; Ionescu et al. 2023).
- ***Genetic Predisposition***: It is estimated that approximately 2–8% of all colorectal cancer (CRC) cases and 10–20% of those diagnosed before the age of 50 (EOCRC) occur in individuals with high genetic risk. Genetic predisposition to CRC is associated with several hereditary conditions, which are traditionally classified into polyposis and non-polyposis

syndromes (Recommendation AIOM 2022). The most common forms of polyposis and non-polyposis syndromes are respectively Familial Adenomatous Polyposis (FAP), characterized by germline mutations in the APC gene, and Lynch syndrome, characterized by germline mutations in DNA mismatch repair genes (10-15% of CRC cases) and microsatellite instability. However, only about 5% of CRC cases are attributable to these hereditary conditions. An additional 20–30% show a familial predisposition without any known or identifiable germline mutations. (Roshandel, Ghasemi-Kebria, and Malekzadeh 2024; Weledji EP 2024).

- ***Family History***: Some meta-analysis studies have shown a familial risk of CRC associated with adenoma in first-degree relatives, with a relative risk (RR) for CRC of 1.99 (Roshandel et al. 2024; Aran et al. 2016).
- ***Abdominopelvic Radiation***: Patients with a history of abdominal irradiation (e.g., those with a history of prostate cancer) are at an increased risk of developing gastrointestinal neoplasms, especially CRC (Roshandel et al. 2024; Ionescu et al. 2023).
- ***Personal History of Other Diseases***: Specific comorbidities were suggested as risk factors for developing CRC. Patients with inflammatory bowel disease (IBD), including ulcerative colitis and Crohn's disease, are at high risk of CRC. The occurrence of long-standing ulcerative colitis was recognised as a histopathological marker for impending or actual malignancy. Indeed, ulcerative colitis should always be considered when large bowel cancer presents at an early age. The incidence of cancer depends on the duration of the disease. After 10 years of colitis, the incidence of colorectal cancer increases by 1% per year (Perspectives on the Aetiology and Pathogenesis of Colorectal Cancer, 2024).

1.2.2 Modifiable risk factors

Several modifiable risk factors have been identified that significantly influence the development of CRC. Unlike non-modifiable factors such as age and genetics, modifiable risk factors are lifestyle-related and can be changed or controlled to reduce the risk of CRC. Key modifiable risk factors for CRC include:

- ***Alcohol Consumption:*** Excessive alcohol intake has been linked to increased CRC risk. Cai et al. found that the quantity of alcohol consumed was directly proportional to the increased risk of death from colorectal cancer. This phenomenon can be attributed to genetic factors that regulate alcohol metabolism. There is evidence that acetaldehyde, a byproduct of ethanol metabolism, may contribute to carcinogenesis by disrupting DNA synthesis and

repair mechanisms, altering the structure and function of glutathione, and promoting the proliferation of colonic mucosal cells (Ionescu et al. 2023; Roshandel et al. 2024).

- ***Smoking:*** Long-term smoking is associated with a higher risk of CRC and colorectal polyps. A large cohort study involving 188,052 individuals found that male smokers had a higher incidence (around 39%) of left colon cancer compared to nonsmokers. In contrast, female smokers had a 20% higher risk of developing right colon cancer as opposed to nonsmokers. Additionally, female smokers have a higher risk of developing rectal cancer, with the risk being directly proportional to the number of packs per year (Gram et al. 2020; Ionescu et al. 2023). Tobacco smoke contains over 7,000 toxic compounds, including around 70 known carcinogens such as nitrosamines, heterocyclic amines, polycyclic aromatic hydrocarbons, and benzene. These substances can reach the colorectal mucosa through inhalation or bloodstream dissemination, exerting a local pro-oncogenic effect. Evidence also suggests that smoking contributes to early colorectal carcinogenesis by increasing the risk of adenoma formation. On a molecular level, a study found smokers have elevated levels of microsatellite instability, BRAF gene mutations, and the CpG island methylator phenotype (CIMP) (Ionescu et al. 2023; Roshandel et al. 2024). Furthermore, it has been observed that smoking is associated with an additional increase in the risk of acquiring colorectal adenomas in patients diagnosed with Lynch syndrome (Winkels et al. 2012).
- ***Obesity:*** Case-control studies and cohort studies have demonstrated a strong association between a high body mass index and the incidence of CRC. The association between obesity and the development of CRC may be explained by different mechanisms, mainly by the effects of hormones and pro-inflammatory cytokines, e.g., interleukin 6, tumor necrosis factor-α, leptin, and adiponectin, produced by adipose tissue. In addition to obesity, insulin resistance is also associated with CRC. Insulin resistance results in hyperinsulinemia and increased activity of IGF (insulin-like growth factor) peptides. High IGF-1 levels are associated with cell proliferation and may increase the risk of colonic neoplasia (Ionescu et al. 2023; Soltani et al. 2019; Baxter et al. 2007).
- ***Physical Inactivity***: Physical inactivity has been identified as a significant modifiable risk factor for colorectal cancer. A growing body of evidence shows that individuals who engage in regular physical activity have a 25–30% lower risk of developing CRC compared to those who are sedentary (Shaw et al. 2018). In contrast, prolonged inactivity and sedentary behaviours, such as sitting for long periods or excessive screen time, have been linked to increased CRC incidence (An et al. 2022). The association between sedentary lifestyle and

CRC risk may be partly explained by higher rates of obesity, higher plasma glucose levels, insulin resistance, and abnormal intestinal peristalsis (Ionescu et al. 2023).

- ***Diet***: There is a well-established link between colorectal cancer (CRC) and diet. Fat, animal protein, and total caloric consumption, as well as dietary fiber and micronutrients such as vitamins and minerals, are all suspected of having potential roles. This can be either protective, as in the case of dietary fiber, particularly insoluble types like cellulose, lignin, and wheat bran, which, by increasing bulk, may reduce carcinogen concentration and speed transit. They may also exert a protective effect by adsorbing co-carcinogens and promoting agents. Additionally, certain dietary patterns, such as the Mediterranean diet, have shown protective effects against CRC (Weledji EP 2024.; Zheng et al. 2022). Conversely, diets high in red and processed meats have been associated with an increased risk of developing CRC. Numerous studies have shown that diets rich in red meat, especially when grilled, smoked, or processed, are associated with an increased risk of CRC. This may be due to the formation of carcinogenic compounds such as heterocyclic amines (HCAs) and polycyclic aromatic hydrocarbons (PAHs) during high-temperature cooking, as well as the presence of heme iron, which can promote the formation of harmful N-nitroso compounds in the gut (Vallis et al. 2022). These findings highlight the crucial role of nutrition in both preventing and managing colorectal cancer.

1.3 Pathogenesis

CRC is a disorder that occurs exclusively in the colon or rectum and is caused by the colon's aberrant proliferation of glandular epithelial cells. There are three principal types of CRC: Sporadic, hereditary, and colitis-associated (Hossain et al. 2022).

CRC is a multi-stage process delineated by four critical junctures: initiation, promotion, progression, and metastasis (***Figure 3***). Irreversible genetic alterations, such as DNA adducts caused by chemical carcinogenesis, characterize the initiation phase. These adducts can either be excised through DNA repair mechanisms or eliminated via cellular apoptosis, which are crucial to maintain the balance between adduct formation and their removal. The persistence of DNA adducts can lead to mutations, which may initiate cancerous developments. When these mutations affect genes involved in the regulation of cell proliferation, they can give rise to small benign tumours (adenomas), which may eventually develop into malignant tumours (carcinomas). During the promotion phase, these genetically altered cells undergo proliferation, forming neoplasms. The progression phase is characterized by further genetic and epigenetic alterations that increase the malignancy of

the neoplasm, granting cells the ability to invade surrounding tissues and metastasize. In the final metastasis stage, cancerous cells disseminate from the primary tumor to distant sites via the bloodstream or lymphatic routes. The temporal span of these stages varies widely, with the entire process often unfolding over several decades (Q. Li et al. 2024). Indeed, up to 18 years may pass between developing a polyp and invasive cancer. On average, it takes nine years to form metastasis (Hossain et al. 2022).

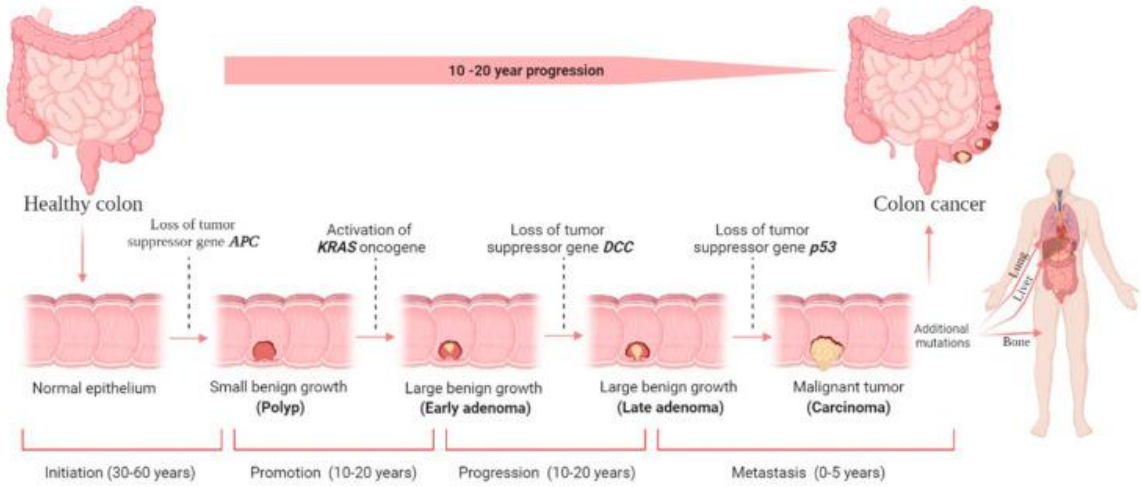

Figure 3. *Colorectal cancer (CRC) stages and development. There are four stages in the development of CRC carcinogenesis: initiation, promotion, progression, and metastasis (Hossain et al. 2022).*

A salient aspect of CRC development is the emergence of benign precursor lesions known as polyps, which manifest as protrusions in the large intestine's lining (Q. Li et al. 2024). Colon polyps, growths within the colon or rectum's inner (mucosal) lining, come in various shapes and types. Some resemble a mushroom on a stalk (pedunculated polyps), while others are flat (sessile polyps). Most colon polyps are benign. However, some can be neoplastic (adenomas) that can grow into cancer. Neoplastic polyps include all adenomas, sessile lesions, and traditional serrated adenomas. A polyp is considered cancerous when abnormal cells spread from the polyp to the surrounding tissue. Cancerous polyps are classified as non-invasive high-grade neoplasia (NHGN) and malignant polyps (T1). NHGN is when the cancer has not yet reached the muscularis mucosa, and T1 is when it has invaded the submucosa. Treating malignant polyps depends on various morphological and histological factors, including sessile or pedunculated morphology, the degree of differentiation of the carcinoma, and the presence of vascular or lymphatic involvement (Kotula et al. 2025).

The histological features of colorectal polyps allow for the classification of several types, including:

- ***Adenomatous***: This lesion, comprising tubular, villous, and tubulovillous adenomas, is a significant category of colorectal polyps, accounting for 70% of cases and serving as precursors to colorectal cancer (CRC) if not removed promptly (Colon and Rectal Polyps, University of Michigan Health, 2025). The development of adenomatous polyps is primarily initiated by mutations in the APC gene, with subsequent alterations in KRAS and TP53 contributing to their progression toward malignancy. Unlike serrated polyps, which are typically driven by BRAF mutations, adenomatous polyps follow the chromosomal instability (CIN) pathway, characterized by widespread genomic alterations and structural abnormalities. Colonoscopy is standard in Western countries to reduce CRC risk (Kotula et al. 2025).
- ***Hyperplastic***: Making up approximately 20% to 30% of non-neoplastic colorectal lesions. These polyps arise from superficial proliferation of epithelial cells, creating their characteristic saw-tooth histological appearance. Unlike serrated lesions such as sessile serrated lesions (SSLs) and traditional serrated adenomas (TSAs), hyperplastic polyps do not exhibit chromosomal instability or CpG island methylation and are generally considered non-neoplastic. Often detected incidentally during colonoscopies, hyperplastic polyps are removed primarily to differentiate them from SSLs, which have a higher malignant potential (Kotula et al. 2025).
- ***Serrated***: These polyps are a broad category that includes hyperplastic polyps, sessile serrated lesions (SSLs), and traditional serrated adenomas (TSAs) (J.-D. Wang et al. 2024). The SSLs and TSAs can potentially become malignant, while the hyperplastic polyps are generally benign. Sessile serrated lesions (SSLs) are characterized by molecular alterations, including hypermethylation of CpG islands in the promoter regions of tumor suppressor genes and BRAF mutations. As they progress, SSLs can give rise to two main types of colorectal cancer: microsatellite instability-high (MSI-H) cancers associated with MLH1 gene silencing, and microsatellite stable (MSS) cancers that lack MLH1 inactivation. Meanwhile, TSAs progress to microsatellite-stable colorectal cancers through the following molecular features: (1) CIMP-high and BRAF mutations without MLH1 inactivation; or (2) KRAS mutations without any of the CIMP-high, BRAF mutations, or MLH1 inactivation (Sano et al. 2020). These distinct molecular pathways reflect the heterogeneity of cancers arising from the serrated neoplasia pathway.
- ***Inflammatory***: They most often occur in people who have inflammatory bowel disease (IBD). These types of polyps are also known as pseudopolyps because they are not true polyps but rather develop as a reaction to chronic inflammation in the colon. Inflammatory

polyps are benign and generally do not carry the risk of developing into colon cancer (Colon and Rectal Polyps, University of Michigan Health, 2025).

- ***Malignant:*** They are colorectal lesions where invasive carcinoma has penetrated the submucosa but remains within the excised polyp. Key features include tumor differentiation, lymphovascular invasion, and resection margin status. The malignant transformation of polyps is driven by key genetic mutations, most notably in APC and TP53, and in some cases, by microsatellite instability (MSI). These molecular changes promote the progression from benign growths to invasive colorectal cancer, highlighting the importance of understanding these pathways to develop more effective targeted therapies (Kotula et al. 2025).

1.3.1 Adenoma–carcinoma sequence

Colorectal cancer (CRC) typically develops through a well-characterized stepwise progression known as the adenoma-carcinoma sequence. This model, proposed by Fearon and Vogelstein, couples specific genetic alterations with advancing histologic features. Adenomatous and serrated polyps are common precursors to colorectal cancer (CRC) (Kotula et al. 2025). Adenoma arises from disruptions of mechanisms that regulate DNA repair and cell proliferation. In the healthy colon, epithelial cells renew continuously, with proliferation restricted only at the crypt base (L. H. Nguyen, Goel, et Chung 2020). However, when mutations occur, most at the level of the *APC* gene, this tightly regulated process is disrupted, leading to adenoma formation and the development of a so-called “dysplastic crypt”. After this stage, the occurrence of additional mutations at the level of K-RAS, p53, and SMAD4 promotes tumor progression, characterized by the increased growth rate of the adenoma and the expansion of malignant clones, with consequent tumor invasion and metastasis (Testa, Pelosi, et Castelli 2018). However, not all adenomas advance to cancer. The accumulation of specific mutations in a particular order is essential for progression to malignancy. The timeline depends upon the specific pathway of tumorigenesis (Nguyen et al. 2020).

1.3.2 Molecular mechanisms of CRC

Colorectal cancer is a heterogeneous disease that develops via stepwise accumulation of well-characterized genetic and epigenetic alterations. The transition from normal colorectal epithelial cells to adenomatous lesions is largely driven by the microsatellite instability (MSI) pathway, chromosomal instability (CIN) pathway, and CpG island methylator phenotype (CIMP) pathway (Li et al. 2025). Each pathway is characterized by distinct genetic alterations, histopathological features, and clinical outcomes (***Figure 4***).

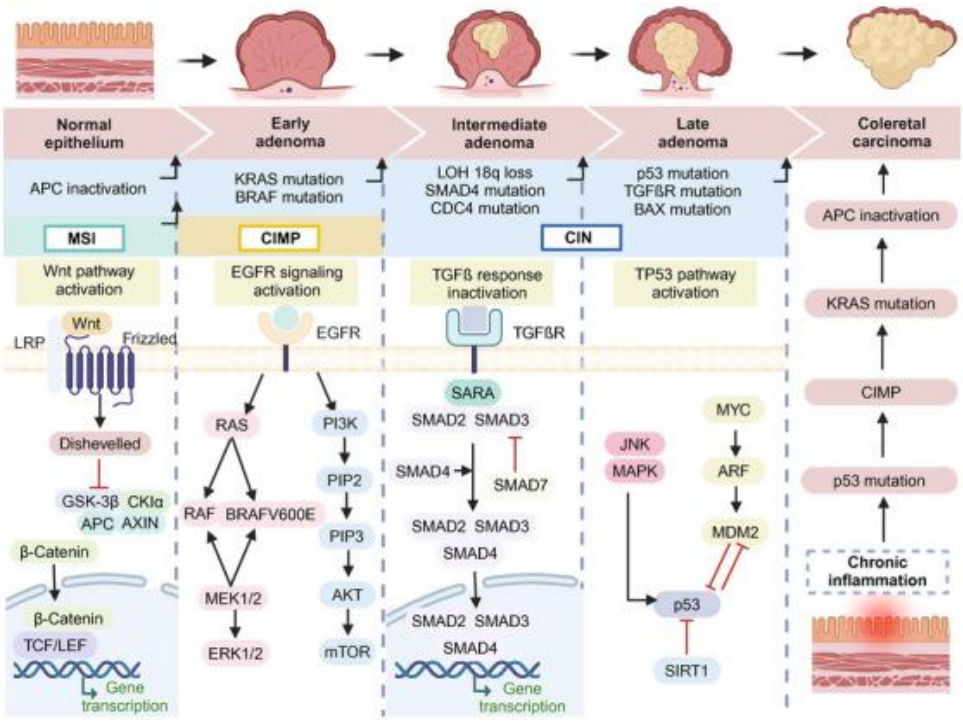

Figure 4. *Molecular mechanisms related to the development of CRC. Mechanistic studies of CRC carcinogenesis primarily focus on CIN, MSI, and CIMP. Cancer progression involves the cumulative mutations of oncogenes and tumor suppressor genes, along with the activation of multiple signaling pathways (Li et al. 2025).*

1.3.3 Chromosomal instability (CIN)

The CIN pathway, observed in 65%–70% of sporadic colorectal tumours, is characterized by chromosome changes that include somatic copy number alterations (SCNA) caused by aneuploidy, deletions, insertions, amplifications, or loss of heterozygosity. Mechanisms that lead to CIN are usually characterized by defects in mitotic errors, telomere dysfunction, dysfunctional DNA damage-response machinery, and loss of heterozygosity (LOH) (Nguyen et al. 2020). CRC tumours arising via the CIN pathway typically follow the classical adenoma–carcinoma sequence, beginning with mutations in the *APC* gene. Loss of APC activity results in hyperactivation of (Wnt)/β-catenin signaling pathway. The abnormal activity of the Wnt/β-catenin signaling pathway promotes the proliferation and differentiation of cancer cells, playing a key role in CRC development. Activating mutations in KRAS usually occur after APC mutations and are found in nearly 40% of colorectal tumours. KRAS is a component of several growth factor signaling pathways, including the epidermal growth factor receptor (EGFR) pathway. In this pathway, activation of KRAS results in constitutive activation of the PI3K/AKT/mTOR pathway. The inactivation of the tumor suppressor *TP53* also plays a key role in the progression of adenomas to cancer. Approximately 60% of CIN tumours contain inactivating mutations in *TP53*. The *TP53* gene

is the most mutated gene in cancer. Its product, p53, regulates transcription of genes that regulate DNA repair and cell responses to oxidative stress. Loss of function in p53 results in disrupting cell cycle arrest and apoptosis. In addition, *TP53* is a marker of invasiveness and metastasis in CRC, and *TP53* mutations are more common in advanced tumours and are associated with poor prognosis (Li et al. 2025; L. H. Nguyen et al. 2020). Together, these sequential genetic events drive the transition from benign adenoma to invasive colorectal carcinoma through the CIN pathway.

1.3.4 Microsatellite instability (MSI)

In contrast to the CIN pathway, characterized by a high frequency of genomic copy number alterations, MSI is characterized by frequent somatic DNA base pair mutations. The MSI pathway is triggered by mutations in the DNA mismatch repair (MMR) genes that result in instability within the microsatellite region. DNA microsatellites are repeated tandem sequences consisting of mono-, di-nucleotide, or even higher-order nucleotide repeats. Cells with MMR deficiency are likely to accumulate DNA errors due to DNA polymerase struggles to efficiently bind these repeating genome sequences. The MMR system is responsible for monitoring and correcting these errors. When MMR mutations occur, code-shifting mutations often arise within the repetitive coding sequences of oncogenes, which are closely associated with the development of Lynch syndrome, the most common hereditary CRC syndrome. However, MSI is observed in nearly 15% of sporadic colorectal tumours. The most common cause of the MSI phenotype is epigenetic silencing of the *MLH1* gene through promoter hypermethylation. Colorectal tumours of the MSI phenotype usually have high levels of methylation at regulatory regions throughout the genome, including the CpG island methylator phenotype (CIMP).

Moreover, one of the more typical mutation types is the v-raf murine sarcoma viral oncogene homolog B1 (BRAF) 600 amino acid substitution mutation from V to E **(**BRAFV600E**),** which is associated with poor prognosis and overall survival in CRC. However, compared to colorectal tumours that develop via the CIN pathway, MSI tumours have a low frequency of *APC* and *TP53* mutations.

MSI mutations include those in the TGFB receptor-2 gene (*TGFBR2*), which encodes a protein responsible for inhibiting the proliferation of colon epithelial cells. In over 90% of microsatellite instability (MSI) colorectal tumours, TGFBR2 is found to be mutated. These mutations typically occur within a specific polyadenine (A) tract, leading to the inactivation

of the receptor. As a result, the receptor loses its ability to transmit signals that normally suppress cell proliferation.

Therefore, MSI has a disruptive effect on cell cycle arrest, apoptosis, DNA repair, and some other genes encoding proteins that regulate proliferation, thus promoting CRC development (Li et al. 2025; L. H. Nguyen et al. 2020).

MSI status is assessed using a standardized panel of microsatellite markers defined by the NCI/Bethesda consensus guidelines. Tumours showing frameshift mutations in 30% or more of these markers are classified as MSI-high. Those with mutations in less than 30% of the markers are categorized as MSI-low, while tumours exhibiting no instability are considered microsatellite stable (MSS). Although MSI-high colorectal tumours often display features such as poor differentiation, they are generally associated with a favourable prognosis, particularly in patients with localized disease. In fact, individuals with MSI-high tumours tend to have longer survival times compared to those with microsatellite stable (MSS) or MSI-low tumours at the same stage (Söreide et al. 2006). Recent studies have shown that MSI-high tumours are highly immunogenic, resulting in the activation of immune cells, such as cytotoxic T cells and natural killer cells, capable of recognizing tumor cells as non-self and facilitating their elimination (Nouri Nojadeh, Behrouz Sharif, et Sakhinia 2018). This immune activation is followed by the expression of checkpoint molecules, such as programmed cell death-ligand 1 (PD-L1), which suppress T-cell activation and cytokine production. As a result, MSI-high tumours are particularly responsive to PD-1 inhibitor therapies, marking a significant paradigm shift in the treatment of colorectal cancer (Le et al. 2017). As a result, routine assessment of MSI status is now recommended during the staging of newly diagnosed colorectal cancer (CRC).

1.3.5 CpG island methylator phenotype (CIMP)

Adenomas with intestinal-type dysplasia are not the only recognized precursors to colorectal cancer (CRC). Serrated polyps are believed to give rise to nearly 15% of CRCs, via the serrated neoplasia pathway (Nguyen et al. 2020).

The serrated pathway refers to the progression of serrated polyps to CRC, which occurs in nearly 20–30% of CRC cases. The serrated pathway is characterized by extensive DNA methylation of CpG islands, which is primarily found in gene promoters and exon regions, and BRAF mutations (Li et al. 2025).

DNA methylation, an important epigenetic modality, is a chemical modification that occurs when methyl groups are added to cytosine bases and is typically associated with repressing transcription. Hypermethylation of these promoter islands often leads to the silencing of oncogenes, contributing to cancer development by inactivating tumor suppressor genes (Gallois, Laurent-Puig, et Taieb 2016). An important mechanism involves the transcriptional repressor MAFG, which recruits BACH1, CHD8, and DNMT3B to target and hypermethylate specific gene promoters, including *MLH1*. Notably, mutant BRAF upregulates levels of MAFG to enhance its binding to promoters (Fang et al. 2014; L. H. Nguyen et al. 2020).

A characteristic trait of the serrated pathway is the activating V600E mutation in BRAF, a component of the MAPK pathway. BRAF mutation leads to the constitutive activation of the MAPK—ERK pathway and uncontrolled cell proliferation. After mutation of *BRAF,* serrated tumours develop via two different pathways: one converges with the MSI pathway, resulting in MMR gene mutations and consequent MSI-high phenotype, or the acquisition of *TP53* mutations, resulting in the activation of several oncogenic pathways, including Wnt signaling, TGFB signaling, and the epithelial to mesenchymal transition. These do not result in MSI-high but rather MSS tumours.

BRAF mutations and DNA methylation are closely linked to the pathogenesis of this pathway. In colorectal cancer (CRC), two distinct patterns of CpG island methylation have been identified. The first is a low-level, age-related methylation. The second involves a high-level, aberrant methylation of specific CpG islands, which leads to the epigenetic silencing of key tumor suppressor genes. CIMP-high tumours exhibit a well-defined molecular profile. They are typically associated with BRAF mutations and frequently display microsatellite instability (MSI) as a consequence of MLH1 promoter hypermethylation, features that describe a large fraction of MSI-H tumours. Although the CIMP is commonly observed in sporadic MSI-high tumours, it is not exclusive to them. In fact, around 50% of CIMP-positive tumours do not exhibit MLH1 promoter methylation or microsatellite instability (MSI), indicating that CIMP can occur independently of these features. On the contrary, CIMP-low tumours are more frequently associated with KRAS, PIK3CA, SOX9, and PCBP1 mutations. Moreover, BRAF mutations represent an early event in the serrated pathway and have been identified in serrated proliferative anomalous crypt foci (Li et al. 2025; Testa et al. 2018; L. H. Nguyen et al. 2020).

Aberrant crypt foci (ACF) are the earliest morphologically identifiable lesions observed in the human colon. Analysis of BRAF and KRAS mutations in hyperplastic aberrant crypt foci (ACF) has shown that BRAF V600E mutations are common in ACF with serrated morphology, while KRAS mutations are more frequently associated with non-serrated lesions. Recent studies using high-resolution chromoendoscopy have identified ACF in the proximal colon in approximately 40% of individuals, especially in patients with synchronous proximal adenomas. Somatic mutations in APC, BRAF, KRAS, NRAS, and ERBB2 were detected in 37% of these proximal ACF. Notably, APC mutations were observed in dysplastic ACF, while mutations in MAPK pathway components (BRAF, KRAS, NRAS, ERBB2) and microsatellite instability (MSI) were found in hyperplastic ACF.

Collectively, the data support the existence of two distinct molecular pathways in early colorectal carcinogenesis (***Figure 5***): the conventional adenoma–carcinoma sequence, characterized by KRAS mutations and somatic copy number alterations via CIN, and the serrated neoplasia pathway, characterized by BRAF mutations followed by gene promoter hypermethylation, which appear to diverge at the earliest stages of tumor initiation (Kasi et al. 2020; Testa et al. 2018).

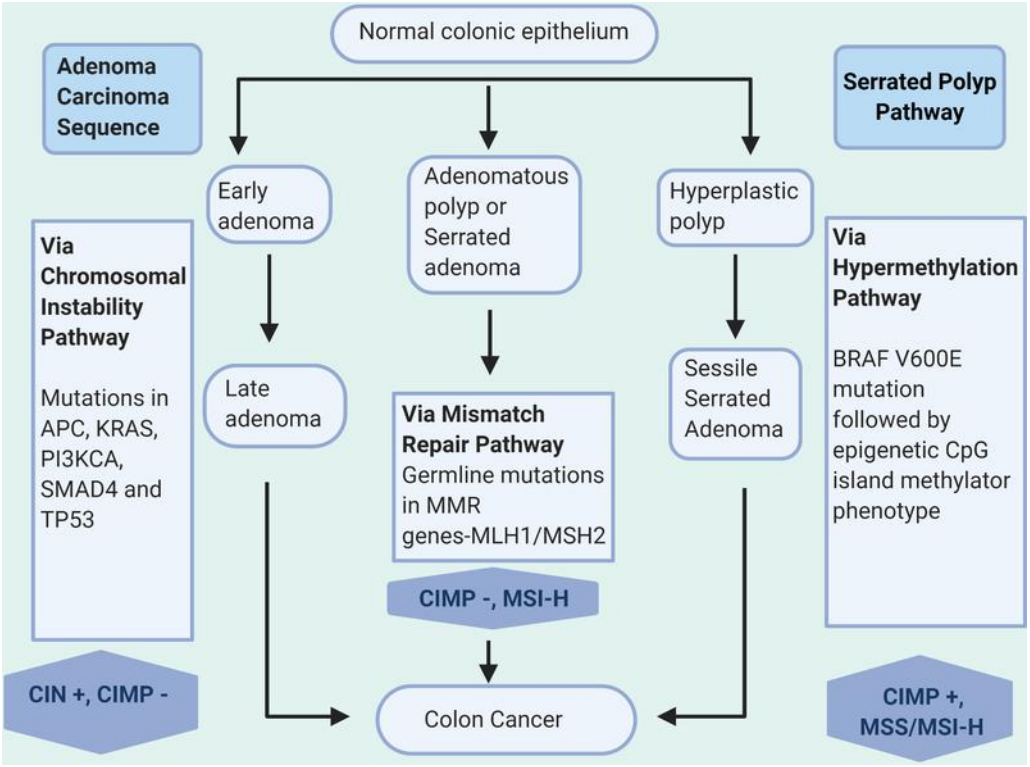

Figure 5. *Key molecular pathways in the development of colorectal cancer* (Kasi et al. 2020).

1.4 Prevention

Preventive methods for CRC may be classified into two main categories, namely primary prevention methods and secondary prevention methods. The primary prevention methods include avoiding CRC risk factors and increasing protective factors for CRC. Secondary prevention strategies, known as colorectal cancer (CRC) screening, involve techniques aimed at detecting, diagnosing, and removing precancerous lesions, specifically neoplastic colorectal polyps such as colorectal adenomas, before they progress to cancer (Roshandel et al. 2024). Current CRC screening may be categorized into two groups: colonoscopic tests and non-invasive tests.

Non-invasive tests are recommended in average-risk men and women from the age of 50 not already taking part in colonoscopic screening programmes. The ideal testing frequency is once per year and should not exceed an interval of three years. A colonoscopy must be carried out at the earliest convenience when the test results are positive (Argilés et al. 2020). The available tests include:

- ***Fecal Occult Blood Test (FOBT)***: The fecal occult blood test (FOBT) is used both in clinical diagnosis and screening of colorectal cancer (CRC), based on the principle that CRCs can release small, invisible amounts of blood into the intestinal lumen. FOBTs detect these traces of occult (hidden) blood in stool samples. Currently, two main types of FOBTs are commonly used: the guaiac-based test (gFOBT) and the immunochemical test (iFOBT). Guaiac-based tests utilize a chemical reaction based on the pseudo-peroxidase activity in hemoglobin. In this test, a stool sample is applied to guaiac paper, and whether hemoglobin is present, a blue colour appears due to an oxidative chemical reaction (Chung, Ali, et Cash 2022). gFOBT remains widely used for CRC screening because it is inexpensive, readily available, and easy to perform. However, it has notable limitations. As a non-specific test for gastrointestinal bleeding, it shows low sensitivity for colorectal cancer, often yielding false positives due to other sources of bleeding, such as ulcers, erosions, inflammatory bowel disease, or use of antiplatelet medications. Additionally, dietary restrictions are required before testing to reduce false-positive results. Studies have reported that gFOBT has a sensitivity of only 11% for advanced adenomas and 12% for carcinomas. Despite its limitations, regular use of gFOBT has been shown to reduce CRC-related mortality by 15–33% (Gude et al. 2023).
- ***Immunochemical Fecal Occult Blood Test (FIT):*** The immunochemical fecal occult blood test (iFOBT), which specifically detects human hemoglobin, offers higher sensitivity than the guaiac-based test (gFOBT) for identifying advanced neoplasia, while maintaining a comparable level of specificity. To identify human hemoglobin, FIT uses specific antibodies.

The test is based on the idea that monoclonal or polyclonal antibodies can detect and bind to the globin portion of human hemoglobin (Mousavinezhad et al. 2016). Therefore, the FIT test is a non-invasive CRC screening method with acceptable accuracy and high adherence to programmatic testing (Roshandel et al. 2024).

Other novel methods are DNA-based or tests using other markers, integrating with imaging tests:

- ***Multitarget Stool DNA Testing:*** Stool DNA tests detect CRC-associated gene mutations in cells shed from the colorectal epithelium into stool. The multitarget stool DNA test includes immunochemical assays for human hemoglobin and molecular assays for abnormally methylated bone morphogenetic protein 3 (BMP3) and N-Myc downstream-regulated gene 4 (NDRG4) promoter regions, mutant Kirsten rat sarcoma (KRAS) virus, and -actin (Gude et al. 2023). Stool DNA tests were proposed as non-invasive accurate methods for detecting colorectal neoplasia, especially when combined with the FIT test (sDNA-FIT test) (Roshandel et al. 2024).
- ***Methylated Septin 9***: In 2016, the Food and Drug Administration approved a second-generation blood assay for a tumor-associated DNA marker for CRC screening. The guanosine triphosphate protein (GTP)-binding protein Septin 9 (SEPT9) is a member of the GTP family involved in apoptosis, pseudopod protrusion, tumor cell migration, and invasion. SEPT9 is hypermethylated in CRC tissue compared with normal colon (Leon Arellano et al. 2022). Plasma-based tests designed to detect methylated SEPT9 identify CRC with a sensitivity of 48% and a specificity of 92% (Chung et al. 2022). While its diagnostic performance is lower than that of the fecal immunochemical test (FIT), the SEPT9 test may still be considered for individuals who decline other CRC screening methods (Nguyen et al. 2020).
- ***Computed Tomographic Colonography (CTC):*** CT colonography (CTC) is a non-invasive imaging technique that simulates the effect of a traditional colonoscopy by examining CT scan images of the colon and rectum. Various studies have demonstrated that CT colonography (CTC) has high accuracy in detecting colorectal neoplasia, particularly large adenomas. However, its sensitivity and overall performance can be influenced by several factors, such as the radiologist's experience, the choice between 2D and 3D imaging modes, and the technical specifications of the CT scanner and detector. These variables are important to consider when evaluating CTC as a screening option for colorectal cancer (Spada et al. 2021; Pickhardt et al. 2018; Roshandel et al. 2024).

- ***Micro RNAs (miRNAs):*** Several unique characteristics contribute to the growing interest in microRNAs (miRNAs). Firstly, miRNAs demonstrate exceptional stability across various experimental and laboratory settings. Secondly, their short length and characteristic hairpin-loop structure make them highly detectable. Although numerous microRNAs (miRNAs) have emerged as promising biomarkers for the early detection of colorectal cancer (CRC), a single miRNA alone is unlikely to fully capture the complex heterogeneity of colorectal polyps and malignancies. To improve diagnostic accuracy, several studies have proposed combining multiple miRNAs into a biomarker panel for more effective identification of colorectal neoplasms (Gude et al. 2023).
- ***Liquid Biopsy***: Liquid biopsies refer to circulating cell-free DNA derived from tumor cells (ctDNA). CtDNA typically comprises 166 base pairs (bp) long short DNA fragments with an estimated half-life of 16 to 2.5 h and can be used to monitor for CRC recurrence and response to treatment. Indeed, liquid biopsy could represent a promising area of investigation (Yamada et al. 2019; L. H. Nguyen et al. 2020).

Colonoscopic techniques, despite being invasive, have the advantage of being both diagnostic and therapeutic (Argilés et al. 2020). Invasive tests, including:

- ***Colonoscopy:*** Colonoscopy is a diagnostic and screening procedure that allows for direct visualization of the entire colon and rectum using a flexible, camera-equipped tube. It is considered the gold standard for colorectal cancer (CRC) screening, as it enables assessing the polyp's features, such as differentiating between an adenoma and a hyperplastic polyp or determining whether a lesion is precancerous or in the early stages of malignancy (Chung et al. 2022). The results of different studies suggest that colonoscopy can lower the incidence of adverse CRC outcomes.
- ***Flexible sigmoidoscopy***: Flexible sigmoidoscopy (FS) is an endoscopic CRC screening that allows the direct visualization of the rectum, sigmoid, and descending colon, as well as biopsy sampling and polyp removal, but is limited to the left side of the colon. Despite this limitation, several clinical trials have shown that FS screening reduces colorectal cancer (CRC) incidence and mortality by 20–30%, with long-lasting benefits, supporting its effectiveness as a reliable CRC screening method (Roshandel et al. 2024).
- ***Colon Capsule Endoscopy (CCE):*** Colon capsule endoscopy (CCE) is a reliable and non-invasive method for detecting colorectal cancer (CRC) and polyps in a screening setting (Vuik et al. 2021). It involves the use of a single-use capsule that travels through the colon via natural peristalsis, capturing colour video images from both ends as it progresses. CCE

is listed as an alternative in the American College of Gastroenterology screening recommendations for people who cannot have a colonoscopy or FIT (Gude et al. 2023).

1.5 Diagnosis

Clinical manifestations of CRC depend on the location and extent of the tumor within the colon or rectum. Common clinical manifestations include changes in bowel habits (e.g., persistent diarrhea, constipation, or a change in stool consistency), rectal bleeding or blood in the stool, abdominal pain or cramping, unexplained weight loss, iron-deficiency anemia, fatigue, and general weakness. Symptoms may be subtle or absent in the early stages, leading to delayed diagnosis (American Cancer Society). Indeed, up to 30% of patients with colorectal carcinoma are primarily diagnosed in an acute stage with sub/obstructing symptoms (De Rosa et al. 2015). This underscores the importance of screening programs for early detection.

The staging of CRC is critical for determining prognosis and guiding treatment decisions. The most commonly used system is the American Joint Committee on Cancer (AJCC) TNM staging system, which classifies cancer according to local invasion depth (T stage), lymph node involvement (N stage), and presence of distant metastases (M stage) (Chen et al. 2021).

As shown in ***Figure 6*****,** stages are typically grouped as follows (American Cancer Society):

- **Stage 0 (Carcinoma in situ):** Abnormal cells are confined to the inner lining of the colon or rectum.
- **Stage I:** The tumor has grown into the submucosa or muscularis propria but has not spread to lymph nodes.
- **Stage II:** The tumor has penetrated through the bowel wall but has not reached regional lymph nodes.
- **Stage III:** The cancer has spread to one or more regional lymph nodes but not to distant sites.
- **Stage IV:** Distant metastases are present, most commonly affecting the liver, lungs, or peritoneum.

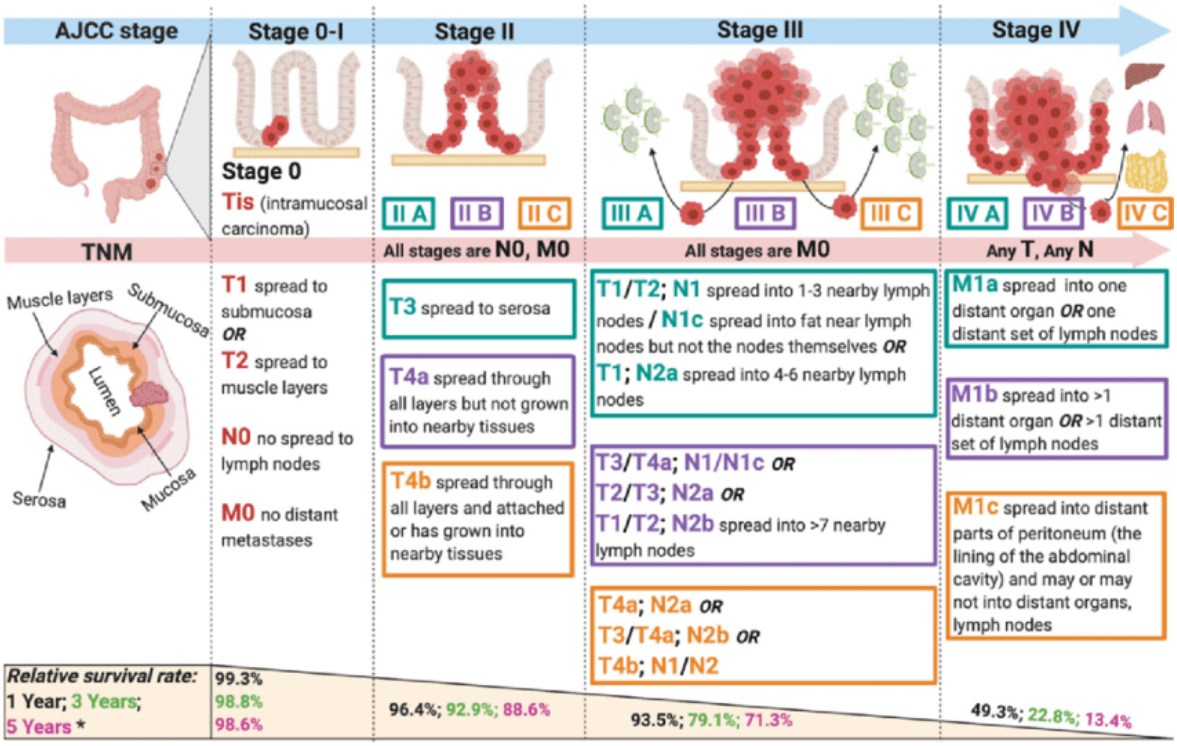

Figure 6. *Colorectal cancer stages according to the American Joint Committee on Cancer (AJCC)* (Shek et al. 2021).

Early-stage CRC (Stages I and II) often has a favourable prognosis when treated surgically, while advanced stages (III and IV) may require multimodal therapy, including chemotherapy, targeted therapy, and immunotherapy (De Rosa et al. 2015).

1.6 Treatment

Colorectal cancer (CRC) remains one of the leading causes of cancer-related mortality worldwide, necessitating the continuous evolution of therapeutic approaches.

Advances in medical research have significantly improved the understanding and treatment of CRC. Therapy typically involves a multidisciplinary approach, including surgery, chemotherapy, radiation therapy, targeted therapies, and, more recently, immunotherapy. The choice of treatment depends on the stage of the disease, molecular characteristics of the tumor, and the overall health of the patient. Personalized treatment strategies are increasingly important in improving outcomes and quality of life for patients with CRC.

The primary therapy for resectable CRC is surgical removal, and for non-resectable CRC, standard therapies include chemotherapy, radiotherapy, and immunotherapy. However, these therapies have certain downsides, such as being non-specific and cytotoxic to normal cells, which leads to secondary complications. Depending on the extent and progression of colorectal cancer (CRC), various therapies may be used in combination. However, despite

these combinational approaches, over half of patients eventually experience relapse due to the development of acquired multidrug resistance. Therefore, there is a need to develop novel CRC therapies that render resistant tumours more sensitive to chemotherapeutic drugs.

1.6.1 Local approaches

In the treatment of locally rectal cancer, neoadjuvant therapy, such as radiotherapy used alone or in combination with chemotherapy, has been recommended and has effectively reduced tumor burden for intermediate and advanced stage cancer. The primary goal of radiotherapy in colorectal cancer is to reduce the risk of local recurrence and potentially enhance overall survival. However, current evidence indicates that preoperative radiotherapy is more effective than postoperative radiotherapy in lowering local recurrence rates, although it does not significantly impact overall survival. The choice between the two available adjuvant radiotherapy approaches, short-course radiotherapy (RT) and long-course RT, has long been a subject of debate. While long-course RT is associated with higher rates of acute toxicity, studies have shown no significant difference in the incidence of late side effects between the two modalities. Radiotherapy, particularly when used as adjuvant treatment, is useful for treating stage II and III CRC. However, it is important to acknowledge the potential long-term toxic effects of radiation on surrounding vital organs (Kumar et al. 2023).

1.6.2 Systemic approaches

I. Chemotherapy

Chemotherapy plays a central role in the treatment of colorectal cancer (CRC), particularly in advanced stages (IIB and IIC) and as an adjuvant therapy after surgery to reduce the risk of recurrence. Chemotherapy aims to destroy cancer cells or inhibit their growth and division. In colorectal cancer, approved cytotoxic agents have proven effective in delaying disease progression and prolonging overall survival, making them a key component of treatment across various stages of the disease. Commonly used agents include fluoropyrimidines, oxaliplatin, and irinotecan, often combined in regimens such as FOLFOX or FOLFIRI (Kumar et al. 2023).

5-FU is a chemotherapy medication that is frequently used to treat a variety of malignant tumours, such as breast, pancreas, skin, stomach, esophagus, head and neck cancers. Since the 1990s, 5-fluorouracil (5-FU), administered both orally and intravenously, along with other fluoropyrimidines (FPs), has constituted the cornerstone of systemic treatment for colorectal cancer (Shaham, Vij, et al. 2025). All 5-FU–based treatment regimens incorporate leucovorin (LV), a chemoprotectant that potentiates the activity of 5-FU by forming a stable

complex and preventing its adverse effects, since it has been demonstrated to improve patient survival and tumor response rate (RR) when combined with 5-FU. Although established efficacy, 5-FU–based chemotherapy presents several drawbacks, including systemic toxicity, poor efficacy, selectivity, and resistance development (Kumar et al. 2023).

Capecitabine, a prodrug of 5-fluorouracil (5-FU), was developed to overcome some of the limitations associated with traditional 5-FU therapy. Its design enables selective conversion to active 5-FU within tumor tissues, thereby increasing intratumoral drug concentration while reducing systemic toxicity. This tumor-specific activation improves the safety profile and tolerability of the treatment (Shaham et al. 2025). In patients with metastatic CRC, two phase III randomized studies compared capecitabine as a single drug to the typical 5-FU/LV therapy combination, and the RR in both studies was as efficient as 5-FU/LV (Kumar et al. 2023).

In 1996, irinotecan**,** which inhibits DNA topoisomerase I**,** received approval in the United States for the treatment of mCRC that was not responding to 5-FU (Fujita et al. 2015).

In patients with mCRC, oxaliplatin**,** a diaminocyclohexane platinum complex that has the potential to generate DNA adducts and interfere with the mechanism of DNA repair, alone has shown moderate efficacy, with response rates (RR) ranging from 10% to 24% (Shaham et al. 2025).

Irinotecan and oxaliplatin were integrated into 5-fluorouracil (5-FU)-based chemotherapy regimens for metastatic colorectal cancer (mCRC). Their addition has been shown to significantly enhance antitumor activity, resulting in higher response rates and prolonged overall survival in patients with advanced disease. However, at the same time, the toxicity levels have increased. In the first-line treatment of metastatic colorectal cancer (mCRC), 5-fluorouracil and leucovorin (5-FU/LV) are commonly combined with oxaliplatin (FOLFOX), irinotecan (FOLFIRI), or both agents simultaneously (FOLFOXIRI). Several trials have demonstrated that combination therapies FOLFOX, FOLFIRI, and FOLFOXIRI an improvement in survival of about 2 years (Kumar et al. 2023).

The second approved oral medication is trifluridine plus tipiracil, which is intended for patients with mCRC who have already received fluoropyrimidine, chemotherapy based on oxaliplatin and irinotecan, an anti-VEGF biological therapy, and, if the patient has RAS wild-type, an anti-EGFR therapy (Raedler 2016).

Considering the several drawbacks of chemotherapy, including low tumor-specific selectivity, unpredictable innate and acquired resistance, unsatisfactory response rate, and systemic toxicity, it is necessary to develop novel strategies to improve and replace current chemotherapy for tumor-specific target therapy for CRC.

II. Targeted therapies

The development of targeted therapy in oncology stems from the paradigm shift toward precision medicine, which focuses on customizing medical treatments based on the unique characteristics of each patient. In contrast to traditional chemotherapy, which non-selectively attacks both cancerous and healthy dividing cells, targeted therapies are specifically designed to act on particular molecular pathways or markers that play a key role in cancer development, progression, and metastasis. The rationale for this approach is grounded in the understanding that cancer is not a single disease but a collection of diverse disorders with varied genetic and epigenetic alterations. The advent of high-throughput genomic technologies has played a pivotal role in enabling the identification of mutations and aberrant signaling pathways that are critical to tumor cell survival, proliferation, and progression. By focusing on these molecular aberrations, targeted therapies can block the growth and spread of tumours while minimizing damage to normal cells, thus offering potentially higher efficacy and lower toxicity (Q. Li et al. 2024).

Cancer cells acquire a set of hallmark capabilities that collectively drive tumor development and metastatic spread. These include sustained proliferative signaling, evasion of growth suppressors, resistance to cell death, replicative immortality, induction of angiogenesis, and activation of invasion and metastasis. The dysregulation of various signaling pathways often underlies these hallmark traits, thereby presenting logical targets for therapeutic intervention.

VEGF/VEGER

Colorectal cancer (CRC) is among the malignancies in which angiogenesis plays a pivotal role. This process, defined as the formation of new blood vessels from pre-existing vasculature or endothelial progenitor cells, is essential for supporting tumor growth, progression, and metastatic dissemination. Vascular endothelial growth factor (VEGF) plays a crucial role as an angiogenic factor in both primary and mCRC in humans (Shaham et al. 2025).

In mammals, the vascular endothelial growth factor (VEGF) signaling pathway comprises five glycoproteins belonging to the VEGF family. The angiogenesis pathway starts with VEGF ligands interacting with tyrosine kinase receptors, predominantly on vascular endothelial cells. VEGF-A, often known as VEGF, is the primary mediator of tumor angiogenesis. VEGF signals are primarily transmitted by VEGF receptor 2 (VEGFR-2). Subsequently, this leads to the activation of downstream signaling pathways such as the PLC-γ/PKC/Ras/Raf/MEK/MAPK signaling pathway (Ntellas et al. 2020).

Several anti-VEGF drugs have been approved to treat CRC. The first VEGF-A-targeted humanized monoclonal antibody was Bevacizumab. This monoclonal antibody plays a crucial role in VEGF signaling pathways, preventing the interaction between VEGF-A and its receptor, VEGFR. Thereby, it inhibits the activation of signaling pathways that promote the formation of new blood vessels, called neovascularization, and normalizes the tumor vasculature, enhancing the delivery of cytotoxic chemotherapy to the tumor. (Ferrara, Hillan, et Novotny 2005).

The combination of FOLFOXIRI (irinotecan, 5-FU, and leucovorin) with bevacizumab enhances the survival rates of individuals suffering from mCRC (Cremolini et al. 2016). Aflibercept is a targeted therapy used in the treatment of CRC. It functions as a specific antagonist by binding to and inactivating circulating VEGF in both the bloodstream and the extravascular compartment. By inhibiting these factors, aflibercept plays a crucial role in preventing angiogenesis, which is vital for tumor growth and metastasis. (Tew et al. 2010).

Regorafenib is a multi-kinase inhibitor that addresses several key hallmarks of CRC development by targeting various pathways crucial for tumor growth and progression. Its mechanism includes anti-angiogenesis through the inhibition of vascular endothelial growth-factor receptors and fibroblast growth-factor receptors, anti-proliferative by inhibiting kinases involved in cell signaling pathways that promote cancer cell growth, combating metastasis by inhibiting pathways related to cancer spread, and, in conclusion, targets immune suppression within the tumor microenvironment by inhibiting colony-stimulating factor 1 receptor (CSF1R), which can enhance anti-tumor immunity. Due to this multi-targeted mechanism, regorafenib is considered a valuable therapeutic option, particularly in cases where conventional treatments may be less effective (Wilhelm et al. 2011).

Another promising target for metastatic CRC treatment is ramucirumab**.** Ramucirumab is distinct from other agents targeting the VEGF pathway, as it specifically binds to an epitope located on the extracellular domain of VEGFR-2. By binding to VEGFR-2, ramucirumab

effectively blocks the interaction of all VEGF ligands, VEGF-C and VEGF-D, to VEGFR-2. Thereby, inhibits their activity and contributes to anti-angiogenic effects in the treatment of cancers, including CRC (Verdaguer, Tabernero, et Macarulla 2016).

Multiple factors contribute to resistance in VEGF-targeted therapy, including elevated serum Angiopoietin-2 (ANG2) levels and FGF, IL-1, PDGF, PIGF, and TGF-β signaling. Hence, efficient, targeted therapy is required to combat tumour resistance (Shaham et al. 2025).

EGF/EGFR

The epidermal growth-factor receptor (EGFR) is a key member of the ErbB family of receptor tyrosine kinases (RTKs). These transmembrane proteins play crucial roles in cell signaling pathways involved in the regulation of cell growth, survival, and differentiation. When activated, EGFR initiates a cascade of downstream signaling pathways that can promote cellular proliferation, angiogenesis, migration, survival, and adhesion. Considering the EGFR pathway is dysregulated in 60–80% of colorectal malignancies, it has emerged as a valuable target in the treatment of mCRC. By inhibiting EGFR activity, therapies can potentially disrupt these critical processes, leading to reduced tumor growth and improved patient outcomes. The EGFR signaling cascade involves an adaptor protein complex that includes growth-factor receptor-bound protein 2 (Grb2) and son of sevenless (SOS). This complex plays a critical role in activating Ras-GTP by binding to phosphorylated tyrosine residues (Janani et al. 2022; Koveitypour et al. 2019). Once Ras is activated, it triggers a cascading effect, activating the MAPK and PI3K/Akt pathways, which are known to regulate cellular proliferation, inhibit apoptosis, and promote angiogenesis (Q. Li et al. 2024). Dysregulation of the EGFR/MAPK signaling pathway plays a critical role in malignant transformations and tumor progression by promoting uncontrolled cell proliferation, survival, angiogenesis, resistance to apoptosis, invasion, and metastasis. Given its strong association with oncogenic processes, this pathway may provide valuable insights for developing therapeutic strategies against CRC (Koveitypour et al. 2019).

Cetuximab is a chimeric IgG1 monoclonal antibody that specifically targets the extracellular domain of the EGFR. By binding to EGFR, cetuximab inhibits ligand-induced receptor signaling, which helps modulate tumor cell growth. The use of cetuximab can enhance treatment efficacy, especially in patients with RAS wild-type tumours, providing a targeted therapeutic approach in combination with other treatments. The combination of cetuximab with immunotherapeutic agents and other targeted therapies expands the therapeutic landscape, offering new treatment avenues for patients with metastatic colorectal cancer who

encounter resistance to conventional therapies (Shaham et al. 2025). The CRYSTAL study demonstrated that the combination of FOLFOX or FOLFIRI regimens with cetuximab has been effective in enhancing progression-free survival and objective response rates in CRC patients (Li et al. 2025). In particular is used as a first-line treatment in patients with KRAS wild-type mCRC (Q. Li et al. 2024). However, considering that cetuximab is a chimeric antibody, it may ultimately result in immunogenic responses.

To minimize the immunogenic responses, the fully humanized antibody panitumumab was developed (Kumar et al. 2023). Panitumumab is a fully humanized IgG2 monoclonal antibody that specifically targets the EGFR. By binding to EGFR, it effectively prevents the interaction of natural ligands, such as EGF and TGF-α, with the receptor. This blockade leads to the inhibition of downstream signaling pathways that promote cell proliferation and survival. Notably, in phase III trials, panitumumab, as a monotherapy or in combination with chemotherapy, has demonstrated efficacy in improving progression-free survival in mCRC patients, particularly those with wild-type KRAS genotype (Q. Li et al. 2024).

Resistance, whether primary or acquired, arises in therapies targeting EGFR due to three different mechanisms: (i) impaired interaction between the therapeutic antibody and the EGFR receptor; (ii) activation of alternative compensatory signaling pathways; and (iii) constitutive activation of downstream signaling components, often driven by KRAS, NRAS, BRAF, and PIK3CA mutations, or KRAS gene amplifications (Testa et al. 2018).

III. Future target therapy

Research continues to uncover a myriad of novel targets and pathways with therapeutic potential in oncology. These include insulin-like growth factor/insulin-like growth factor 1 receptor (IGF/IGF-1R), transforming growth factor (TGF), Wnt/β-catenin, Notch, and Hedgehog, which can be potentially targeted for CRC treatment (Figure 7) (Shaham et al. 2025).

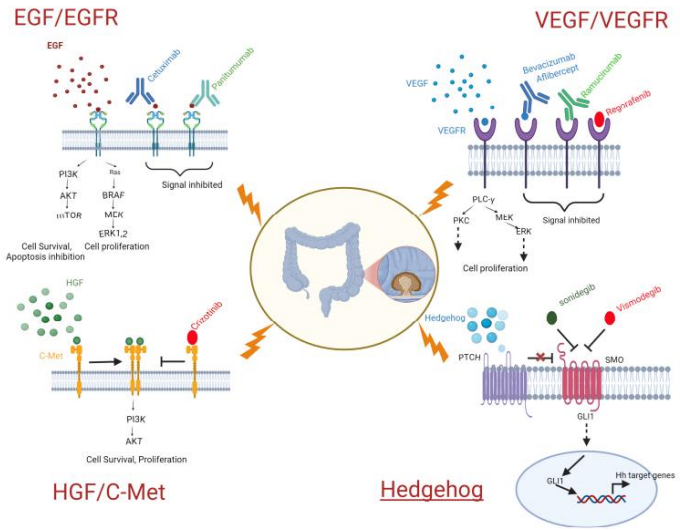

Figure 7. *Target therapy for colorectal cancer* (Shaham et al. 2025).

IV. Immunotherapy

Immunotherapy has been established as a prominent therapeutic strategy for a variety of solid tumours, including CRC. Several immunotherapy strategies are used to treat colorectal cancer, including monoclonal antibody (mAb) therapy, immune checkpoint inhibitor therapy, cancer vaccines, adoptive cell therapy, complement inhibition, and cytokine treatment (***Figure 8***) (Q. Li et al. 2024).

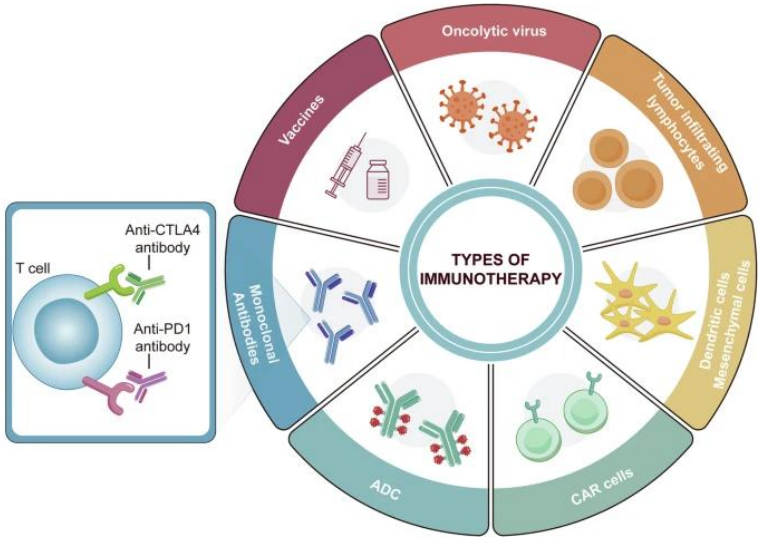

Figure 8. *Immunotherapeutic strategies for CRC* (Q. Li et al. 2024).

CRC characterized by microsatellite instability-high (MSI-H) or deficient mismatch repair (dMMR) are more susceptible to immunotherapy due to their high mutational burden. In this context, immune checkpoint inhibitors such as pembrolizumab and nivolumab (anti-PD-1 antibodies) have demonstrated significant clinical benefit, including durable responses and

improved progression-free survival, particularly in metastatic CRC (mCRC). By inhibiting PD-1, these drugs allow cytotoxic T cells to recognize and destroy tumor cells (Romero-Zoghbi et al. 2025).

Furthermore, the exploration of novel immunotherapeutic targets, as well as personalized neoantigen vaccines and adoptive cell therapies (e.g., CAR-T cells), may hold promise for expanding the benefits of immunotherapy to a broader population of CRC patients (Q. Li et al. 2024).

2.0 Epigenetic and cancer

Epigenetics refers to a set of molecular modifications that affect gene expression without altering the underlying DNA sequence. In the context of CRC, epigenetic regulation plays a fundamental role in the initiation, progression, and metastasis of the disease. The main epigenetic mechanisms regulating gene expression in colorectal cancer include DNA methylation, histone modifications, lncRNAs, and miRNAs (***Figure 9***). These modifications can lead to the inactivation of tumor suppressor genes and the activation of oncogenes, thereby disrupting the delicate balance of cellular homeostasis (Q. Li et al. 2024). The reversible nature of many epigenetic modifications makes them an attractive target for therapeutic intervention, offering the potential for novel CRC treatments either as monotherapy or in conjunction with existing therapies (Tahghighi et al. 2025).

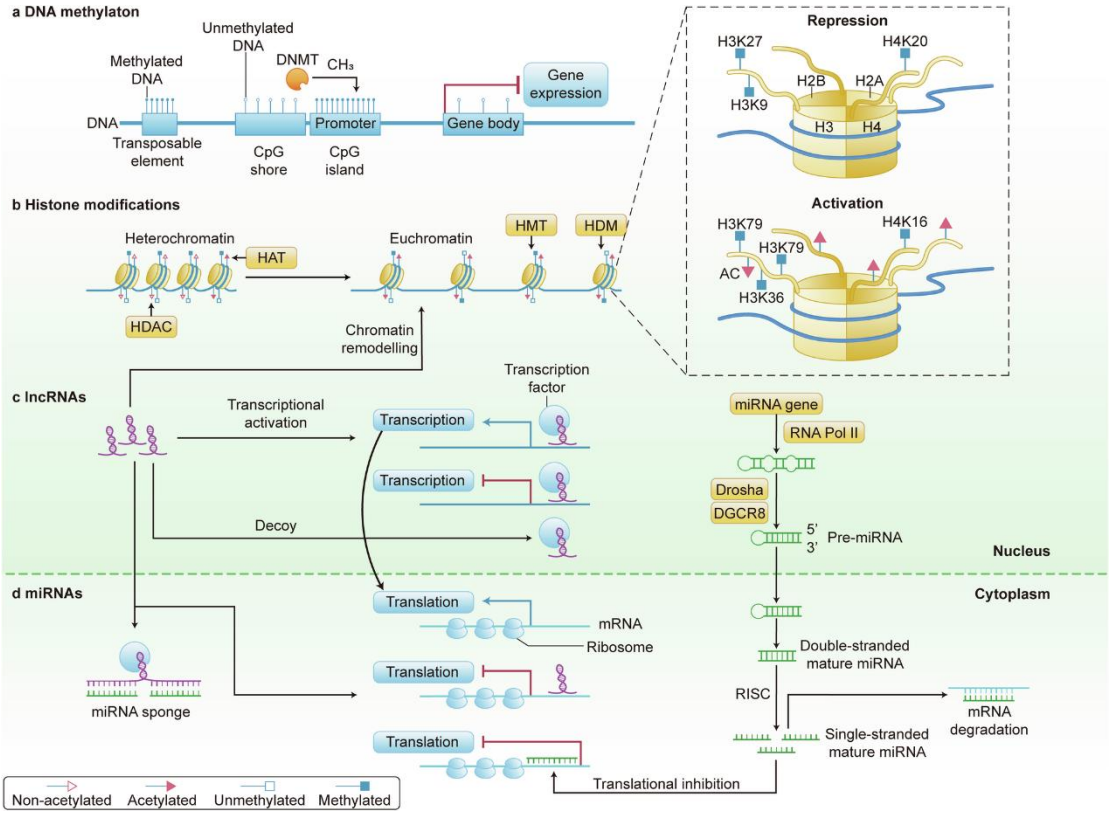

Figure 9. *The landscape of epigenetic modulation in colorectal cancer signaling cascades.*

2.1 Histone modification

Histone modifications, including acetylation, methylation, phosphorylation, and ubiquitination, are dynamic processes that modulate chromatin structure and accessibility. In CRC, dysregulated patterns of histone modifications can promote carcinogenesis by altering the expression of genes involved in crucial cellular functions. For instance, the overexpression of histone deacetylases (HDACs) has been observed in CRC and is associated with poor prognosis, highlighting the potential of HDAC inhibitors as therapeutic agents. These compounds have shown promise in preclinical models, and several are currently under clinical evaluation (Q. Li et al. 2024).

2.1.1 Histone acetylation

Histone acetylation is a reversible epigenetic modification regulated by two opposing enzymes, HATs and HDACs, which transfer acetyl groups to and from lysine residues of target proteins, respectively. Histone acetyltransferases (HATs) facilitate the recruitment of acetyl coenzyme A (acetyl-CoA) to transfer acetyl groups to lysine side chains, neutralizing the positive charges on histone tails This process disrupts the electrostatic interaction between histones and negatively charged DNA, leading to an “open” chromatin configuration that enhances transcription factor accessibility and promotes gene expression

(King et al. 2021). They are divided into Gcn5 *N*-acetyltransferases (GNATs) and MYST HATs. GNATs include Gcn5 (General control non-repressed protein 5), PCAF (p300-CREB-binding protein-associated factor), Elp3 (Elongator protein 3), Hat1 (Histone acetyltransferase 1), Hpa2 (Hrp-associated 2 protein), and Nut1 (Component of the RNA polymerase II mediator complex). MYST is an acronym for the members of a protein family: Morf, Ybf2 (Sas3), Sas2, and Tip60 (Eckschlager et al. 2017).

Opposingly, histone deacetylases (HDACs) catalyse the removal of acetyl groups from lysine residues in both histone and non-histone proteins. This results in a more compact, "closed" chromatin structure, reducing the accessibility of transcription factors and thereby suppressing gene expression (King et al. 2021). Beyond histones, HDACs also target non-histone proteins, such as RUNX3 (Core binding factor α3 subunit), STAT3 (Signal transduction and activation of transcription 3), β-catenin, estrogen receptor, Myc (Avian myelocytomatosis viral oncogene homolog), EKLF (Erythroid Kruppel-like factor), GATA family (GATA-binding factors), HIF-1α (Hypoxia-inducible factor 1α), MyoD (Myogenic regulatory factor), NF-κB (Nuclear factor κB) or Foxp3 (Forkhead box P3 protein) (Li et al. 2025; Eckschlager et al. 2017).

In humans, 18 known HDACs are classified into four categories that differ in structure, localization, and cofactor requirement. Class I HDACs are usually located in the nucleus and include HDACs 1, 2, 3 and 8, while class II HDACs are found in the nucleus and cytoplasm and include HDACs 4, 5, 7 and 9. HDAC11 is the only class IV HDAC. It is active in the nucleus, shares a similar structure to class I/II HDACs, and regulates the stability of CDT1, a DNA replication factor. Class I, II, and IV HDACs are all zinc-dependent. The zinc ion stabilizes the acetylated substrate in the catalytic centre of the enzyme and polarizes the carbonyl group, making the carbon a better target for the nucleophilic water molecule. On the other hand, class III HDACs, known as Sirtuins, are NAD^+ dependent, being capable of forming *O*-acetyl ADP ribose and nicotinamide as a result of the acetyl transfer. The primary structure of Sirtuins is similar to that of the yeast Sir2 protein, and they can be active in the nucleus, mitochondria, or cytoplasm (***Figure 10***) (Y. Li et al. 2024). Most of the classic HDACs are incorporated into multiprotein complexes that include various transcriptional co-repressors, such as SIN3, NuRD (nucleosome remodeling and deacetylase complex), NCoR (nuclear receptor co-repressor), and SMRT (silencing mediator for retinoic acid and thyroid hormone receptors), all of which are involved in chromatin remodelling. These complexes mediate gene repression primarily through two mechanisms: targeted recruitment

by specific transcriptional repressors and their constitutive binding to chromatin (Eckschlager et al. 2017).

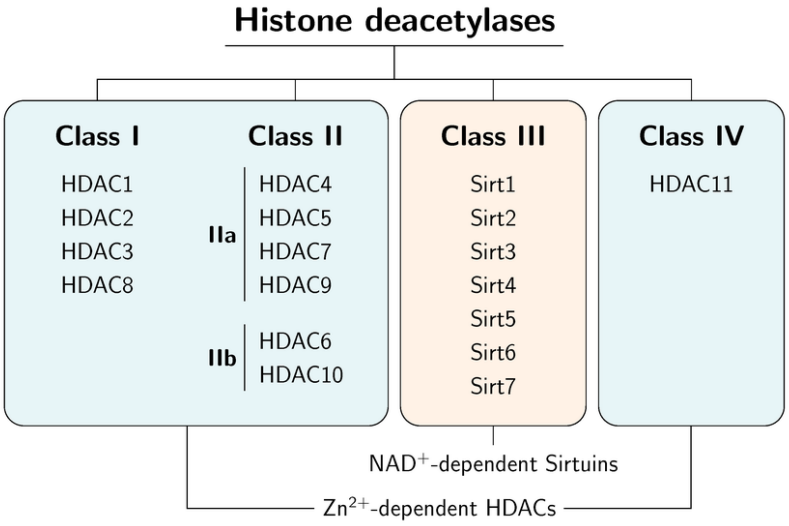

Figure 10. *HDAC classification* (Behnisch-Cornwell et al. 2021).

Alterations in the expression or activity of these epigenetic regulators, through either mutations or changes in expression levels, are frequently observed in cancer and can contribute to tumorigenesis. Under physiological conditions, normal cells maintain a tightly regulated balance between histone acetyltransferases (HATs) and histone deacetylases (HDACs), which is essential for proper gene expression and chromatin remodelling. Disruption of this epigenetic balance is a hallmark of several types of cancer. In particular, aberrant upregulation of HDACs has been observed in various solid tumours, including colorectal cancer, leading to a global decrease in histone acetylation. This shift toward a more deacetylated chromatin state suppresses the transcription of critical genes, including those involved in tumor suppression and other antitumor responses (Shi et al. 2024). Given the significant role of aberrant HDAC overexpression in cancer, HDAC inhibitors have emerged as promising therapeutic agents.

2.2 HDAC inhibitors

In recent years, a deeper understanding of epigenetic mechanisms has facilitated the development of novel therapeutic strategies targeting epigenetic alterations, particularly in the treatment of various malignancies, including colorectal cancer (CRC). Compared to genetic mutations, epigenetic modifications are more frequently implicated in the dysregulation of gene expression associated with CRC pathogenesis, highlighting their pivotal role in tumor initiation and progression. Epigenetic therapy, aimed at reversing aberrant epigenetic modifications, has emerged as a novel strategy in CRC management.

Epidrugs, such as DNA methyltransferase inhibitors (DNMTi) and HDAC inhibitors (HDACi), are at the forefront of this approach. These drugs have the potential to reactivate silenced tumor suppressor genes and induce growth arrest, differentiation, or apoptosis in cancer cells. Furthermore, when administered either as monotherapy or in combination with conventional chemotherapy or immunotherapy, these agents have been shown to enhance anti-tumor efficacy, mitigate drug resistance, and potentiate host immune responses (Tahghighi et al. 2025; Q. Li et al. 2024).

HDAC inhibitors may act specifically against only several isoforms of HDACs (HDAC selective inhibitors), but also against all types of HDACs (pan-inhibitors). ***Figure 11*** shows that the HDAC inhibitors may be classified as members of five classes of compounds (Eckschlager et al. 2017):

i. **Hydroxamic acids (hydroxamates):** Vorinostat (suberoylanilide hydroxamic acid, SAHA) is the first HDAC inhibitor that has already been approved by the United States Food and Drug Administration (FDA) for the treatment of relapsed and refractory cutaneous T-cell lymphoma (CTCL). Other pan-HDAC inhibitors recently tested in clinical studies are givinostat (ITF2357), resminostat (4SC201), abexinostat (PCI24781), and quisinostat (JNJ-26481585). Selective HDAC inhibitors in the group of hydroxamic acids, including rocilinostat (ACY1215), which is a selective inhibitor of HDAC class II, as well as practinostat (SB939) that inhibits all classical classes of HDACs (I, II, and IV), and CHR-3996, the selective inhibitor of class I, are under clinical studies.

ii. **Short-chain fatty acids:** Valproic acid (VPA), butyric acid, and phenylbutyric acid are known to be weak inhibitors of HDAC class I and II. VPA is registered for the therapy of epilepsy, bipolar disorders, and migraines, but more recently it has been tested in clinical studies as an anticancer drug.

iii. **Benzamides:** Entinostat (MS-275-SNDX-275), tacedinaline (CI994), and 4SC202, which inhibit the class I HDACs, are tested in clinical studies.

iv. **Cyclic tetrapeptides:** Include the bicyclic depsipeptide romidepsin (FK228, FR901228), a compound that has been approved by the FDA and EMA (European Medicines Agency) to treat CTCL.

v. **Sirtuin inhibitors:** Include the pan-inhibitor nicotinamide and the specific SIRT1 and SIRT2 inhibitors sirtinol, cambinol, and EX-527. They might act against different types of neurodegenerative diseases and cancers.

Class	HDAC Inhibitor	Target HDAC Class	Clinical Status
hydroxamic acids	Trichostatin A	pan	preclinical
	SAHA	pan	approved for cutaneous T-cell lymphoma
	Belinostat	pan	approved for peripheral T-cell lymphoma
	Panabiostat	pan	approved for multiple myeloma
	Givinostat	pan	phase II clinical trials—relapsed leukemia and multiple myeloma
	Resminostat	pan	phase I and II clinical trials—hepatocellular carcinoma
	Abexinostat	pan	phase II clinical trial—B-cell lymphoma
	Quisinostat	pan	phase I clinical trial—multiple myeloma
	Rocilinostat	II	phase I clinical trial—multiple myeloma
	Practinostat	I, II and IV	phase II clinical trial—prostate cancer
	CHR-3996	I	phase I clinical trial—advanced/metastatic solid tumors refractory to standard therapy
short chain fatty acids	Valproic acid	I, IIa	approved for epilepsia, bipolar disorders and migraine, phase II clinical trials—several studies
	Butyric acid	I, II	phase II clinical trials—several studies
	Phenylbutyric acid	I, II	phase I clinical trials—several studies
benzamides	Entinostat	I	phase II clinical trials—breast cancer, Hodgkin´s lymphoma, non-small cell lung cancer, phase III clinical trial—hormone receptor positive breast cancer
	Tacedinaline	I	phase III clinical trial—non-small cell lung cancer and pancreatic cancer
	4SC202	I	phase I clinical trial—advanced hematological malignancies
	Mocetinostat	I, IV	phase II clinical trials—Hodgkin´s lymphoma
cyclic tetrapeptides	Romidepsin	I	approved for cutaneous T-cell lymphoma
sirtuins inhibitors	Nicotinamide	all class III	phase III clinical trial—laryngeal cancer
	Sirtinol	SIRT 1 and 2	Preclinical
	Cambinol	SIRT 1 and 2	Preclinical
	EX-527	SIRT 1 and 2	cancer preclinical, phase I and II clinical trials—Huntington disease, glaucoma

Figure 11. *HDAC inhibitors classification* (Eckschlager et al. 2017).

SAHA

VRS, also known as suberoylanilide hydroxamic acid (SAHA), is an orally bioavailable broad-spectrum HDAC inhibitor that commonly targets HDAC class I and II. SAHA, a second-generation HDAC inhibitor, was approved by the US FDA for the treatment of cutaneous T cell lymphoma (CTCL). As mentioned above, the activity of HDAC is known to be involved in CRC progression, making it a potential target for CRC treatment. SAHA exerts its antitumor effects in part by disrupting the interaction between FLICE-inhibitory protein (FLIP), a key inhibitor of apoptosis, and the DNA repair protein Ku70, which is known to stabilize FLIP. SAHA enhances the acetylation of Ku70, thereby impairing its ability to bind FLIP. This disruption promotes FLIP polyubiquitination and subsequent proteasomal degradation, ultimately restoring caspase-8 activation and triggering apoptosis in CRC cells (Q. Li et al. 2024; Kerr et al. 2012).

ITF2357 (Givinostat)

ITF2357, also known as Givinostat, is a pan-histone deacetylase (HDAC) that has shown both anti-inflammatory and antitumor properties. Originally developed for the treatment of inflammatory and autoinflammatory conditions, such as systemic juvenile idiopathic arthritis and Duchenne muscular dystrophy, has since shown significant anticancer potential in various preclinical models, including melanoma and colorectal cancer. Several clinical

trials have investigated its efficacy in hematological malignancies, including relapsed/refractory Hodgkin lymphoma, chronic lymphocytic leukemia (CLL), and multiple myeloma. Previous studies conducted in the laboratory where the present project was carried out have demonstrated the antitumor action of the pan-HDAC inhibitors SAHA and ITF2357 in different tumour cells, describing their action mechanism (Emanuele et al. 2007). More recently, it has been shown that both ITF2357 and SAHA were capable of targeting BRAF protein, an oncogene specifically activated in tumour forms, including melanoma and colon cancers. Evidence was also provided that these HDACi promote a switch from pro-survival autophagy to caspase-dependent apoptosis in BRAF-mutated melanoma cells (Celesia et al. 2022). Furthermore, it was demonstrated for the first time that oncogenic BRAF interacts with p53 in melanoma cells. The HDAC inhibitor ITF2357 targets oncogenic BRAF localized in both the cytoplasm and nucleus and modulates p53 protein levels depending on its mutational status. Consequently, ITF2357 decreases the interaction between mutant BRAF and p53, and silencing experiments confirmed that the cellular response to ITF2357 depends on the functional integrity of p53, whose presence may render melanoma cells more sensitive to HDAC inhibitor treatment (Celesia et al. 2023). Additionally, evidence has been provided that ITF2357 potentiates the effects of chemotherapeutic agents, such as pemetrexed in lung cancer and doxorubicin in sarcoma cells (Del Bufalo et al. 2014) (Di Martile et al. 2018).

2.3 Mechanisms of HDAC inhibitors

HDAC inhibitors exert their anticancer effects through multiple mechanisms, including the induction of cell cycle arrest, promotion of cellular differentiation, and activation of programmed cell death. Additionally, these compounds have been shown to inhibit angiogenesis and modulate the immune response, contributing further to their antitumor activity. The hypothesis of “epigenetic vulnerability of cancer cells”, which has been proposed by Dawson and Kouzarides, offers a possible explanation for the relative specificity of HDAC inhibitors. According to this hypothesis, normal cells have, in contrast to some cancer cells, several epigenetic regulatory mechanisms. Consequently, inhibition of HDACs can selectively disrupt the epigenetic balance in cancer cells, leading to their death, while sparing normal cells. It is important to note, however, that the mechanisms of anticancer effects of HDAC inhibitors are not uniform. Indeed, they can vary significantly depending on the cancer type, the specific HDAC inhibitor used, its dosage, and other cellular or molecular factors. For instance, VPA has been shown to inhibit the invasiveness in bladder cancer but not in prostate cancer cells.

2.3.1 Cell cycle arrest

A major effect of HDAC inhibitors in cells is the activation of tumor suppressor pathways and the blocking of cell cycle progression. Cell cycle progression is a tightly regulated process essential for maintaining cellular homeostasis, and its disruption can lead to cellular senescence, apoptosis, or other forms of cell death. The activities of major tumor suppressors such as p53 and p21 are tightly linked to cell cycle regulation (Chen 2016). A number of studies have shown that HDAC inhibition induces p21 expression and cell cycle arrest. In particular, the expression of p21 is regulated by the tumor suppressor protein p53, which binds to the *p21* promoter and competes with HDAC1, a histone deacetylase that represses p21 transcription. After treatment with HDAC inhibitors, HDAC1 is displaced from the Sp1 transcription factor (a promoter-specific component of RNA polymerase II), leading to increased p21 expression. Finally, the p21 levels are increased, thereby mediating cell cycle arrest and apoptosis. Additionally, HDAC inhibition enhances the acetylation of p53, which not only stabilizes the protein by increasing its half-life but also improves the interaction with the p21 promoter. Further studies have shown that HDAC inhibitors can also inhibit the expression of genes coding cyclin D and cyclin A, resulting in the absence of activities of the corresponding kinases, CDK2 and CDK4. For example, HDAC3 directly regulates cell cycle progression and cyclin A degradation by modulating cyclin A acetylation. Overall, while HDAC inhibitors are known to impair cell cycle progression through both direct and indirect pathways, the specific mechanisms remain to be fully elucidated (Eckschlager et al. 2017; Karagiannis et Rampias 2021).

2.3.2 Cell death

HDAC inhibitors induce apoptosis in tumor cells by regulating pro-apoptotic and anti-apoptotic genes. The mechanisms by which different HDAC inhibitors induce apoptosis include activation of both extrinsic and intrinsic apoptotic pathways. HDAC inhibitors have been shown to modulate the expression of several key death receptors, including TRAIL (TNF-related apoptosis-inducing ligand), DR5 (Death Receptor 5), Fas (CD95/TNF receptor superfamily member 6), and TNF (Tumor Necrosis Factor), as well as their corresponding ligands such as FasL, LIGHT (TNF superfamily member 14), and TLA1 (Transparent Leaf Area peptide). Inhibition of those death receptors and their ligands can impair the apoptotic response induced by HDAC inhibitors. HDAC inhibitors also activate the intrinsic apoptotic pathway by regulating transcription of pro-apoptotic genes such as *Bid* (BH3 interacting domain death agonist protein), *Bad* (Bcl-2 associated agonist of cell death protein), and *Bim* (Eckschlager et al. 2017). Several studies have established a mechanistic link between

HDAC inhibitor (HDACi)-induced apoptosis and the generation of reactive oxygen species (ROS), primarily through mitochondrial membrane depolarization in a caspase-independent manner (Karagiannis et Rampias 2021). Notably, the use of ROS scavengers has been shown to reduce HDACi-mediated cell death, supporting the role of ROS in this process. However, lower concentrations of HDAC inhibitors can still induce moderate cell death without a significant increase in ROS levels, suggesting that ROS generation contributes to, but is not solely responsible for, HDACi-induced apoptosis (Jing et al. 2018).

Moreover, HDACs play a significant role in the regulation of autophagy. However, the role of HDAC inhibitors in inducing autophagy in cancer cells remains controversial. Some studies have reported that HDACi-induced autophagy may explicate dual roles: acting as a pro-survival mechanism in some contexts, while contributing to autophagic cell death in others. As described by Zhang et al. in their study, inhibition of autophagy or knockdown of autophagy-related genes (ATGs) was shown to reduce the anticancer efficacy of HDAC inhibitors. Moreover, using various in vivo models, the combined inhibition of HDACs and autophagy significantly suppressed the growth of HCT116 colon cancer cells. In contrast, in hepatocellular carcinoma cells, SAHA-induced cytotoxicity was significantly reduced by treatment with 3-methyladenine, an autophagy inhibitor that blocks autophagosome formation by inhibiting class III PI3K. Similarly, genetic knockout of Atg5, a key autophagy-related gene, also diminished the cytotoxic effects of SAHA (Liu et al. 2010). Several signaling pathways play a role in the induction of autophagy by HDAC inhibitors. Among them, mTOR (mechanistic target of rapamycin) is a key negative regulator of autophagy, acting through the phosphorylation and inactivation of the ULK1 complex (Unc-51-like autophagy activating kinase 1), an upstream component of the autophagy pathway. mTOR inactivation by SAHA restores the functions of ULK1. In addition, SAHA has been shown to induce the overexpression of ATG genes through activation of NF-κB, specifically via modulation of RelA/p65 (NF-B p 65 subunit) signaling. Other studies have also reported that SAHA promotes autophagy through the generation of reactive oxygen species (ROS) in both leukemic and hepatocellular carcinoma cell lines (Eckschlager et al. 2017). Notably, SAHA has also been shown to induce necroptosis, a caspase-independent form of cell death (Natarajan et al. 2018). In conclusion, HDAC inhibitors have been found to induce cell death through several pathways, which could be due to direct roles of HDACs in cell death pathways or results of other effects of HDACi, such as DNA damage or gene expression dysregulation.

2.3.3 Cellular signaling pathways

Another mechanism of anticancer effects of HDAC inhibitors is the regulation of cell differentiation by activation of some protein kinases. Protein kinases modulate several biological processes, such as cell growth, differentiation, and apoptosis. HDAC inhibitors have been shown to enhance DNA binding and transactivation activity of the AP-1 transcription factor through ERK pathway activation, leading to increased expression and phosphorylation of c-Jun in SH-SY5Y neuroblastoma cells. HDAC inhibitors also increase the expression of genes that are involved in the regulation of ERK/AP-1 signaling, e.g., the growth-associated protein-43 (GAP-43) and Bcl-2, thereby increasing the growth of some cancer cells. Loss of function of APC and β-catenin leads to the overexpression of HDAC2, which contributes to the survival of HT29 colorectal cancer cells. This suggests that HDAC2 may be a downstream target of the APC/β-catenin signaling pathway. Furthermore, treatment with HDAC inhibitors reduces polyp formation in APC-deficient mouse models of colon cancer, probably via damage to HDAC2 by degradation in proteasomes (Eckschlager et al. 2017).

2.3.4 The antiangiogenic effect

HDAC inhibitors can affect cancer angiogenesis and inhibit cellular stress response pathways, thereby interfering with the metastatic process. Their anti-angiogenic activity is linked to the downregulation of pro-angiogenic genes, including those encoding vascular endothelial growth factor (VEGF) and endothelial nitric oxide synthase (eNOS). Moreover, HDAC inhibitors promote hyperacetylation of HIF-1α, a key pro-angiogenic transcription factor, leading to its degradation. Valproic acid (VPA) reduces angiogenesis by increasing the expression of anti-angiogenic proteins such as thrombospondin-1 and activin A, while simultaneously downregulating pro-angiogenic factors like basic fibroblast growth factor (bFGF) (Eckschlager et al. 2017).

2.4 Selective HDAC inhibitors

Pan-HDAC inhibitors have emerged as a promising tool in cancer therapy. However, their lack of isoform specificity often results in pleiotropic effects that can be associated with undesirable clinical outcomes, including dose-limiting toxicities, including fatigue, gastrointestinal disturbances, haematological complications, and alterations in serum biochemistry profiles, which severely limit their clinical utility in chronic disease indications (Subramanian et al. 2010). These adverse effects have limited their clinical application and highlighted the need for more targeted strategies. Given the distinct tissue distribution and cellular localization of HDAC isoforms, as well as their specific associations with various

cancer types, a wealth of evidence supports that isoform-selective HDAC inhibitors could offer a better therapeutic index and reduced side effects. In this context, increasing efforts are focused on developing isoform-selective HDAC inhibitors as epigenetic therapeutics (Yang et al. 2019).

2.4.1 Selective HDAC6 inhibitors

Among epigenetic regulation processes of HDACs, HDAC6, a cytoplasmic class II b HDAC, stands out for its unique structure and physiological functions. HDAC6 is the only HDAC containing two catalytic domains in tandem, CD1 and CD2, along with a C-terminus hydrolase–like zinc finger domain with conserved regions rich in cysteine and histidine for ubiquitin binding (ZnF-UBP). The second catalytic domain (CD2) is mainly responsible for the deacetylation of non-histones proteins, such as alpha-tubulin, heat shock protein 90 (HSP90), and cortactin. Therefore, HDAC6 regulates cytoskeletal stability, cell motility, vesicle trafficking, axonal transport in neurons, and the degradation of misfolded proteins via the aggresome–autophagy pathway (Zhang et al. 2021; Zhang et al. 2023). Additionally, elevated expression of HDAC6 has been implicated in various diseases. In cancer, its overexpression can promote tumorigenesis, metastasis, and chemoresistance (Yang et al. 2019; Yano et al. 2021). More recently, HDAC6 has also been associated with metabolic disorders, including obesity and diabetes. Previous studies have shown that inhibitors of HDAC6 act as potent leptin sensitisers and anti-obesity agents in diet-induced obese mice. Specifically, the HDAC6 inhibitor Tubastatin A (TA) has been shown to alleviate leptin resistance by targeting HDAC6 activity in adipose tissue, leading to reduced food intake, decreased body weight and fat mass, and improved systemic glucose homeostasis in obese mice. Interestingly, HDAC6 upregulation was observed exclusively in the adipose tissue of obese mice, and its inhibition had no significant impact on body weight, food intake, or key metabolic parameters in normal mice. However, earlier findings reported that adipocyte-specific HDAC6 deletion resulted in increased fat accumulation and impaired insulin sensitivity in mice. The mechanism may be that loss of HDAC6 in white adipose tissue leads to increased acetylation of the cell death-induced DNA fragment factor subunit alpha-like effect C (CIDEC) protein, resulting in increased lipid droplet storage (Qian et al. 2017; Y. Li et al. 2024). In another study, Yan et al. 2019 have demonstrated that HDAC6 regulates lipid droplet turnover in response to nutrient deprivation via p62-mediated selective autophagy, and HDAC6 deletion causes steatosis in response to starvation.

Currently, the most widely investigated inhibitors of selective small molecule HDAC6 mainly include Ricolinostat (ACY-1215), Citarinostat (ACY-241), Tubacin, CKD-506, Tubastatin A, BML-281, and LTB2 (Zhang et al. 2023). Tubacin is the first reported HDAC6 inhibitor developed by Schreiber and co-workers. Studies have indicated that Tubacin exhibits different effects on HDAC1, HDAC6, and HDAC8, which are primarily derived from the surface differences between class I and class II HDACs. Unfortunately, its high lipophilicity made it more useful as a chemical tool rather than a drug candidate (Yang et al. 2019). The most successful anti-tumor HDAC6 inhibitors are ACY-1215 and ACY-241, which are oral selective HDAC6 inhibitors under clinical investigation for the treatment of refractory multiple myeloma (MM) (Zhang et al. 2023). Particularly, low doses of ACY-1215 combined with bortezomib or lenalidomide in multiple myeloma can produce synergistic therapeutic effects (Santo et al. 2012). Therefore, HDAC6 represents a potential target for further investigation considering its therapeutic applications.

3.0 Metabolism and cancer

The hallmarks of cancer, first proposed by Hanahan and Weinberg in 2000, describe the key aberrant cellular processes that enable malignant cells to sustain uncontrolled growth. These hallmarks now include avoiding growth suppressors, evading immune destruction, tumour-promoting inflammation, activating invasion and metastasis, inducing angiogenesis, genome instability and mutation, deregulating cellular metabolism, sustaining proliferative signaling, acquiring phenotypic plasticity, engaging in non-mutational epigenetic reprogramming, senescent cells, and polymorphic microbiomes. Recent advances in understanding cancer metabolism further highlight that reprogrammed lipid metabolism is a pervasive and fundamental feature across diverse cancer types. During cancer transformation, a metabolic shift known as the "Warburg effect" occurs. The Warburg effect refers to a metabolic alteration characteristic of cancer cells, in which they preferentially generate energy through aerobic glycolysis and lactic acid fermentation rather than oxidative phosphorylation to support rapid proliferation. This metabolic switch in glucose and glutamine metabolism enhances lipid metabolism via increasing exogenous dietary lipids and lipoproteins, or upregulating cholesterol and *de novo* lipid biosynthesis (Salita et al. 2022). For example, fatty acid synthase (FASN), which catalyzes the synthesis of fatty acids (FAs) from malonyl-CoA and acetyl-CoA via *de novo* FAs synthesis, is upregulated in colorectal cancer (Ecker et al. 2021). Furthermore, the inhibition of FASN in CRC-associated fibroblasts and the inhibition of FA uptake in CRC cells have been shown to attenuate cell migration (Gong et

al. 2020). This may lead to structural changes in their membranes, disruption of energy homeostasis, cell signaling, gene expression, and protein distribution, affecting several cell functions, such as apoptosis, autophagy, necrosis, proliferation, differentiation, growth, and chemotherapy resistance (Pakiet et al. 2019). Over the past decade, several studies highlighted the importance of lipid dysregulation in carcinogenesis, suggesting FAs metabolism could be exploited as a potent vulnerability (Krauß, Fari, et Sibilia 2022).

3.1 Lipogenesis

CRC is characterized by an altered lipid profile and the dysregulation of several lipid metabolic pathways. In particular, it is acknowledged that lipogenesis is upregulated, involved in the *de novo* FAs and triglycerides (TAGs) synthesis, and increased FAs uptake (***Figure 12***).

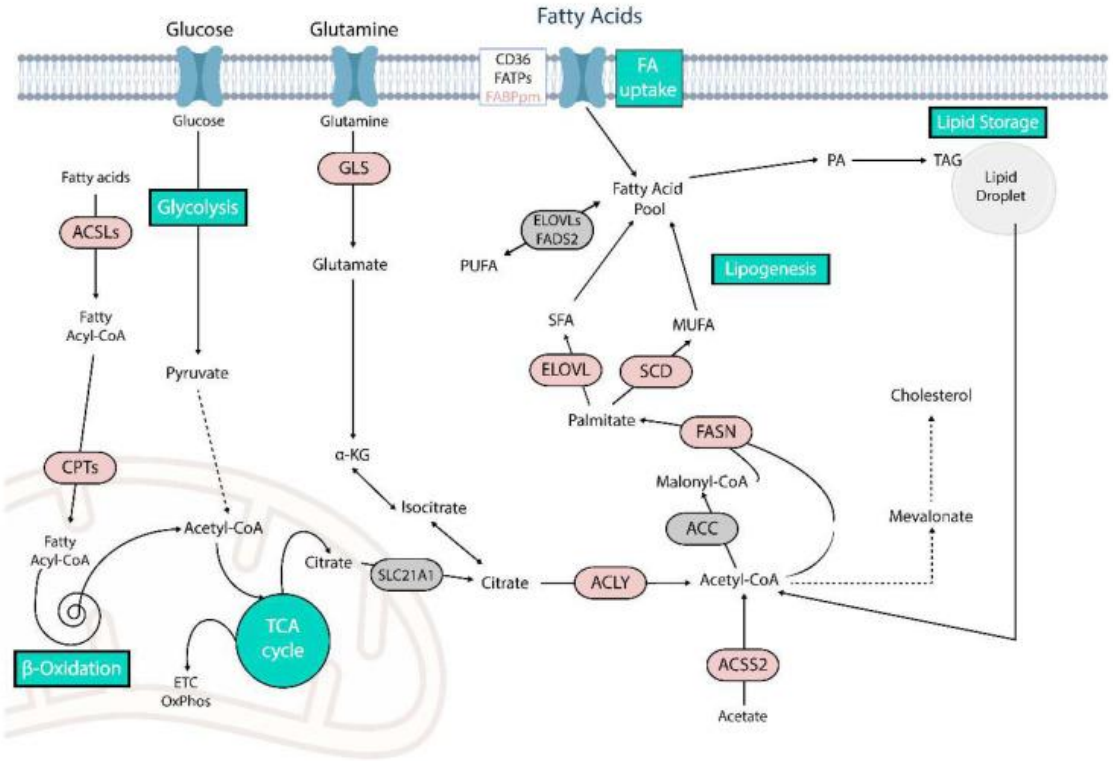

Figure 12. *Schematic representation of fatty acid metabolic reprogramming in CRC. Enzymes shown to be upregulated in CRC are highlighted in red. ACC, acetyl-CoA-carboxylase; ACLY, ATP-citrate lyase; ACSS, acyl coenzyme A synthetase; aKG, alpha-ketoglutarate; ACSL, acyl-CoA synthetase long-chain family; CPT, carnitine palmitoyltransferase; ELOVL, elongation of very-long-chain fatty acids protein; ETC, electron transport chain; FA, fatty acid; FABP, fatty acid binding protein; FADS, fatty acid desaturase; FASN, fatty acid synthase; FATP, fatty acid transport protein; GLS, glutaminase; MUFA, monosaturated fatty acid; PA, phosphatidic acid; PUFA, polyunsaturated fatty acid; SCD, stearoyl-CoA desaturase; SFA, saturated fatty acid; TAG, triacylglycerols (Krauß et al. 2022).*

Most somatic cells primarily obtain extracellular FAs from circulating dietary sources, and endogenous lipid biosynthesis is typically limited to hepatocytes, adipose tissue, and mammary glands. In contrast, cancer cells enhance both extracellular FAs uptake and reactivating de novo FAs synthesis, regardless of extracellular lipid availability, providing them with metabolic flexibility and alternative sources of energy. Extracellular free FAs can be transported across the membrane via different membrane-associated proteins. Membrane-associated proteins that have been described to mediate FAs uptake include fatty acid transport proteins (FATP), fatty acid binding proteins (FABP), and the best characterized scavenger receptor, CD36, also known as fatty acid translocase (FAT). Upregulation of CD36 was associated with poor prognosis, increased storage of FAs in LDs, resulting in inhibition of proliferation and induced apoptosis in CRC. Particularly, Drury et al. demonstrate that upregulation of CD36 expression is a potential compensatory mechanism for FAs synthase inhibition and that inhibition of CD36 can improve the efficacy of FAs synthase-targeted therapy.

The starting point of FAs synthesis is the conversion of cytosolic acetyl-CoA to malonyl-CoA, followed by condensation, elongation, and desaturation. The main source of cytosolic acetyl-CoA is either glycolytic flux or other anaplerotic sources, such as glutamine, which is used to produce TCA-derived citrate. Citrate generated in the mitochondria is exported into the cytosol via the SLC25A1 transporter, where FAs synthesis is initiated. In this rate-limiting step, ATP-citrate lyase (ACLY) catalyses the cleavage of citrate into acetyl-CoA and oxaloacetate, thereby coupling carbohydrate metabolism with FAs biosynthesis. Under low-glucose conditions, an alternative source of cytosolic or extramitochondrial acetyl-CoA is provided by acetate, which is converted into acetyl-CoA through the action of acetyl-CoA synthetase (ACSS) family enzymes. These are the only enzymes that use acetate as a substrate to produce acetyl-CoA by ATP-dependent ligation to CoA. Particularly, CRC cells are exposed to high local acetate concentration, and hypoxic CRC cells were shown to increase acetate uptake through activation of ACSS2 and endogenous generation via histone deacetylases that remove acetyl from histones. Further, acetyl-CoA can be activated to malonyl-CoA through acetyl-CoA carboxylases (ACC1/2), also known as ACACA/ACACB. This irreversible carboxylation step of *de novo* lipogenesis is regulated by phosphorylation and allosteric regulation as feedback control, for example, by high concentrations of palmitoyl-CoA. It couples mitochondrial FAs synthesis with β-oxidation through the activity of palmitoyltransferases (CPTs). The subsequent condensation of one acetyl-CoA with seven malonyl-CoA to create the saturated FA (SFA) palmitate (C16:0) is

catalysed by FASN. Finally, SFA palmitate can be modified through elongation and desaturation, creating a variety of different FAs. FAs are converted into monounsaturated FAs (MUFAs) by stearoyl-CoA desaturase 1 (SCD1), and their chains are elongated by elongases (ELOVLs). It has been shown that SCD1 drives tumor proliferation and invasiveness through increased lipogenesis and a misbalance of fine-tuned MUFA/SFA ratios. The activated FAs may serve as substrates for the synthesis of TAGs and phospholipids (PHLs) or are transported to mitochondria, where they undergo oxidation (Krauß et al. 2022; Pakiet et al. 2019).

TAGs are stored in lipid droplets (LDs), which are dynamic organelles characterized by a phospholipid monolayer containing lipid metabolism-associated proteins, and a neutral lipid core consisting of TAGs and sterol-esters. More than 200 structural and functional proteins, including DGAT2, RAB18, and members of the perilipin (PLIN) family, are localized on the surfaces of LDs, where they regulate LDs homeostasis and interactions. For example, DGAT2 catalyses the synthesis of triacylglycerols, while perilipin family proteins are involved in the regulation of RAB18 activity and in LDs metabolism. Cancer cells can accumulate TAGs as a consequence of upregulated FAs uptake and lipogenic enzymes, which ultimately serve as a reservoir of FAs that can be metabolized for bioenergetic β-oxidation or membrane biosynthesis. Tirinato et al. 2015 demonstrated that CRC stem cells accumulate LDs compared to normal colon epithelial cells, and this accumulation is directly correlated with increased expression of lysophosphatidylcholine acyltransferase-2 (LPCAT2) (Salita et al. 2022). As a result of TAGs upregulation, LDs accumulation has become an emerging feature of cancer. Lipotoxicity, resulting from excessive accumulation of FAs, glycerolipids (GLs), and sterols, underscores the crucial role of neutral lipid synthesis and accumulation within cells. These lipids can induce cellular stress, apoptosis, mitochondrial dysfunction, and inflammation. Research has shown that inhibiting specific lipid metabolism pathways can reduce lipotoxicity. Thanks to research advancements, LDs are now recognized as fully functional organelles. Beyond their well-known roles in lipid storage and metabolism, LDs also contribute to protein storage and degradation, and actively participate in a variety of intracellular processes, including membrane trafficking and inter-organelle communication. Advancements in understanding LD features have enriched knowledge of disease mechanisms in obesity, metabolic liver disease, and neurological disorders. In addition, LDs also have a role in cellular autophagy (Zhang et al. 2024).

Some FAs, such as linoleic acid (LA, 18:2) and α-linolenic acid (ALA, 18:3), cannot be synthesized by human cells and must be provided in the diet. Fatty acyl desaturases (FADS1-3) mediate polyunsaturated FAs (PUFAs) generation from the essential FAs LA and ALA. FADS2 is frequently upregulated in tumours that display resistance to SCD inhibition, enabling the maintenance of intracellular MUFAs levels. This prevents the accumulation of saturated FAs (SFAs) and preserves the balanced MUFA/PUFA ratio, a condition that helps cells evade lipid peroxidation and ferroptosis. Consistent with this function, increased FADS2 expression in CRC was shown to promote cancer proliferation and tumor growth. PUFAs can be classified into two categories, ω-6 PUFAs and ω-3 PUFAs. A recent lipidomic study of CRC tissues revealed that both ω-6 PUFAs (20:4), such as arachidonic acid (AA), and ω-3 PUFAs, for instance eicosapentaenoic acid (EPA, 20:5) and docosahexaenoic acid (DHA, 22:6), were up-regulated in CRC compared to normal tissue. PUFAs are generally more susceptible to oxidation because of their multiple double bonds. Moreover, the position of these double bonds is crucial from the functional perspective, since metabolites derived from ω-6 PUFAs typically exert pro-inflammatory effects, whereas those derived from ω-3 PUFAs display anti-inflammatory properties (Krauß et al. 2022).

Recently, more and more evidence has demonstrated that SREBP-1 participates in metabolic reprogramming in different cancers, including colorectal cancer. In mammalian cells, three SREBP isoforms, SREBP-1a, SREBP-1c, and SREBP-2, from two genes, *SREBF1* and *SREBF2*, have been identified, which regulate the synthesis of FAs and cholesterol. SREBP-1 and SREBP-2, which are tightly regulated by Insig-1 and SREBP-cleavage activating protein (SCAP) complexes, function in response to cholesterol levels. Decreased levels of cholesterol result in the dissociation of Insig-1 from the SREBP1-c/SCAP complex, stimulating SREBP-1c cleavage in the Golgi. After the cleavage, SREBP-1 translocates to the nucleus, where it binds to sterol regulatory elements (SREs) to stimulate the transcription of genes for FAs synthesis, including ATP citrate lyase (ACLY), acetyl-CoA carboxylase (ACC), fatty acid synthase (FASN), and stearoyl-CoA desaturase 1 and 2 (rodent)/5 (human) (SCD-1 and -2/5), and for lipid uptake, such as low-density lipoprotein receptor (LDLR) (***Figure 13***). Furthermore, it has been reported that SREBP-1 activation stimulates *de novo* lipogenesis to regulate cell growth, cell cycle progression, and metastatic characteristics for cancer progression.

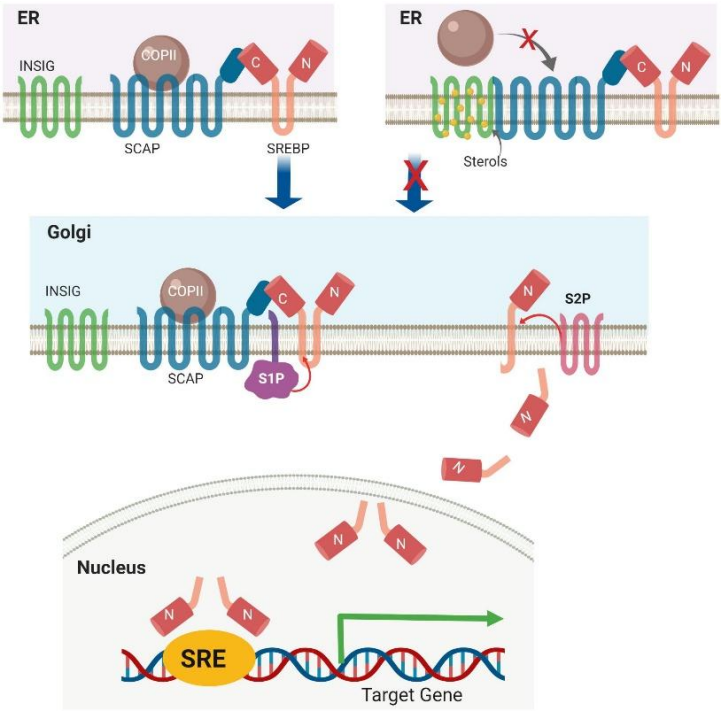

Figure 13. *Sterol-mediated proteolytic activation of SREBP. Under basal conditions, the SREBP-SCAP-INSIG complex is retained in the ER membrane. High levels of cellular sterol induce INSIG degradation, followed by translocation of the SREBP-SCAP complex from the ER to the Golgi apparatus. In the Golgi, SREBP is activated via a two-step proteolytic mechanism with S1P and S2P (Dorotea, Koya, e Ha 2020).*

Meanwhile, multiple signaling pathways control SREBP-1 activation to regulate the downstream genes for lipogenesis, including the EGFR, PI3K/Akt/mTOR, and p53 mutation pathways. Indeed, hyperactivation of the PI3K/Akt/mTOR signaling pathway can suppress oxidative stress and ferroptotic cell death by regulating SREBP-1/SCD-1-mediated lipogenesis. Activation of Akt promotes the synthesis of full-length SREBP-1 and facilitates its nuclear accumulation, leading to increased intracellular lipid levels, including FAs and PHLs. This process contributes to the activation of the FASN promoter. Li et al. demonstrated that colocalization of SREBP-1 and FASN has been observed in colorectal cancer (CRC) tissues, and the transcriptional regulation of the FASN promoter by SREBP-1 serves as a compensatory mechanism in response to impaired endogenous FAs synthesis in colorectal neoplasia. Furthermore, the mammalian/mechanistic target of rapamycin complex 1 (mTORC1) regulates both the transcription and translation of SREBP-1 and SREBP-2, thereby promoting de novo lipid biosynthesis in response to nutrients or insulin. Through these mechanisms, mTORC1 influences cell proliferation, mitochondrial metabolism, and glycolytic capacity in cancer (Zhao, Lin, et Wang 2022). In the context of chemotherapy resistance in CRC, SREBP-1 is overexpressed in chemoresistant CRC samples and is associated with poor patient survival. Interestingly, SREBP-1 can enhance

gemcitabine chemosensitivity by downregulating caspase-7, suggesting its potential as a novel prognostic biomarker for CRC (Shen et al. 2019). Conversely, overexpression of SREBP-1 promotes resistance to 5-fluorouracil (5-FU) by modulating caspase-7-dependent PARP1 cleavage in CRC cells (Gao et al. 2019).

3.2 The role of HDAC in metabolism

Histone deacetylases (HDACs) are increasingly recognized as key regulators of cellular metabolism. Beyond their classical role in chromatin remodelling, HDACs modulate the expression and activity of enzymes involved in critical metabolic pathways, including glycolysis, oxidative phosphorylation, lipid metabolism, and the tricarboxylic acid (TCA) cycle. HDAC3 has been reported to regulate lipid metabolism and homeostasis in several tissues, and the directionality of this effect varies depending on the tissue. For instance, liver-specific deletion of HDAC3 increased the expression of genes that drive lipid synthesis and storage (Knutson et al. 2008). In contrast, intestine-specific deletion of HDAC3 ($HDAC3^{IKO}$) has been shown to protect mice from diet-induced obesity. Intestinal epithelial cells (IECs) isolated from $HDAC3^{IKO}$ mice upregulate genes and proteins involved in mitochondrial and peroxisomal β-oxidation, leading to enhanced FAs oxidation and extensive lipidome remodelling. Simultaneously, analysis of gene and protein enrichment induced by $HDAC3^{IKO}$ mice showed that the PPAR target gene was significantly enriched. This also provides evidence that HDAC3 inhibits genes involved in FAs oxidation in enterocytes by repressing the transcriptional targets of the PPAR family of nuclear receptors (Dávalos-Salas et al. 2019). Peroxisome proliferator-activated receptors (PPARs), including PPARα, PPARβ/δ, and PPARγ, are key regulators of lipid metabolism and energy homeostasis. PPARα primarily controls cholesterol balance and bile acid metabolism, whereas PPARβ/δ enhances glycolysis, glucose uptake, and FAs catabolism while limiting lipid synthesis. PPARγ, on the other hand, promotes adipocyte differentiation and regulates insulin sensitivity and FAs storage by modulating genes involved in lipid transport and deposition (King et al. 2021; Y. Li et al. 2024). Another instance of how metabolism is affected by HDACs, HDAC2, HDAC4, HDAC5, and HDAC6 play a significant role in the development of obesity. Particularly, HDAC4 promoted lipolysis and reduced TAGs in Drosophila and mammals. The knockdown of HDAC5 led to the upregulation of lipogenic genes and the accumulation of TAGs in the cells. Moreover, studies have indicated that HDAC6 plays an important role in modulating fat accumulation, adipocyte lipid droplet sizes, and TAG levels. Furthermore, HDAC6 regulates the differentiation of mesenchymal stem cells into adipocytes, and its expression is altered during differentiation (Mukhtar Yusif 2024). In

addition, high concentrations of HDAC1 and HDAC2 are found in HCC tissues. Particularly, HDAC1 and HDAC2 suppress the expression of Fructose-1,6-bisphosphate (FBP1), the rate-limiting enzyme in the gluconeogenesis pathway, by deacetylating histone H3K27 in the *FBP1* enhancer (Yang et al. 2017). Understanding how HDACs impact cancers through metabolism can provide novel targets for potential treatments.

Objectives

Histone deacetylase inhibitors (HDACi) have emerged as promising anti-cancer agents due to their ability to modulate gene expression and interfere with various cellular processes involved in tumor progression. Recent evidence also suggests a strong connection between HDAC6 activity and lipid metabolism, which represents a hallmark of cancer.

The main objective of the thesis was to characterize the effects of HDAC inhibitors in CRC cells and to clarify their role in lipid metabolic reprogramming. To achieve this, the pan-HDAC inhibitor ITF2357 or the selective HDAC6 inhibitor ITF3756 was used to treat CRC cells.

Specifically, the connection between HDAC inhibition and lipid metabolism and accumulation was a major goal.

Moreover, considering that HDAC6 is overexpressed in CRC and plays a role in lipid metabolism, the specific aims were:

- To verify that selective HDAC6 inhibition induces lipogenesis and clarify the role of this process.
- To evaluate the effects of the combination of ITF3756 with lipogenesis-producing agents such as the proteasome inhibitor bortezomib.
- To clarify the role of HDCAI-induced lipogenesis (pro-survival or death promoter) to assess whether this can be exploited as a therapeutic strategy to target CRC cells selectively.

Materials and methods

Cell culture

HCT116 and HT29 cells (ATCC-LGC Standards S.r.l., Italy) were cultured in Dulbecco's Modified Eagle's Medium (DMEM, Euroclone, UK) supplemented with 10% Fetal Bovine Serum (FBS), 1% Antibiotic Antimycotic Solution (100X, cat. n°30-004-CI, Corning®, USA), 1% Sodium Pyruvate (100 mM, cat. n° ECM0542D, Euroclone, UK), and 1% L-Glutamine 100X (200 mM, cat. n°AU-X0550-100, Aurogene S.r.l., Italy).

Cells were maintained in a humidified atmosphere 5% CO_2 at 37 °C and used at early passages for all experiments.

Chemicals and reagents

ITF2357 and ITF3756 were synthesized and provided by the pharmaceutical company Italfarmaco S.p.A (Cinisello Balsamo, Milan, Italy), dissolved in dimethyl sulfoxide (DMSO) (20 mM stock solution) and stored at -20 °C. For the experiments, the stock solution was diluted in DMEM, not exceeding 0.01% (v/v) DMSO, to realize the proper final concentrations. The results presented are strictly limited to the use of the selective HDAC6 inhibitor.

Bortezomib (BTZ, Velcade or PS-341) was obtained from Millennium Pharmaceuticals (London, UK), solubilized in DMSO to reach a 5 mM stock solution, and stored at -20 °C. It was used at various final concentrations.

The lipogenic inhibitors, DGAT-1i (Diacylglycerol Acyltransferase 1 A922500, cat n° 252801, Sigma-Aldrich, St. Louis, MO, USA) and DGAT-2i (Diacylglycerol Acyltransferase 2 PF-0642439, cat n° PZ0233, Sigma-Aldrich, St. Louis, MO, USA), were solubilized in DMSO or water according to the datasheet instructions (Stock solution: 5 mM and 10 mM, respectively), stored at -20 or 4°C and used for the experiments at different final concentrations.

SSO (cat n° SML2148, Merck, Darmstadt, Germany) was provided by the Université Catholique de Louvain (Brussels, BE). SSO was solubilized in DMSO to prepare a stock solution at 10 mM and stored at −20 °C. For experiments, SSO was diluted in the appropriate medium to achieve a final concentration of 10 μM.

Fatty acid preparation

The FA/BSA complex was prepared as described by (Knight et al. 2021). Docosahexaenoic acid (DHA, cat n°10–2206, Larodan) was complexed with fatty acid–free bovine serum

albumin (FA-free BSA, cat n° A7030, Merck, Darmstadt, Germany) in 150 mM NaCl solution to achieve a fatty acid/BSA ratio of 4:1 (mol:mol). The aliquoted fatty acid solutions were stored at −80 °C, protected from light, and used immediately after thawing by adding the required concentration directly to the wells. The stock solution was prepared at an initial concentration of 4.5 mM and subsequently diluted to a final concentration of 100 µM for the experiments.

Cell treatments

For synergistic experiments with ITF3756 and BTZ, cells were treated with both compounds in a 3:5 ratio. The analysis and generation of the synergism curve were performed using CompuSyn Software version 1.0 (CompuSyn, Inc., Paramus, NJ, USA), a program for drug combination studies and their synergy quantification using the Chou-Talalay method. The resulting combination index (CI) theorem of Chou-Talalay offers a quantitative definition for synergism (CI < 1), antagonism (CI > 1), and additive effect (CI = 1) in drug combinations (Chou 2010).

For establishing the role of lipogenesis, HCT116 and HT29 cells were treated with DGAT-1/2 inhibitors, SSO, or DHA, either alone or in combination with ITF2357 or ITF3756 and BTZ for 24 or 48 h. In particular, cells were pre-treated for 1 hour with the DGAT-1/2 inhibitors at the established concentration of 7.5 µM and 10 µM, respectively.

At the end of the treatment, cell viability was quantified by MTT assay or using an Incucyte® Live-Cell Analysis System (Sartorius). The instrument acquires time-lapse phase-contrast images and quantifies cell proliferation by measuring the percentage of surface area occupied by cells (confluence). Confluence values from treated cells were normalized to those of the control, allowing for the assessment of treatment-induced effects on cell viability.

MTT (3-[4,5-Dimethyl-2-thiazolyl]-2,5-diphenyl-2H-tetrazolium bromide) assay

Cell viability was evaluated by MTT assay (cat n° M5655 6494, Sigma-Aldrich, USA) following the manufacturer's instructions. Briefly, HCT116 and HT29 cells were seeded in 96-well plates (2.5 x 10^4 cells/cm^2) 24 h post-seeding, cells were treated with the compounds for the established time. MTT (1 mg/mL) was added for 2 h The medium was then replaced with lysis buffer (20% sodium dodecyl sulfate, 40% N,N-dimethylformamide, pH 4.7) and

the absorbance was measured by bio-photometer (Dynex Opsys MR^{TM} Microplate Reader, Technologies, Chantilly, VA, USA) at 570 nm (Test wavelength) and 630 nm (Reference wavelength), using the lysis buffer as blank.

Oil Red O (ORO) staining

Oil Red O staining (ORO, cat n° O0625, Sigma-Aldrich, St. Louis, MO, USA) was used to detect neutral lipid content in HCT116 and HT29 cells, following the manufacturer's instructions. ORO stock solution was prepared by dissolving 0.35 g of ORO in 100 mL of 100 % isopropanol. Cells (2.4 x 10^4 cells/cm^2) were seeded in 24-well plates, allowed to adhere overnight, and then treated with the compounds. After 48 hours, the medium was removed, and the cells were washed with Phosphate-Buffered Saline (PBS), fixed in 4% paraformaldehyde (PFA) for 10 minutes at room temperature, and washed with PBS. Then, 60% isopropanol was added for 15–20 seconds to remove PFA and then removed until completely dry. Subsequently, a freshly prepared (3:2 ratio ORO stock solution diluted with distilled water) and filtered ORO working solution was added to the cells and incubated for 30 minutes at room temperature. ORO solution was then removed, and the cells were washed three times with distilled water. Stained cells were visualized under a Leica DM-IRB microscope at 400× magnification. Representative images of the experimental conditions were acquired with the Leica DC300F digital camera. ImageJ software was used to quantify LDs. First, the proper threshold was set and applied to all images, resulting in a binary image. Then, the pixels referred to the area covered by a single cell were used to measure the intensity of the LDs in each image. The average of the intensity of an established number of areas was then normalized to the number of cells counted.

BODIPY 495/503 staining

20 x 10^4 HCT116 cells were seeded in µ-slide 8-well high (cat n°80 806, Ibidi) and treated the day after with different concentrations of ITF2357. After 48 h, cells were washed with warmed PBS twice and incubated with a solution of 2 µM BODIPY 493/503 in PBS for 20 min at 37 °C and 5% CO_2. After washing with warmed PBS, cells were maintained in DMEM medium without phenol red, containing 1% FBS and 1µg mL^{-1} Hoechst33342 (cat n°H3570, Invitrogen) during live cell microscopy acquisition. Pictures were taken with an LSM 800 confocal microscope, objective 40x. The percentage of pixels associated with LD was quantified using ImageJ. The threshold was determined to discriminate the LDs from

the background and applied to the different conditions of the same cell line and experiment. The percentage area of LDs was normalised by the number of nuclei.

Cell cycle distribution

HCT116 cells were seeded in 6-well plates (1.8 x 10^4 cells/cm^2). 24 h post-seeding, cells were treated with 2 μM ITF3756, 5 nM BTZ, either alone or in combination, and maintained in a humidified atmosphere of 5% CO_2 at 37 °C. After 48 h treatment, cells were harvested (0.025% Trypsin-EDTA), washed in PBS, and resuspended in hypotonic solution (25 μg/mL Propidium Iodide, 0.1% Sodium citrate, 0.1% Nonidet P-40, and 10 μg/mL RNase A). The cell cycle phase distribution was evaluated by CytoFLEX LX Flow Cytometer (Beckman Coulter, Life Sciences, USA) using CytExpert 2.5 Software (Beckman Coulter, USA). Cell debris and aggregates were excluded by opportune gating, and 50.000 events were acquired for each sample.

Annexin V/PI apoptosis detection assay

Annexin V/PI apoptosis detection assay (Annexin V-FITC Kit, cat n° 130-092-052, Miltenyi Biotec, Germany) was used to identify early and late apoptotic cells. HCT116 cells were seeded (1.8 x 10^4 cells/cm^2), allowed to adhere overnight, treated with 2 μM ITF3756, 5 nM BTZ either alone or in combination, and maintained in a humidified atmosphere of 5% CO_2 at 37 °C. After 48 h treatment, the percentage of cells in early or late apoptosis and cell necrosis was measured. Following the manufacturer's instructions, cells were harvested, centrifuged, and the resulting cell pellet was washed with PBS and resuspended in Annexin V binding buffer. The cells were then labelled with Annexin V and Propidium Iodide and incubated for 15 minutes at room temperature in the dark. Samples were then analysed by flow cytometry using a FACSCanto cytometer (Becton Dickinson, Franklin Lakes, NJ, USA). Approximately 50.000 events were acquired for each sample. Flow cytometry data were analyzed using FlowJo 10 software (BD Biosciences, San Diego, CA, USA), using a gating strategy excluding debris and doublet cells.

Western blotting

HCT116 cells were seeded in 6-well plates (1.8 x 10^4 cells/cm^2); 24 h post-seeding, cells were treated with 2 μM ITF3756, 5 nM BTZ either alone or in combination. At the end of

treatment, cells were lysed using ice-cold lysis RIPA buffer (1% NP-40, 0.5% sodium deoxycholate, 0.1% SDS, and protease inhibitors in PBS, pH 7.4) supplemented with a protease inhibitor cocktail for 20 minutes. Cell debris was removed by centrifugation and the supernatant, containing total protein lysate, was sonicated (10 seconds, three times at 10 rev) and quantified by Bradford assay (Pierce™ Coomassie Plus Assay Kit, cat N° 23236, Thermo Fisher Scientific, USA) using Bovine Serum Albumin (BSA, cat n° A2153, Sigma-Aldrich, USA), as previously reported (44).

The amount of 30 µg protein from each sample was separated by sodium dodecyl sulphate-polyacrylamide gel electrophoresis (SDS-PAGE) and transferred to nitrocellulose membrane. To verify the correct loading of all samples, the membranes were stained with 0.1% Ponceau Red in 5% acetic acid. The membranes were then washed with Tris-buffered saline-Tween 20 (TBS-T - 20 mM Tris, 140 mM NaCl, 0.1% Tween-20) and first incubated for 1 hour in blocking solution (5% milk in TBS-T) at room temperature. After blocking, incubated overnight at 4 °C with primary antibodies: anti-p53 (DO-1, 1:200, cat n° sc-126, Santa Cruz Biotechnology, CA, USA), anti-caspase 3/anti-cleaved caspase-3 (1:1000, cat n° 9662S, Cell Signaling Technology, USA), anti-PPARγ (1:1000, cat n°sc-7273, Santa Cruz Biotechnology, CA, USA), anti-SREBP-1 (1:1000, cat n°#bs-140R, BioSS, Dundee, UK), anti-Poly ADP-Ribose Polymerase-1 (PARP-1, 1:700, cat n° sc-8007, Santa Cruz Biotechnology, CA, USA), anti-α-acetylated-tubulin (1:1000, cat n° T6793, Sigma Aldrich, Milan, Italy) and anti-γ-tubulin (1:10000, cat n° T6557, Sigma Aldrich, Milan, Italy).

After washing in TBS-T, the membranes were incubated with appropriate HPR-conjugated secondary antibodies anti-Rabbit IgG (1:10.000, cat n° W4011, Promega Corporation, Madison, WI, USA) or anti-Mouse IgG (1:10.000, cat n° W4021, Promega Corporation, Madison, WI, USA) at room temperature for 1 hour.

The chemiluminescent signal was visualized by chemiluminescence solution (ECL™ Prime Western Blotting Detection Reagents, cat n° RPN2232, Amersham™, UK) and was detected using the ChemiDoc, XRS acquisition instrument (Bio-Rad, Hercules, CA, USA). The images were analysed using the Image Lab software (Bio-Rad, USA), using γ-tubulin as a housekeeping protein.

Depending on the molecular weight of the protein, if required, the membranes were subjected to stripping (15g glycine, 1g SDS, and 10 ml TWEEN-20 in distilled water, pH 2.2), before proceeding with further incubation with other antibodies.

Extraction of cytosolic and nuclear fractions

HCT116 cells were seeded in 60 mm-dishes (1.9 x 10^4 cells/cm^2); 24 h post-seeding, cells were treated with 2 μM ITF3756, 5 nM BTZ either alone or in combination and maintained in a humidified atmosphere of 5% CO_2 at 37 °C. Cells were then washed in PBS and scraped in subcellular fractionation buffer (250 mM sucrose, 20 mM HEPES, 10 mM KCl, 1.5 mM MgCl2, 1 mM EDTA, 1 mM EGTA, 1 mM DTT, and protease inhibitors, pH 7.4). Subsequently, cells were passed 10 times through a needle of 25 G and kept on ice for 20 min. The homogenates were centrifuged at 720x g for 5 min at 4 °C. The pellets were resuspended in lysis buffer and passed 10 times through a needle of 25 G and centrifuged again at 720x g or 10 min at 4 °C. The pellets (nuclear fraction) were lysed with nuclear buffer (standard lysis buffer with 10% glycerol and 0.1% SDS–1% NP-40, 0.5% sodium deoxycholate, 0.1% SDS, and protease inhibitors: s, 25 μg/mL aprotinin, 1 mM PMSF, 25 μg/mL leupeptin and 0.2 mM sodium pyrophosphate) and sonicated (10 seconds at 10 rev, three times). The supernatants obtained from the first centrifugation were considered as cytosolic fractions. Nuclear or cytosolic protein lysates were quantified by Bradford assay method (Pierce™ Coomassie Plus Assay Kit, cat n° 23236, Thermo Fisher Scientific, USA) using Bovine Serum Albumin (BSA, cat n° A2153, Sigma-Aldrich, USA) and western blotting was performed as previously reported. Nuclear and cytosolic fractions were used to evaluate Cleaved SREBP-1 (1:1000, cat n° #bs-1402R, BioSS, Dundee, UK). Lamin-B (1:1000, cat n°365962, Santa Cruz Biotechnology, CA, USA) and β-tubulin (1:1000, cat n° sc-55529, Santa Cruz Biotechnology) were used as nuclear and cytoplasmic protein housekeeping, respectively.

Triacylglycerol quantification assay

The content of TAGs was quantified using a spectrophotometric commercial kit for TAGs determination (Gesan Production s.r.l, Campobello di Mazara, Italy). HCT116 cells were seeded in 60 mm-dishes (1.9 x 10^4 cells/cm^2); 24 h post-seeding, cells were treated with 2 μM ITF3756, 5 nM BTZ either alone or in combination for 48 hours. The TAGs accumulation was then measured. Briefly, after removing the medium, cells were washed in PBS and lysed with 5% NP-40 on ice. Then, to solubilize TGs, the samples were repeatedly subjected to heat shock, slowly heated at 80-100°C, and cooled to room temperature. After centrifugation, the reagent was added to the recovered supernatant, and the samples were incubated in the dark at room temperature for 10 minutes. The amount of TAGs for each

sample was measured as absorbance using a Varian Cary 50 Scan UV-Visible Spectrophotometer at 546 nm and calculated by a standard curve (in nmol) obtained with the standard triacylglycerol and normalized to the same cell number (nmol/1x10^6 cells).

RNA Extraction and RT-qPCR

HCT116 cells were lysed with TRIzol Reagent after treatment with different concentrations of ITF2357. Briefly, total RNA was recovered after chloroform separation (aqueous part), precipitation with isopropanol, washing with 70% ethanol, and resuspension in RNAse-free water. The RNA quantity and quality were evaluated with a Nanodrop 1000 spectrophotometer (Thermo Fischer Scientific). 1 µg of total RNA was used for reverse transcription with RevertAid Reverse-Transcriptase, oligo-dT, and random hexamers (Thermo Fisher Scientific). Then, quantitative PCR amplification was performed using the CFX Connect Real-Time PCR detection system (cat n°#1 855 201, Bio-Rad), with GoTaq qPCR Master Mix (cat n°A6001, Promega) and sequence-specific primers for the PLIN2, CD36, DGAT-1, and SBREF-1 genes. Relative gene expression was calculated using the ddCq method, with RLPL0 as the housekeeping gene.

siRNA transfection

HCT116 cells were seeded in 96-well plates or in 6-well plates at 2.5 x 10^4 cells/cm^2; 24 h post-seeding, cells were transfected with 80 pMoles/cm^2 of Silencer® Select SREBP-1 (Cat n° #4390824, Thermo Fisher Scientific, USA), or Silencer® Select Negative Control (Cat n° #4390843, Thermo Fisher Scientific, USA). For cell transfection, Lipofectamine™ RNAiMAX Transfection Reagent (Cat n°13778030, Thermo Fisher Scientific, USA) was used following the manufacturer's standard instructions. 16 h after transfection, the cells were treated with 2 µM ITF3756 and 5 nM BTZ, either alone or in combination, in fresh medium and maintained for 24 h in a humidified atmosphere of 5% CO_2 at 37 °C. After this incubation, cells were subjected to an MTT assay or harvested to obtain protein lysates. The siRNA knockdown efficiency was assessed by western blotting 40 h post-transfection.

Statistical analysis

The data shown in all graphs represent the mean ± standard deviation (SD) of at least three independent biological replicates. Statistical analyses were conducted using the following

tests: Student's t-test (for comparing two groups), Ordinary one-way ANOVA (for comparisons across three or more groups), and two-way ANOVA (for the analysis of multiple variables between two groups). All analyses were performed using GraphPad Prism 10 software (GraphPad Software, USA).

P-values are indicated in the graphs as follows: * $p < 0.05$; ** $p < 0.01$; *** $p < 0.001$; **** $p < 0.0001$. p-value ≤ 0.05 was considered statistically significant.

Results

PART 1: The pan-HDAC inhibitor ITF2357

The effects of the pan-HDACI ITF2357 (Givinostat) on HCT116 cell viability and lipid accumulation.

This part of the project was carried out in collaboration with the Université Catholique de Louvain, where I spent six months abroad as part of my academic training.

Given that HDACs play key roles in regulating lipid metabolism, the inhibition of HDACs activity through the pan-HDAC inhibitor (HDACi) could promote lipogenesis via transcriptional activation of genes involved in lipid synthesis and storage (King et al. 2021; Pakiet et al. 2019). Therefore, the effect of the pan-HDACi on CRC HCT116 cell viability was assessed by MTT assay using increasing concentrations of ITF2357. As shown in ***Figure 1A***, the epigenetic compound decreased cell viability in a dose-dependent manner after 48 h of treatment, with approximately a 50% reduction observed at the 0.5 µM concentration. To evaluate the effects of ITF2357 on LDs formation, cells were stained with BODIPY 493/503, a neutral lipid-specific fluorescent dye. Fluorescence microscopy analysis revealed a progressive increase in both the number and size of LDs in treated cells compared to the control group (***Figure 1B***). Quantitative analysis showed that LDs accumulation was significantly enhanced in a concentration-dependent manner (***Figure 1C***). Given the effects of the compound on lipid accumulation, the transcriptional regulation of genes involved in lipid metabolism in response to the treatment was investigated. To this end, the expression levels of a selected panel of genes related to lipid biosynthesis and storage were determined using quantitative real-time PCR (qRT-PCR). The results showed a significant upregulation of *SREBF-1* and *CD36* (***Figure 1D***). Sterol regulatory element-binding proteins (SREBPs) are crucial transcription factors in lipid metabolism, regulating the expression of genes involved in the synthesis of FAs, cholesterol, and triglycerides (Li et al. 2025). FAs can either be synthesized within the cell (*de novo* lipogenesis) or transported across the membrane via different membrane-associated proteins. A key player in the uptake of extracellular FAs is the membrane protein CD36, also known as fatty acid translocase. CD36 facilitates the transport of long-chain and ultra-long-chain free FAs across the plasma membrane (Krauß, Fari, et Sibilia 2022; Drury et al. 2022). The results demonstrate that CRC cells alter their lipid sources by increasing both extracellular lipid uptake and *de novo* FAs synthesis. In cancer cells, excess lipids are converted into cholesterol esters and TAGs within the endoplasmic reticulum, leading to the formation of LDs (Li et al. 2025). Consistent with this, an increase in expression levels of *PLIN2* and *DGAT-1* was observed

(***Figure 1D***). DGAT-1 is a key enzyme involved in the final step of TAGs synthesis, catalyzing the esterification of diacylglycerol (DAG) with fatty acyl-CoA to form triacylglycerol. DGAT-1 plays a crucial role in lipid metabolism by regulating lipid storage and energy homeostasis (L. Wang et al. 2024).

Although TAGs synthesis is its predominant function, DGAT-1 has an important role in detoxifying excess lipids that are taken up from outside the cell. As such, *DGAT1* may be important for preventing activation of ER stress pathways due to lipotoxic lipids (Walther, Chung, et Farese 2017). Following TAGs synthesis, PLIN2 localizes to the surface of nascent LDs, where it plays a key role in LDs formation (Yang et al. 2025; Doncheva et al. 2023). Indeed, PLIN2 helps to sequester those neutral lipids into stable droplets, preventing their immediate breakdown. Without proper PLIN2 coating, LDs can be more susceptible to lipolysis or autophagic degradation (Tsai et al. 2017).

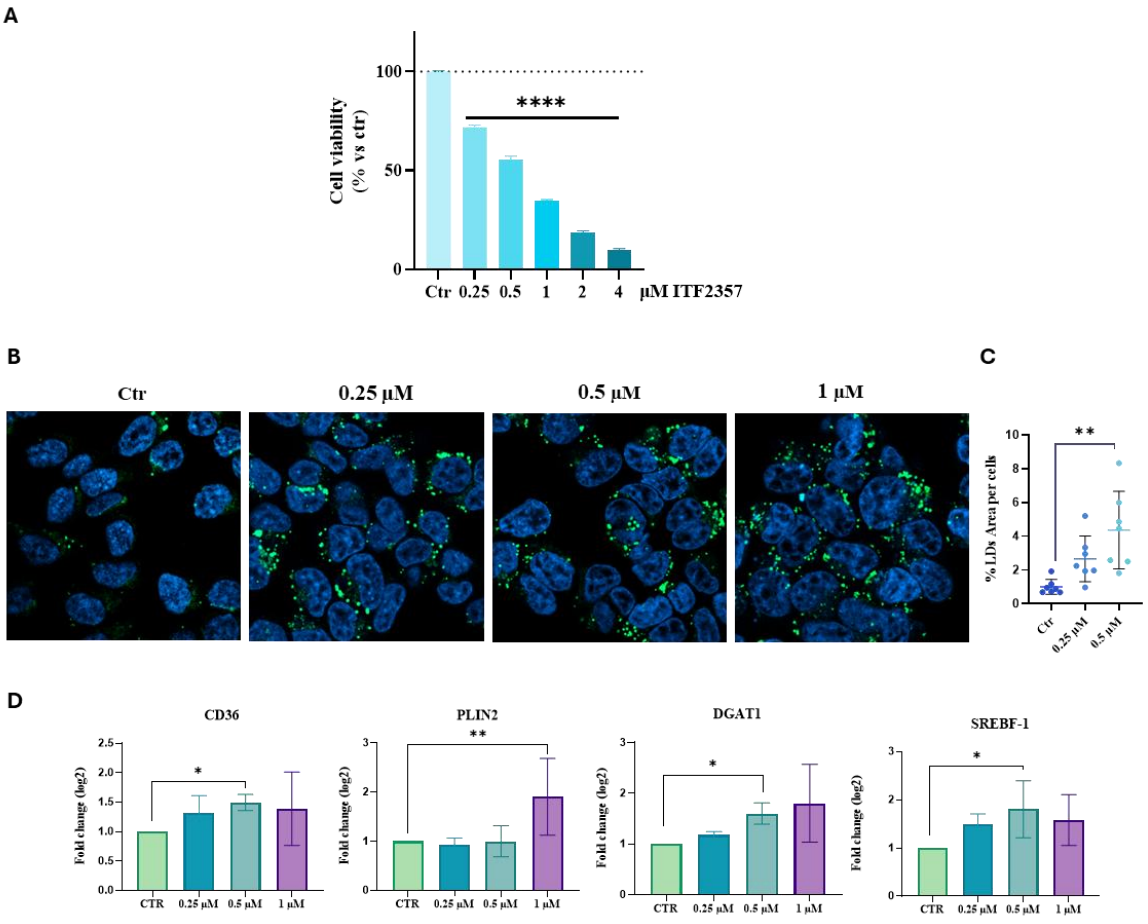

Figure 1. ***The effects of ITF2357 on HCT116 cell viability and lipid accumulation***.

HCT116 cells were treated with increasing concentrations of ITF2357 for 48 h. Cell viability was evaluated by MTT assay. Data are expressed as cell viability percentages compared to the control Ctr (**A**). The results

reported in the graph are the mean ± SD of three independent experiments. Statistical analyses were performed using ordinary one-way ANOVA with multiple comparison test, **** $p < 0.0001$.

Confocal microscopy images of HCT116 cells showing LDs accumulation after 48 h of treatment. LDs were stained using BODIPY 493/503 (green), while nuclei were counterstained with DAPI (blue). Images were acquired using a confocal microscope with a 600x oil immersion objective and analysed using ImageJ/Fiji software. The images are representative of three independent experiments (**B**). For the quantification, data are expressed as LDs area/cells compared to the Ctr **(C**). Statistical analyses were performed using Ordinary one-way ANOVA with multiple comparison test, ** $p < 0.01$.

HCT116 cells express high levels of genes involved in lipogenesis regulation. Gene expression analysis (qRT-PCR) of Perilipin 2 (PLIN2), Cluster of Differentiation 36 (CD36), Sterol Regulatory Element Binding Transcription Factor 1 (SREBF-1), Diacylglycerol O-Acyltransferase 1 (DGAT-1) on HCT116 cells treated with different concentrations of ITF2357 for 48 h. Gene expression levels are reported in $2^{\wedge-\Delta\Delta Ct}$ compared to HCT116 Ctr cells, and Ct was normalized to RLP0 (housekeeping). The results reported in the graph are expressed as the mean ± SD of six independent biological replicates. Statistical analyses were performed using ordinary one-way ANOVA with multiple comparison test, * $p < 0.05$, ** $p < 0.01$ (**D**).

The role of lipogenesis induced by ITF2357.

Finally, to better understand the functional role of lipid accumulation induced by ITF2357, DGAT-1/2 inhibitors (DGAT-1/2i) and CD36 inhibitors were employed. It should be noted that DGAT-2 also contributes significantly to TAGs synthesis, particularly for *de novo*-synthesized FAs and DAGs, indicating that inhibition of DGAT-1 alone may be insufficient to fully block the pathway. To guarantee complete blockage of LDs assembly, both DGAT-1 and DGAT-2 were inhibited by specific inhibitors, A922500 and PF-06424439 respectively. Co-treatment with DGAT-1/2i or CD36 inhibitors significantly potentiated the effects of ITF2357 on cell viability compared to treatment with ITF2357 alone (***Figure 2A-B***).

To further support the notion that LDs accumulation plays a protective role, cells were treated with DHA, a highly unsaturated FA. As shown in ***Figure 2C,*** when DHA was added to the ITF2357/DGAT-1/2i combination, an even more pronounced reduction in cell viability was observed.

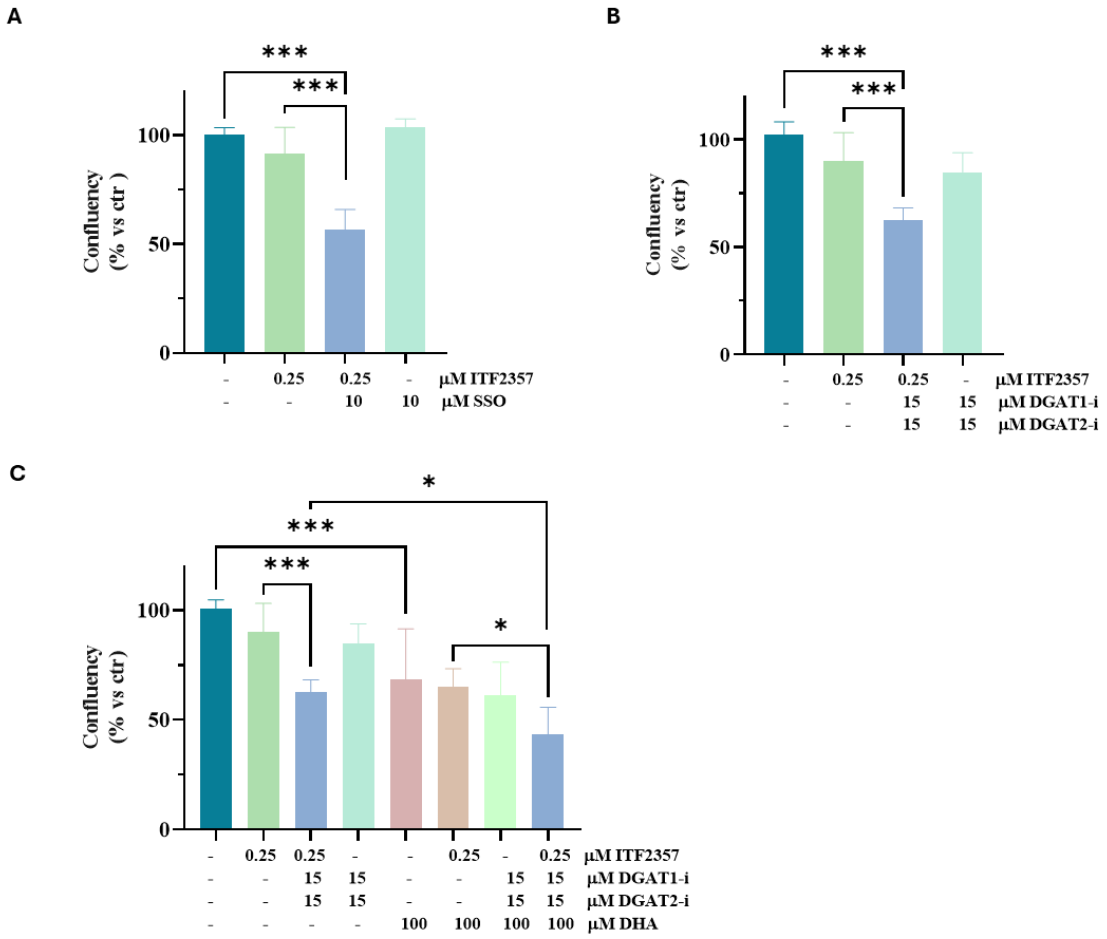

Figure 2. DGAT-1/2i and CD36 inhibitors exacerbate the effects of ITF2357.

HCT116 cells were treated with 15 µM A922500 (DGAT-1 inhibitor) and 15 µM PF-06424439 (DGAT-2 inhibitor) (**A**), 10 µM SSO (CD36 inhibitor) (**B**), or 100 µM DHA (**C**) alone or in combination with 0.25 µM ITF2357 for 48 h. Data are expressed as cell confluency percentages compared to vehicles. The vehicle consists of an equivalent concentration of FA-free BSA for DHA or DMSO at the highest concentration for the drugs. The results reported in the graph are expressed as the mean ± SD of three independent biological replicates. Statistical analyses were performed using ordinary one-way ANOVA with multiple comparison test, *$p < 0.05$, *** $p < 0.001$.

PART 2: The selective HDAC6 inhibitor ITF3756

The effects of selective HDAC6 inhibitor ITF3756 and bortezomib on HCT116 cell viability and lipid accumulation.

Since pan-HDAC inhibitors have a broad-spectrum action as they inhibit different HDACs belonging to class I/II, a selective HDAC inhibitor was used to achieve more specific targeting of tumor cells (W. Li, Fu, and Wang 2024). Considering that specific HDACs are overexpressed in different tumour types, the development of selective HDACi has corroborated the idea of a focused targeted therapy. In particular, the attention of this study was focused on HDAC6. This histone deacetylase is upregulated in colon cancer and is

specifically related to lipid metabolism (Zhang et al. 2019a; Qian et al. 2017). The selective HDAC6 inhibitor ITF3756 was used for this purpose. This study was conducted at the biochemistry laboratory of the BI.N.D Department at the University of Palermo.

To evaluate the efficacy of ITF3756 in colon cancer cells, its effects on cell viability and morphology in the HCT116 and HT29 CRC cell lines were assessed.

The results reported in ***Figure 3A*** show a comparative analysis indicating that the ITF3756 reduces the viability of both cell lines in a dose-dependent manner after 48 hours of treatment. The effect was more pronounced in HCT116 cells, with approximately a 50% reduction in cell viability observed at 5 µM. In contrast, the same concentration produced only about a 25% reduction in cell viability in HT29 cells. Morphological analysis in HCT116 cells revealed that this concentration mainly induced a cytostatic effect with minimal signs of cell death. In contrast, treatment with 7 µM leads to pronounced morphological changes characterized by cell shrinkage, rounding, and detachment from the substrate, reflecting significant cytotoxicity. On the other hand, HT29 appeared to be viable even with 7 µM ITF3756 but reduced in number (***Figure 3B***).

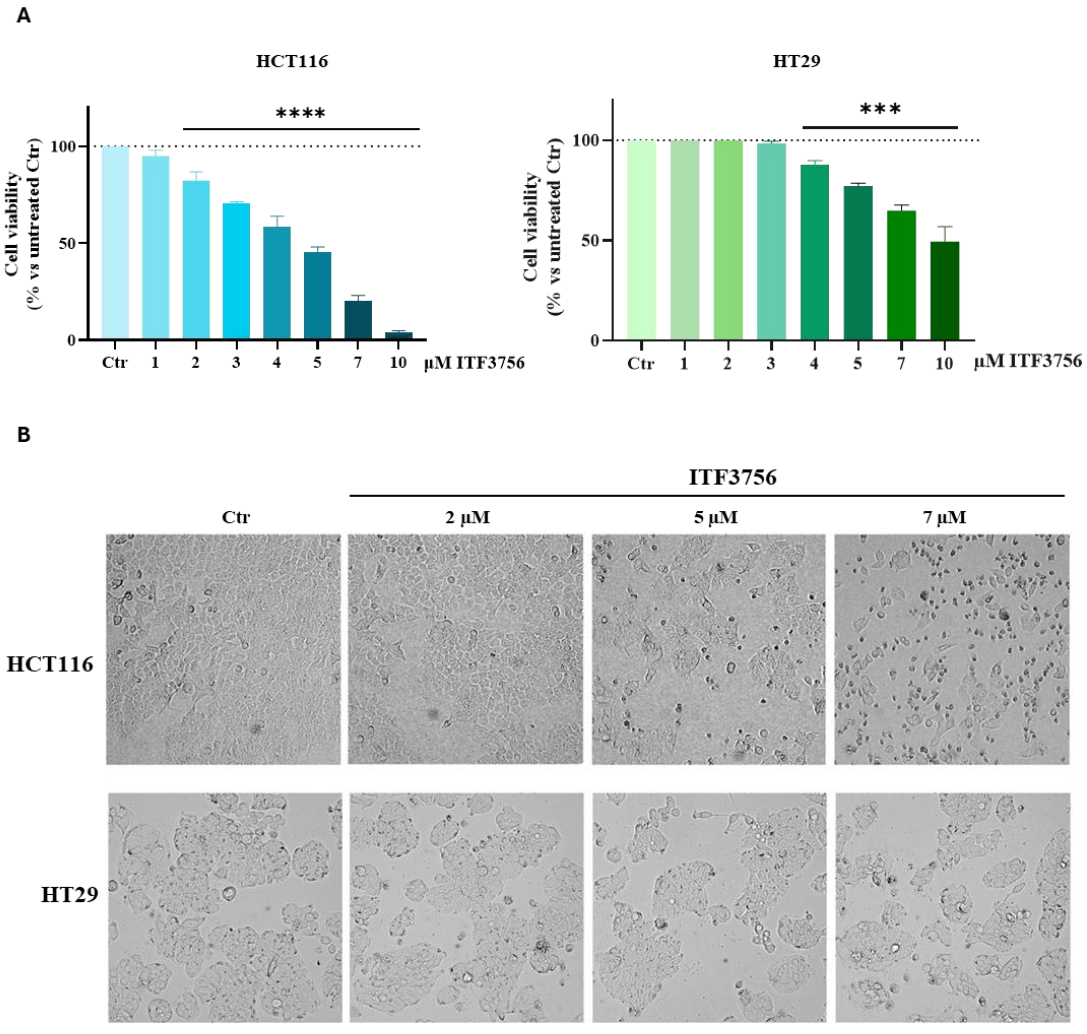

Figure 3. ***The Effects of ITF3756 on colon cancer cell viability and morphology.***

HCT116 and HT29 cells were treated for 48 h with increasing concentrations of ITF3756. Cell viability was evaluated by MTT assay. Data are expressed as cell viability percentages compared to Ctr. The results reported in the graph are the mean ± SD of three independent experiments. Statistical analyses were performed using Ordinary one-way ANOVA with multiple comparison test, *** $p < 0.001$, ****$p < 0.0001$ (**A**). The effect of different concentrations of ITF3756 on cell morphology (**B**) at 48 h treatment is shown. All images were visualized under a light microscope at 200x (morphology) original magnification and acquired by OPTIKA PRO VIEW Digital Camera Software. The images are representative of three independent experiments.

Since selective HDAC6 inhibition can promote lipid accumulation through multiple mechanisms (Qian et al., 2017), ORO staining was performed, a dye that specifically detects LDs in cells. As shown in ***Figure 4A***, HT29 cells display a basal LDs content which was not detected in HCT116 cells. Notably, treatment with the compound induced lipid accumulation in HCT116 cells, which became noticeable at 5 μM and significantly increased at 7 μM ITF3756. Despite the high basal levels of LDs in HT29 cells, treatment with the HDAC6 inhibitor resulted in a further dose-dependent increase. Specifically, LDs were larger than those observed in control cells and exhibited a markedly more intense staining. ImageJ quantification of LDs confirmed these results as reported in the respective histograms (***Figure 4B)***.

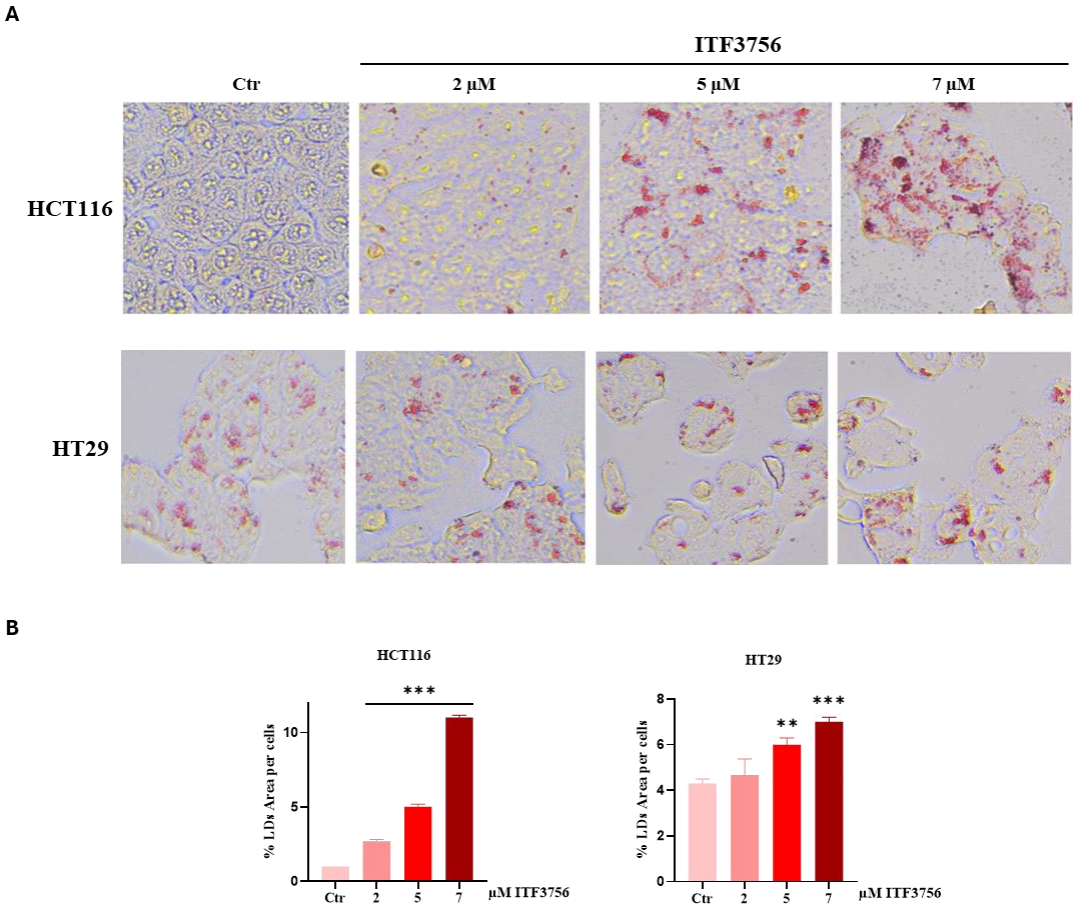

Figure 4. ***Lipid accumulation in colon cancer cells. The effects of ITF3756.***

Representative ORO staining images of HCT116 and HT29 cells treated with increasing concentrations of ITF3756 for 48 h (**A**). The cells were visualized under a light microscope at 400x magnification, and the pictures were acquired by OPTIKA PRO VIEW Digital Camera Software. Representative histograms showing quantification of ORO-stained image area in pixels corrected for cell number by ImageJ software (**B**). Images and histograms are representative of three independent experiments. Statistical analyses were performed using Ordinary one-way ANOVA with multiple comparison test, $^{**}p < 0.01$, $^{***}p < 0.001$.

To clarify the role of lipogenesis and possibly induce a potentiation of the antitumor activity of the HDAC6 inhibitor, combinations with agents that also produce lipid accumulation were considered. Among the lipogenic compounds tested in our laboratory, the proteasome inhibitor bortezomib (BTZ) was selected based on its ability to dose-dependently reduce the viability of both cell lines, even with a different efficacy (***Figure 5A***), and to induce a dramatic LDs accumulation at the active concentration of 10 nM (***Figure 5B-C***).

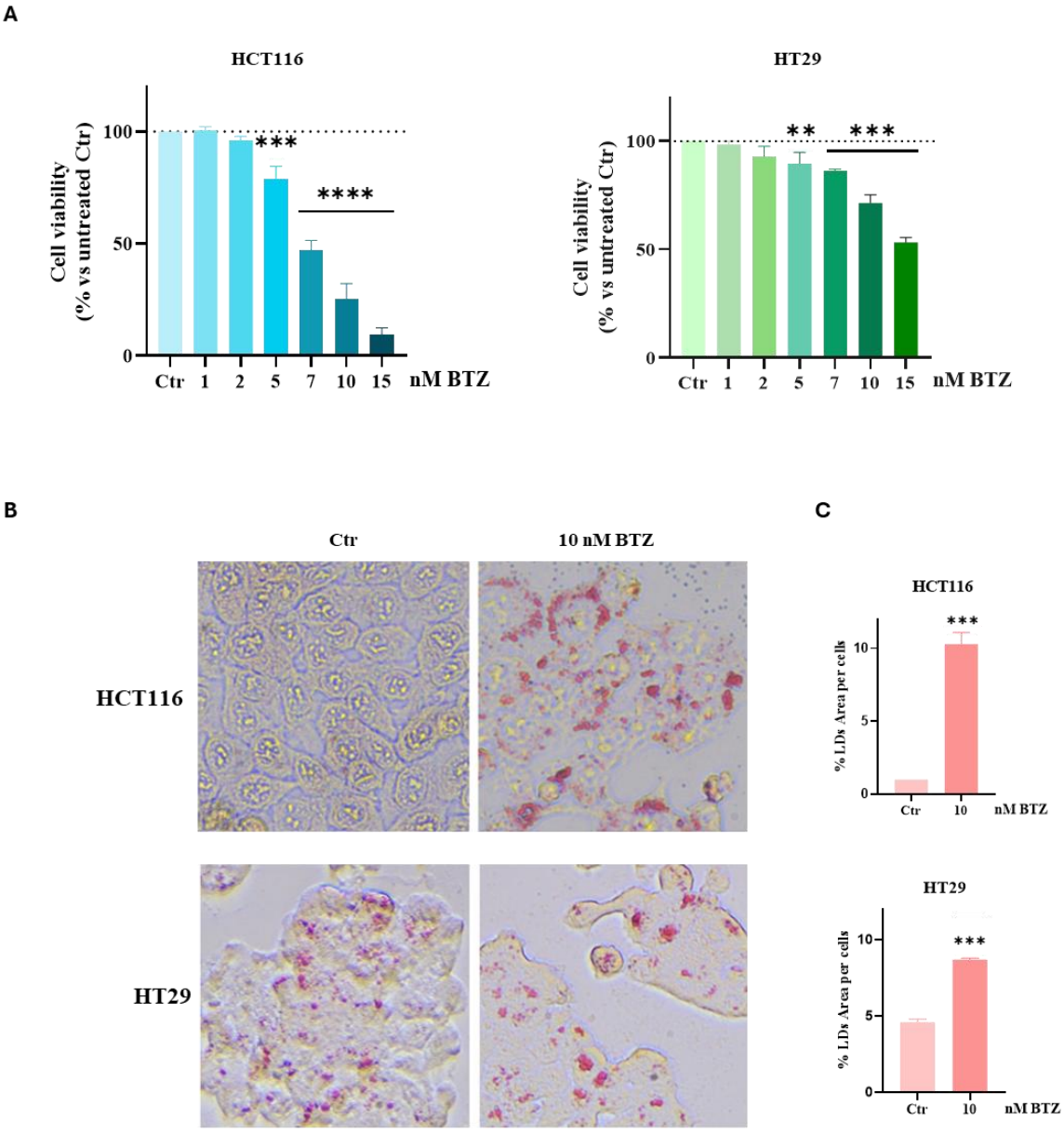

Figure 5. ***The Effects of bortezomib on colon cancer cell viability and lipid accumulation.***

Cell viability was evaluated by MTT assay in HCT116 and HT29 cells treated with different concentrations of BTZ for 48 h (**A**). Data are expressed as cell viability percentages compared to Ctr. The results reported in the graph are the mean ± SD of three independent experiments. Statistical analyses were performed using Ordinary one-way ANOVA with multiple comparison test, ** $p < 0.01$, *** $p < 0.001$, **** $p < 0.0001$.

Representative ORO staining images of HCT116 and HT29 cells treated with BTZ for 48 h (**B**). The cells were visualized under a light microscope at 400x magnification, and the pictures were acquired by OPTIKA PRO VIEW Digital Camera Software (**C**). Representative histograms showing quantification of ORO-stained image area in pixels corrected for cell number by ImageJ software. The images and the histograms are representative of three independent experiments. Statistical analyses were performed using Ordinary one-way ANOVA with multiple comparison test, *** $p < 0.001$.

The combination effects of ITF3756 and bortezomib.

Given that high concentrations of selective HDAC6 inhibitors are often associated with a loss of target specificity and increased cytotoxicity due to off-target effects on other HDAC isoforms (Depetter et al. 2019), subtoxic concentrations of the HDAC6 inhibitor were combined with BTZ. Specifically, 2 μM ITF3756 was used in combination with 5 nM BTZ (***Figures 3A-5A***). The effects of associating the two compounds in both CRC cell lines were thus evaluated. As shown in ***Figure 6A***, the combination of the two compounds results in a dramatic reduction of cell viability (about 70%) after 48 h treatment in HCT116 cells. Notably, the single compounds only slightly reduced cell viability, due to a modest cytostatic effect, as confirmed by morphological analysis. In contrast, cells treated with the combination exhibited clear morphological features of cell death (***Figure 6B***).

HT29 cells also responded to the ITF3756/BTZ combination. However, the effects were less pronounced, as cell viability was reduced by approximately 50% (***Figure 6A***), accompanied by a lower extent of cell death and a predominant decrease in cell number (***Figure 6B***).

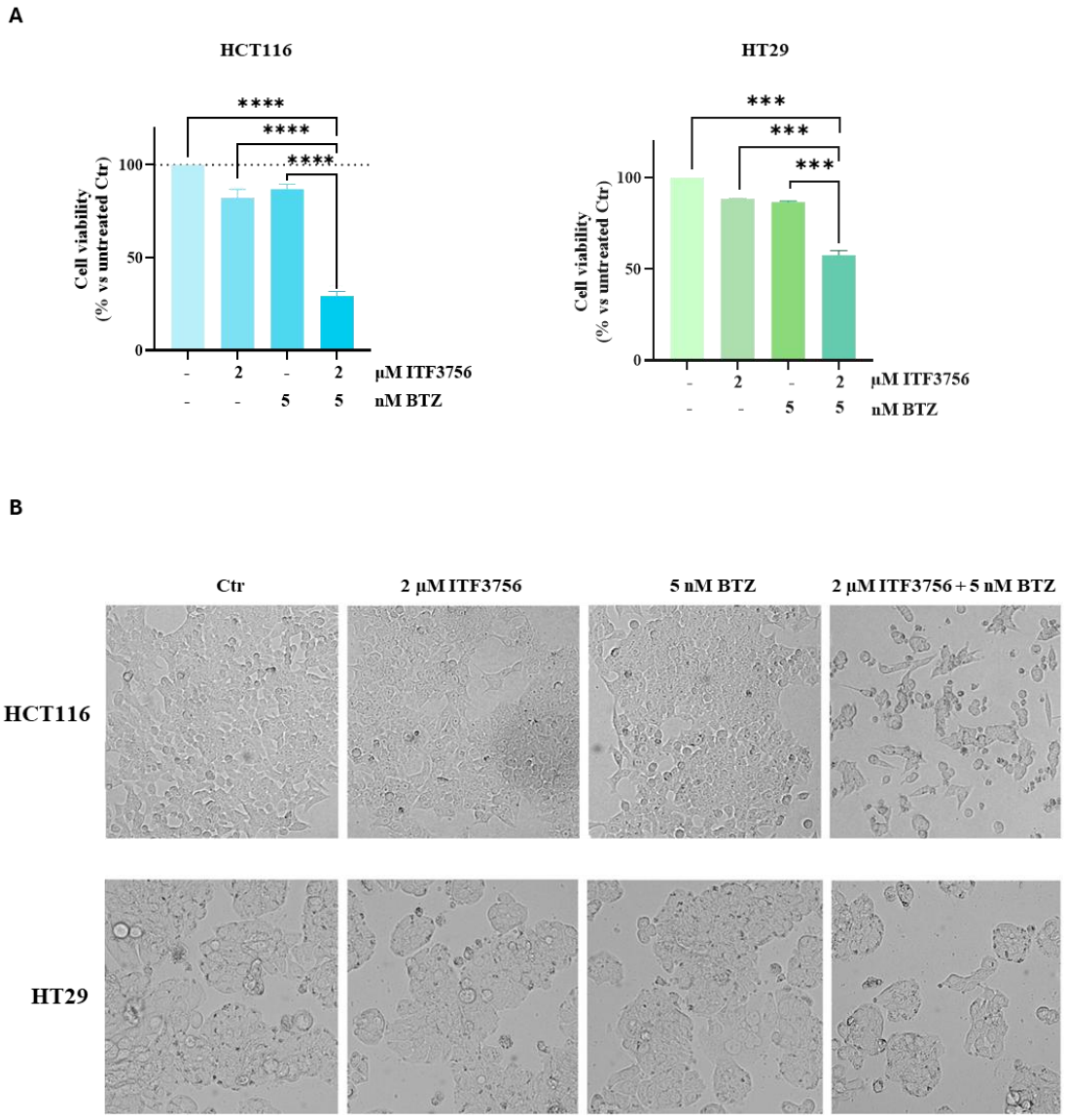

Figure 6. ***The combination effects of ITF3756 and bortezomib in colon cancer cells.***

HCT116 and HT29 cells were treated for 48 h with 2 µM ITF3756 and 5 nM BTZ either alone or in combination. Cell viability was determined by MTT assay. Data are expressed as cell viability percentages compared to Ctr (**A**). Representative morphological images revealing the effects of the ITF3756/BTZ combination. Images were visualized under a light microscope at 200x magnification, and the pictures were acquired by OPTIKA PRO VIEW Digital Camera Software (**B**). The results reported in the graphs are the mean ± SD of three independent experiments. Statistical analyses were performed using two-way ANOVA with multiple comparison test (**A**) and Student's t-test (**B**), *** $p < 0.001$, ****$p < 0.0001$.

Considering the higher susceptibility of HCT116, this cell line was mainly considered for subsequent experiments. To verify the selectivity of ITF3756 toward HDAC6, levels of acetylated α-tubulin, the cytoplasmic HDAC6 substrate, were assessed at the same treatment conditions. The results clearly indicate that 2 µM concentration of the selective HDACi markedly increased α-tubulin acetylation either alone or in combination with BTZ,

confirming the selectivity for HDAC6 inhibition (***Figure 7A***). Subsequently, to test whether the combination of subtoxic doses of ITF3756 and BTZ display a synergistic effect, cell viability was evaluated at different doses in a 3:5 ratio. The results were then analysed using CompuSyn Software for synergism calculation developed by the mathematical model of Chou-Talalay. Data shown in ***Figure 7B*** confirmed that the selective HDAC6 inhibitor and BTZ exerted an evident synergistic effect when used in combination.

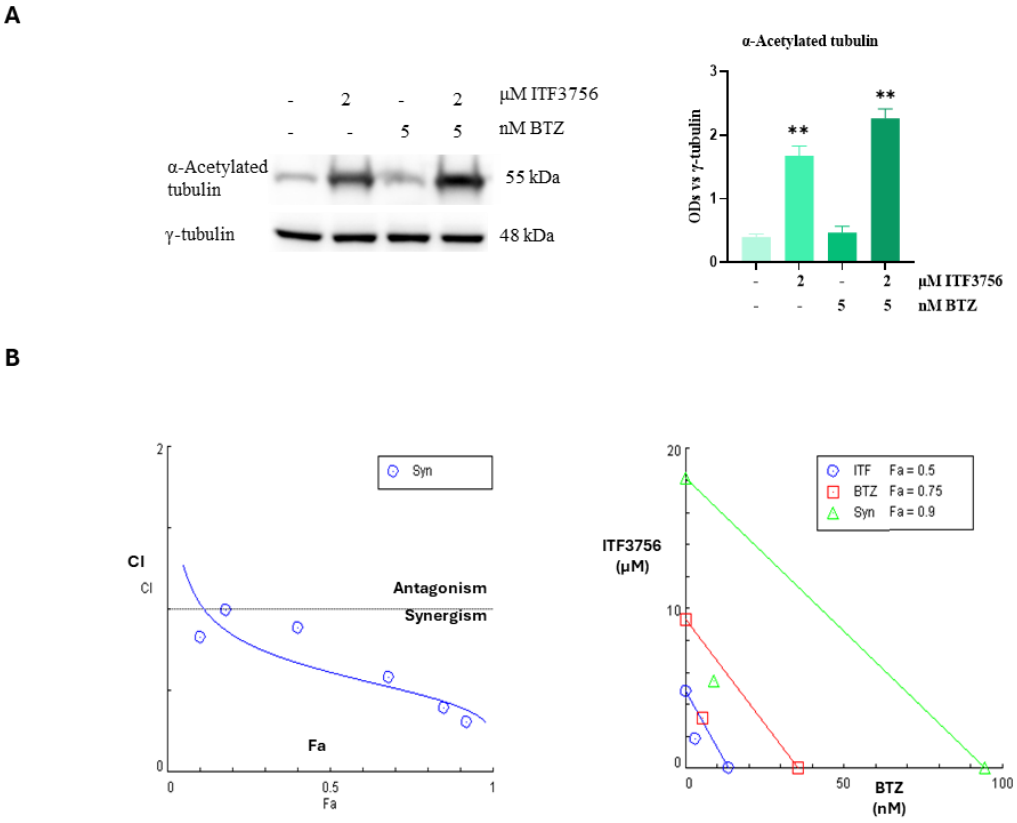

Figure 7. ***The selectivity of HDAC6 inhibition and the synergistic effects of the ITF3756/BTZ combination in HCT116 cells.***

Cells were treated for 48 h with 2 µM ITF3756 and 5 nM BTZ either alone or in combination. Representative images and densitometric analysis of western blots of Acetylated tubulin from HCT116 cells treated with ITF3756 and BTZ either alone or in combination for 48 h. The graphs show the OD (Optical Density) of the indicated proteins normalized for the housekeeping OD (γ-tubulin) (**A**). Data are expressed as the mean ± SD of three independent biological replicates. Statistical analysis was performed using Student's t-test, ** $p < 0.01$. Synergistic effects were evaluated after combining different doses of ITF3756 and BTZ, maintaining 3:5 ratio. The graphs represent the combination index plot (left) and the isobologram (right) obtained using CompuSyn software (**B**). All data are representative of three independent experiments. Abbreviations: CI, combination index; Fa, fraction affected; Syn, synergism.

To confirm this, cell cycle distribution was analysed by flow cytometry. As shown in ***Figures 8A*** and ***8C,*** the combination of 2 µM ITF3756 and 5 nM BTZ increased the percentage of HCT116 cells in the subG0-G1 phase of the cell cycle after 48 h of treatment, indicating DNA fragmentation. To further investigate the nature of cell death suggested by the cell cycle analysis, Annexin V/propidium iodide (PI) staining was performed. The results showed a high percentage of double positivity only with the combination of the two compounds under the same treatment conditions (***Figures 8B*** and ***8D***).

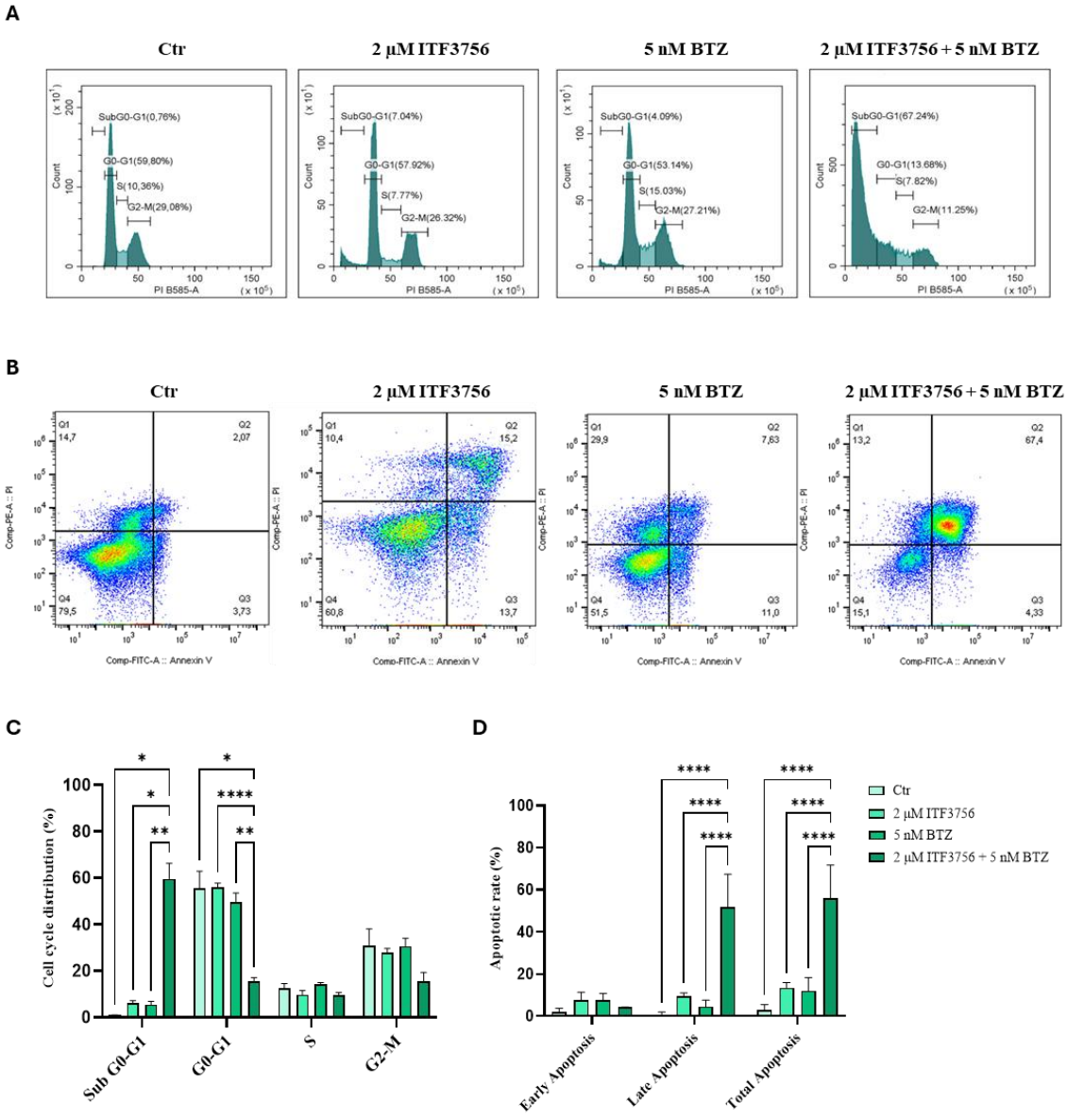

Figure 8. ***Flow cytometric analysis of cell cycle distribution and apoptosis induced by the ITF3756 /bortezomib combination.***

HCT116 cells were treated for 48 h with 2 µM ITF3756 and 5 nM BTZ either alone or in combination. Hypotonic propidium iodide staining or propidium iodide/annexin V double staining was carried out to determine cell cycle distribution (**A**) or apoptosis (**B**). The histograms indicate the percentage of cell cycle

phase distribution (**C**) and the percentage of early apoptotic, late apoptotic, and total apoptotic cells (**D**) compared to Ctr. The results reported in the graphs are the mean ± SD of three independent biological replicates. Statistical analyses were performed using two-way ANOVA with multiple comparison test, *$p <$ 0.05, **$p < 0.01$, ****$p < 0.0001$.

Apoptosis induced by the ITF3756/BTZ combination was also shown to involve the tumor suppressor and pro-apoptotic protein p53, as revealed by western blot at 24 and 48 h (***Figure 9A***). Moreover, the expression level of two apoptotic markers at 48 h of treatment, caspase-3, a key executioner caspase, and PARP-1, a primary caspase-3 substrate**,** was evaluated. As illustrated in **Figures *9B*** and ***9C*,** the combined treatment induced an increase in caspase 3 cleavage, indicating its activation. Concomitantly, a marked increase in cleaved PARP-1 was observed, consistent with caspase-3-mediated apoptosis. These effects were not observed with the single agents alone.

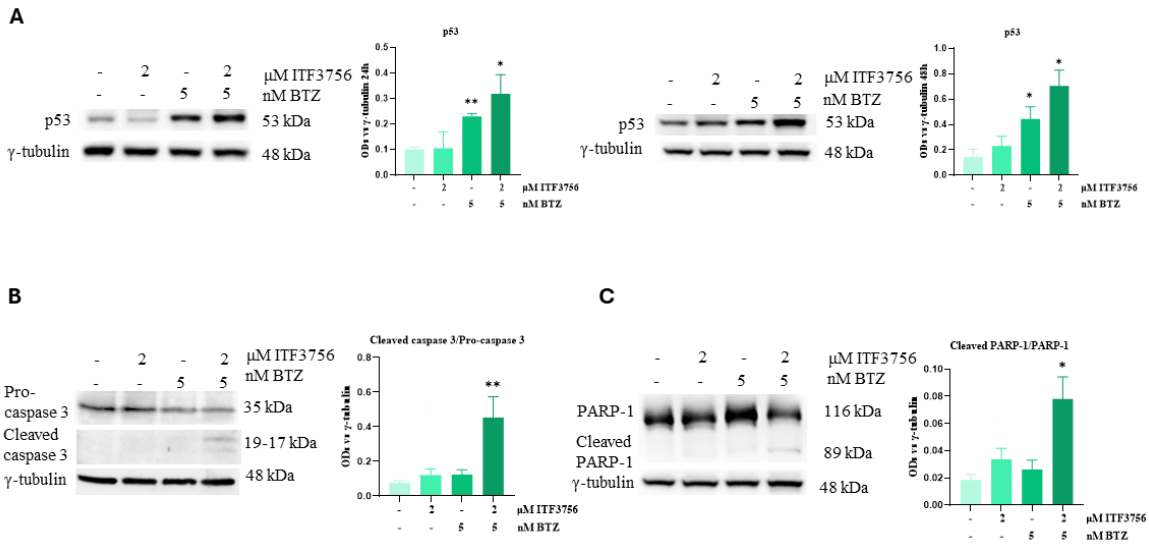

Figure 9. ***The effects of the ITF3756/BTZ combination on apoptotic markers.***
Representative images and densitometric analysis of western blot of p53 (**A**), pro-caspase 3 cleaved caspase 3 (**B**), PARP-1 and cleaved PARP-1 (**C**) from HCT116 cells treated with 2 µM ITF3756 and 5 nM BTZ either alone or in combination for 24 or 48 h (p53) or 48 h (caspase 3 and PARP-1). The graphs show the OD of the indicated proteins normalized for the housekeeping OD (γ-tubulin). Data are expressed as the mean ± SD of three independent biological replicates. Statistical analyses were performed using Student's t-test, * $p < 0.05$, ** $p < 0.01$.

The ITF3756/BTZ combination produces lipid accumulation and SREBP-1 cleavage.

To investigate whether the ITF3756/BTZ combination produces lipid accumulation, ORO staining, as well as a TAGs quantification assay, was performed. As shown in ***Figure 10A***, treatment with the single agents led to a modest increase in LDs formation after 48 h. In contrast, the combination of two compounds induced a much more significant effect,

although the number of cells was reduced due to the combined treatment. Both LDs quantification by ImageJ (***Figure 10B***) and triacylglycerols quantification (***Figure 10C***) confirmed these results. Indeed, the level of the lipids appeared significantly higher with the combination compared to either the control or the single compounds.

Among the key players of lipogenesis, the mammalian target of rapamycin (mTOR), sterol regulating element binding protein 1 (SREBP-1), and peroxisome proliferator-activated receptor gamma (PPARγ) axis have been widely described (C. Cheng et al. 2018; Khan et al. 2024). Interestingly, western blot analysis revealed dramatic phosphorylation of mTOR, which was detected in cells treated with the ITF3756/BTZ combination. One of the key downstream effects of mTORC1 activation is the induction of lipid biosynthesis, largely mediated by SREBP (Sterol Regulatory Element-Binding Protein) transcription factors. Specifically, mTORC1 promotes the processing and nuclear translocation of SREBP-1, allowing it to activate the transcription of lipogenic genes, including *FASN*, *ACC*, and *SCD-1*. Following mTOR activation, the results show a decrease in the levels of the full-length SREBP-1, as well as an increase in the levels of the cleaved and active form (X. Cheng, Li, and Guo 2018). In addition, a modest increase in the levels of PPARγ, another main promoter of TAGs synthesis, was observed (***Figure 10D***). To confirm SREBP-1 activation, the translocation of the cleaved SREBP-1 active fragment was detected in the nucleus of HCT116 cells after treatment with the ITF3756/BTZ combination (***Figure 10E***). A faint band was also present after treatment with the single agents, thus confirming their role in promoting lipogenesis.

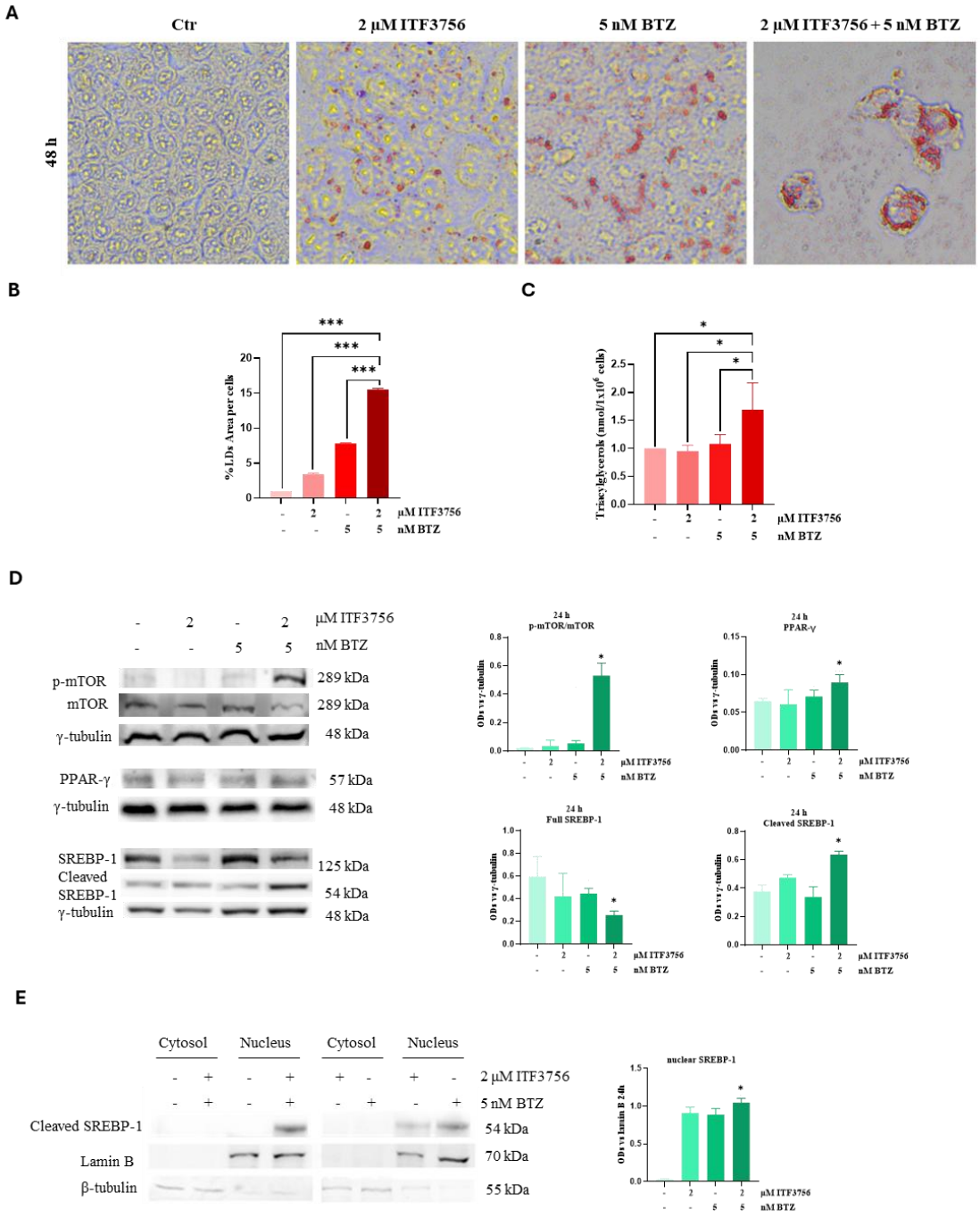

Figure 10. ***The ITF3756/BTZ combination stimulates lipogenesis.***

HCT116 cells were treated with 2 µM ITF3756 and 5 nM BTZ either alone or in combination for 48 h and subjected to ORO staining (**A, B**), triacylglycerol quantification assay (**C**), or western blot analysis (**D**).

For ORO staining, cells were visualized under a light microscope at 400x magnification and the pictures were acquired by OPTIKA PRO VIEW Digital Camera Software. Representative histograms showing quantification of ORO-stained image area in pixels corrected for cell number by ImageJ software (**B**). For triacylglycerol quantification, data are expressed as nmol/10^6 compared to the Ctr. Data are expressed as the mean ± SD of three independent biological replicates. Statistical analyses were performed using two-way ANOVA with multiple comparison test, *$p < 0.05$, ***$p < 0.001$.

Representative images and densitometric analysis of Western Blots of phospho-mTOR (p-mTOR), mTOR, full SREBP-1, cleaved SREBP-1, and PPARγ are shown (**D**). The graphs indicate the OD of the proteins normalized for the housekeeping OD (γ-tubulin). All data are expressed as the mean ± SD of three independent biological replicates. Statistical analyses were performed using Student's t-test, $*p < 0.05$.

Cleaved SREBP-1 subcellular localization (**E**). Representative images and densitometric analysis of western blots obtained from nuclear/cytoplasmic fractions of HCT116 cells treated for 24 h with ITF3756 and BTZ either alone or in combination. The histogram shows the OD of nuclear SREBP-1 normalized for nuclear housekeeping OD (Lamin B). Data are expressed as the mean ± SD of two independent experiments. Statistical analysis was performed using Student's t-test, $*p < 0.05$.

Blocking lipogenesis increases the effects of the combination ITF3756/BTZ.

To gain a deeper understanding of the role of LDs accumulation, lipogenesis inhibitors were used. Specifically, DGAT-1 and DGAT-2 were targeted using specific inhibitors. The results shown in ***Figure 11*** indicate that DGAT-1/2i increased the effect of the ITF3756/BTZ combination. This was observed either by cell viability evaluation (***Figure 11A***) or cell morphology observation (***Figure 11B***). Indeed, co-treatment with ITF3756 and BTZ in the presence of DGAT-1/2i led to a further reduction in cell viability. In contrast, DGAT-1/2i alone caused only a slight decrease in cell number, with most cells remaining viable **(*Figure 11B***). To further confirm the efficacy of DGAT-1/2i, ORO staining demonstrated that the two lipogenesis inhibitors completely prevent the LDs accumulation induced by the ITF3756/BTZ combination (***Figure 11C-D***).

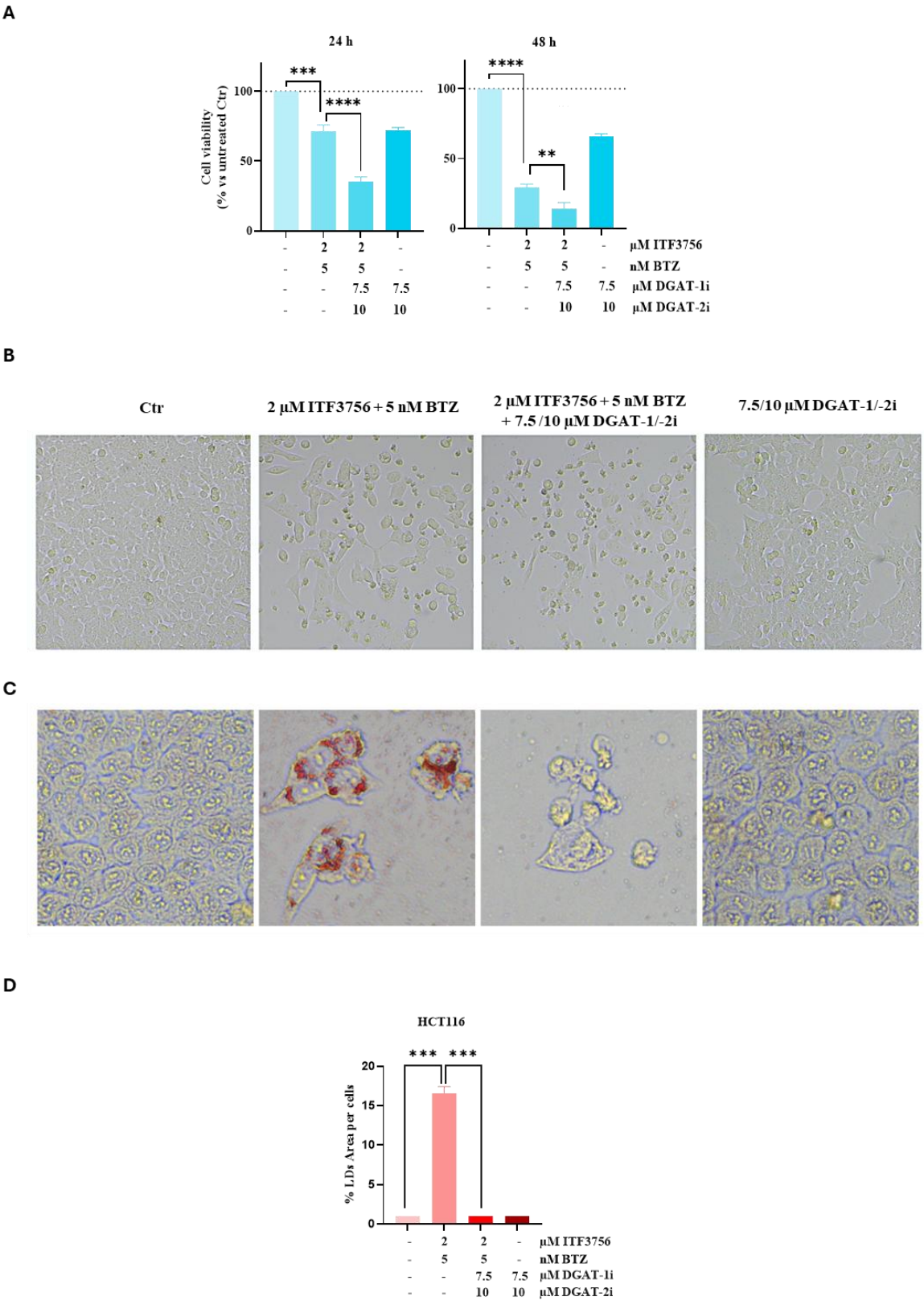

Figure 11. ***DGAT inhibitors prevent lipogenesis and exacerbate the effects of the ITF3756/BTZ combination in the HCT116 cells.***

Cells were pre-treated for 1 h with 7.5 µM A922500 (DGAT-1 inhibitor) and 10 µM PF-06424439 (DGAT-2 inhibitor). Then 2 µM ITF3756 and 5 nM BTZ were added either alone or in combination for an additional 24

or 48 h. Evaluation of cell viability (**A**) and cell morphology (**B**). Treatment with 2 μM ITF3756 or 5 nM BTZ alone did not produce significant modifications (not shown). Data are expressed as cell viability percentages compared to Ctr. Lipid accumulation was evaluated by ORO staining (**C**) after 48 h of treatment. All images were visualized under a light microscope at 200x (morphology) or 400x (ORO staining) original magnification and acquired by OPTIKA PRO VIEW Digital Camera Software. The images are representative of three independent experiments. Representative histograms showing quantification of ORO-stained image area in pixels corrected for cell number by ImageJ software (**D**). The results reported in the graph are the mean ± SD of three independent experiments. Statistical analyses were performed using two-way ANOVA with multiple comparison test, ** $p < 0.01$, *** $p < 0.001$, **** $p < 0.0001$.

To further verify the role of LDs and validate the combination strategy, experiments to inhibit lipogenesis were also performed in HT29 cells. Data reported in ***Figure 12*** indicate that DGAT-1/2i completely abolished lipid accumulation and exacerbated the effects of the ITF3756/BTZ combination, thereby confirming that colon cancer lipogenesis exerts a pro-survival role.

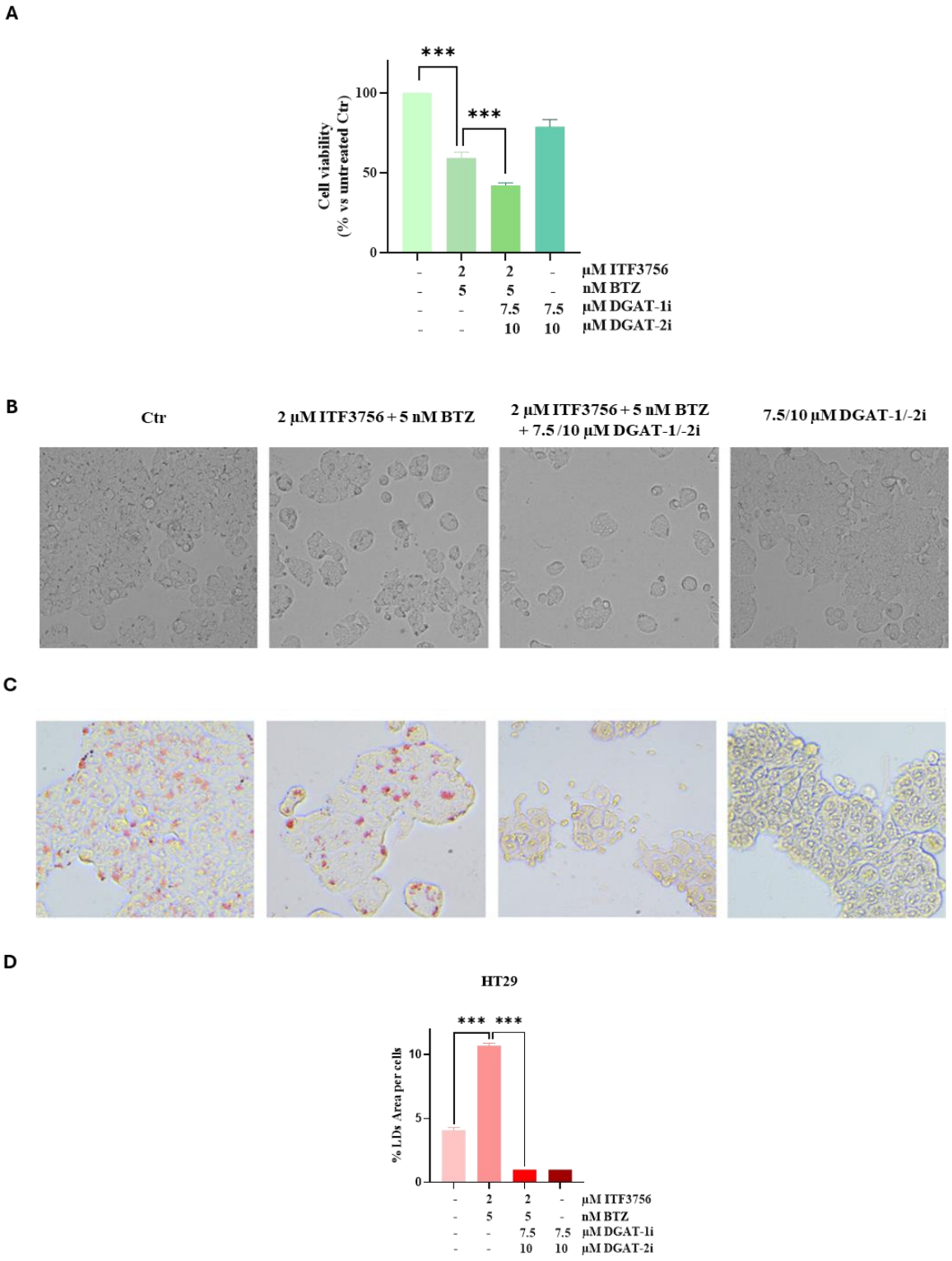

Figure 12. ***DGAT inhibitors prevent lipogenesis and exacerbate the effects of the ITF3756/bortezomib combination in HT29 cells.***

Cells were pre-treated for 1 h with 7.5 µM DGAT-1 inhibitor and 10 µM DGAT-2 inhibitor. Then, 2 µM ITF3756 and 5 nM BTZ were added either alone or in combination for an additional 48 h. Evaluation of cell viability (**A**) and cell morphology (**B**). Treatment with single compounds in the presence of DGAT-1/2i did not produce significant modifications (not shown). Data are expressed as cell viability percentages compared to

Ctr. Lipid accumulation was evaluated by Red Oil O staining (**C**) after 48 h of treatment. Representative histograms showing quantification of ORO-stained image area in pixels corrected for cell number by ImageJ software (**D**). All images were visualized under a light microscope at 200x (**B**) or 400x (**C**) original magnification and acquired by OPTIKA PRO VIEW Digital Camera Software. The images and the graphs are representative of two independent experiments. Statistical analyses were performed using two-way ANOVA with multiple comparison test, *** $p < 0.001$.

Given the role of SREBP-1 in lipogenesis, knockdown of this factor by a specific SREBP-1 siRNA was performed in HCT116 cells to corroborate the data obtained with DGAT-1/2i. As shown in ***Figure 13A***, SREBP-1 siRNA transfection produced a significant reduction in the SREBP-1 protein level. Moreover, the effect of the ITF3756/BTZ combination was more pronounced in SREBP-1-silenced cells compared to scramble control cells, as revealed by morphological analysis (***Figure 13C***) and evaluation of cell viability (***Figure 13B***).

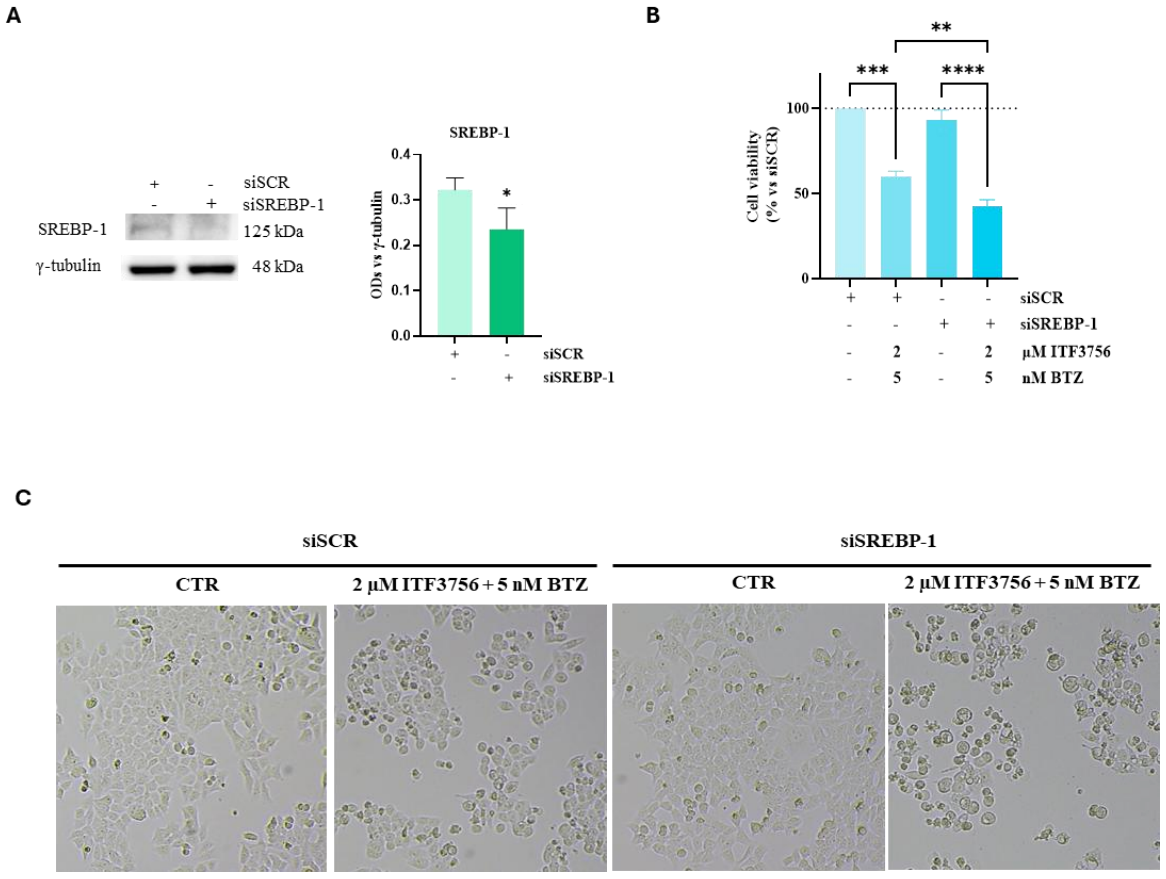

Figure 13. ***SREBP-1 silencing increased the effects of the ITF3756/BTZ combination.***
HCT116 cells were transfected for 16 h with 80 pmol/cm^2 of Silencer® Select SREBP-1 (siSREBP-1), or Silencer® Select Negative Control (siSCR). The silencing efficiency was determined by SREBP-1 western blot (**A**). After transfection, the cells were treated with 2 μM ITF3756 and 5 nM BTZ in combination and subjected to cell viability (**B**) and cell morphology (**C**) evaluation. Data are expressed as cell viability percentages compared to siSCR control. The results reported in the graphs are the mean ± SD of three independent experiments. Statistical analyses were performed using Student's t-test (**A**) and two-way ANOVA

with multiple comparison test (**B**), * $p < 0.05$, **$p < 0.01$, *** $p < 0.001$, **** $p < 0.0001$. Images were visualized under a light microscope at 200x magnification, and the pictures were acquired by OPTIKA PRO VIEW Digital Camera Software and they are representative of three independent experiments.

Discussion and conclusion

Pan-HDACis have shown considerable promise as anti-tumor agents, largely due to their multifaceted effects on cell proliferation, apoptosis, and metabolic pathways. In this study, the treatment with the epigenetic compound ITF2357 (Givinostat) reduces cell viability and promotes lipid accumulation by stimulating *de novo* lipogenesis but also enhancing lipid storage and uptake in the HCT116 CRC cell line, highlighting the link between HDAC inhibition and lipid metabolic reprogramming. Specifically, Givinostat upregulated lipogenic factors, including SREBP-1, CD36, PLIN2, DGAT-1, and DGAT-2. Preliminary data seem to indicate that lipogenesis induced by Givinostat has a pro-survival function, since DGAT-1/2 and CD36 inhibitors increased the antitumor efficacy of the compound. The combination of ITF2357 and DGAT-1/2i produced a decrease in cellular viability, but not as marked as expected. However, when ω-3 polyunsaturated FA DHA was supplemented, an even more pronounced decrease in viability was observed.

DHA, being a highly unsaturated FA, is particularly susceptible to lipid peroxidation. When incorporated into cellular membranes, its high degree of unsaturation promotes the formation of lipid hydroperoxides, which can accumulate and trigger ferroptotic cell death, an oxidative-dependent process (Salita et al. 2022).

Additionally, treatment with DHA alone resulted in a marked reduction in cell viability, consistent with its detrimental role. Interestingly, co-treatment with DHA and ITF2357 leads to only a modest additional decrease in viability compared to DHA alone. Presumably, this response depends on the initial incorporation of DHA into LDs, which function as a protective mechanism by sequestering potentially toxic FAs. As demonstrated by Dierge et al., when DHA is supplemented, cells can initially sequester it in LDs, reducing its incorporation into membranes and mitigating its cytotoxic effects. However, when DGAT-1/2i are added to the ITF2357/DHA combination, triglyceride synthesis is blocked, preventing DHA storage in LDs. As a result, DHA is directed into membranes, where its susceptibility to peroxidation leads to oxidative damage and possibly ferroptosis. As supporting data are not presently available, this hypothesis provides a rationale for future studies.

Taken together, these findings strongly support the hypothesis that, in this context, lipogenesis and LDs formation serve as critical pro-survival mechanisms. Moreover, these data highlight the therapeutic potential of combining HDAC inhibitors with DHA supplementation to sensitize tumor cells to ferroptosis and improve anti-cancer efficacy.

This work also provides evidence that the selective HDAC6 inhibitor ITF3756 exerts a synergistic antitumor effect when combined with the proteasome inhibitor BTZ. Although previous studies have reported that selective HDAC6 inhibition can enhance the anticancer efficacy of BTZ, a precise mechanism has not been described. Most papers attribute this synergistic interaction to a stress condition resulting from proteasome inhibition and impaired aggresome formation, a cellular structure that sequesters misfolded or non-degraded proteins. In particular, Huang et al. demonstrated that combined treatment with an HDAC6 inhibitor and BTZ could increase the accumulation of ubiquitinated proteins and enhance BTZ-induced cell cytotoxicity, thereby leading to caspase-dependent apoptosis in multiple myeloma (MM) cells. Mechanistically, they proposed that HDAC6 inhibition prevents the interaction between HDAC6 and dynein, a cytoskeletal motor protein, thereby blocking the transport of misfolded proteins to the aggresome. It is not surprising that most studies describing the synergistic interaction between HDAC6 inhibitors and BTZ have been conducted in multiple myeloma (MM) cells, as BTZ is the first FDA-approved proteasome inhibitor for the treatment of MM at various disease stages (Sogbein et al. 2024; Park, Cho, et Song 2020). However, the clinical application in solid tumors has been restricted by adverse effects, such as nephrotoxicity and peripheral neuropathy (Sogbein et al. 2024). Consistent with this evidence, few clinical studies have investigated the efficacy of BTZ in colorectal cancer treatment, reflecting the challenges associated with this drug in solid tumors (Feng et al. 2022; Mao et al. 2024). Nevertheless, some pre-clinical studies encourage the association of BTZ with other antitumor agents in colon cancer models to get synergistic effects (Caldiran et al. 2023; Qing et al. 2021). Indeed, this combination strategy is considered particularly promising to lower drug doses while minimizing side effects in vivo. This work represents the first evidence that an HDAC6 inhibitor exerts a synergistic apoptotic effect with BTZ in colon cancer cells. Specifically, ITF3756, a selective HDAC6 inhibitor produced by Italfarmaco, was used. HDAC6 is a unique HDAC member that deacetylates cellular proteins regulating the cell fate (Zheng et al. 2023) and has recently emerged as an intriguing antitumor target (Oliveira-Silva et al. 2025). Considering the involvement of HDAC6 in lipid metabolism, the original idea was to block HDAC6 to clarify the effects on lipogenesis in colon cancer cells. To this purpose, the study was conducted in two colon cancer cell lines, HCT116 and HT29, that differ in HDAC6 expression levels (Zhang et al. 2019b) and may also display different lipid metabolism profiles. Our findings show that HT29 cells display a higher basal content of LDs compared with HCT116 cells and are less responsive to HDAC6 inhibition, either alone or in combination with BTZ. Both

compounds, ITF3756 and BTZ, were able to enhance lipogenesis when used alone at active concentrations or in combination at subtoxic doses.

Given the higher susceptibility of HCT116 cells, attention was focused on this cell line to characterise the cell death mechanism. Combination of the two compounds at sub-toxic doses resulted in a synergistic apoptotic effect, as evidenced by annexin V positivity and activation of apoptotic markers. It is interesting to note that apoptosis was accompanied by p53 increase, a well-known tumor suppressor and proapoptotic factor, which is wild type in HCT116 and mutated in HT29 cells, a condition that may further explain the different response of the two cell lines (Abu El Maaty et al. 2017). Additionally, the ITF3756/BTZ combination induces a dramatic increase in LDs accumulation, evidenced either by ORO staining, quantification of triacylglycerols, and activation of lipogenesis markers, including phospho-mTOR, SREBP-1, and PPARγ. SREBP-1 is well known to exert a crucial role in lipogenesis. Specifically, cleaved SREBP-1, which is the active form, acts as a transcription factor regulating genes related to cholesterol biosynthesis, FAs synthesis, and lipid production. The nuclear localization of cleaved SREBP-1 in HCT116 confirmed its involvement in the lipogenic action of the ITF3756/BTZ combination. Lipogenesis is known to exert a double role in tumor cells. On the one hand, it represents a key metabolic hallmark of cancer, supporting tumor cell survival and progression (Mounier, Bouraoui, et Rassart 2014). On the other hand, excessive lipid accumulation can trigger lipophagy, the process of autophagic degradation of LDs and a form of cell death that can be exploited to target tumor cells (Xu et al. 2016; Mukhopadhyay et al. 2017). The results of this study indicate that lipogenesis induced by the ITF3756/BTZ combination plays a pro-survival role. Indeed, inhibition of lipogenesis, either through DGAT inhibitors or SREBP-1 silencing, potentiates the antitumor efficacy of the combination. Interestingly, these effects were observed in both HCT116 and HT29 cells, thereby reinforcing the hypothesis of the pro-survival role of lipogenesis. These data are in accordance with the findings of Wang et al., who found that SREBP-1 silencing inhibits the proliferation of human oesophageal squamous carcinoma cells. The pro-tumorigenic role of SREBP-1 has also been documented in other cancer types, including renal cell carcinoma (Shen et al. 2019) and non-small cell lung cancer (Tiong et al. 2022). A recent review by He et al. summarizes the mechanisms through which SREBP-1 contributes to cancer progression and chemoresistance, while Zhao et al. have highlighted SREBP-1 targeting as a potential therapeutic strategy in oncology.

Overall, this thesis demonstrated that targeting lipogenesis enhances the pro-apoptotic effects of both pan-HDAC inhibitors and the selective HDAC6 inhibitor when combined

with BTZ. Therefore, these data highlight the therapeutic potential of combining HDAC inhibitors with strategies that modulate lipid metabolism, including DHA supplementation, to enhance anticancer efficacy. Collectively, this work provides a strong rationale for the development of combinatorial approaches that target both epigenetic regulation and lipid metabolic pathways, offering a potentially innovative avenue for clinical intervention in colon cancer. Obviously, the clinical feasibility of combining DGAT inhibitors/SREBP-1-targeted drugs with ITF3756/BTZ is beyond the scope of this work, which represents a preliminary *in vitro* evaluation. Encouraging data support the clinical use of either selective HDAC6 inhibitors (Amengual et al. 2021) or DGAT inhibitors (Deng et al. 2024) as anti-tumor agents. According to our observations, pre-treatment with DGAT-1 and DGAT-2 inhibitors together guarantees complete blockage of lipogenesis, suggesting a hypothetical sequence of administration. However, clinical evaluations and toxicity profiles remain to be determined.

In a pre-clinical scenario, future perspectives include to evaluate the co-treatment of CRC cells with polyunsaturated fatty acids in order to engulf LDs and to verify the induction of ferroptosis, a type of programmed cell death specifically induced by lipid peroxidation.

References

Abu El Maaty, Mohamed A., Wendy Strassburger, Tooba Qaiser, Yasamin Dabiri, e Stefan Wölfl. 2017. «Differences in P53 Status Significantly Influence the Cellular Response and Cell Survival to 1,25-dihydroxyvitamin D3-metformin Cotreatment in Colorectal Cancer Cells». *Molecular Carcinogenesis* 56(11):2486–98. doi:10.1002/mc.22696.

Amengual, Jennifer E., Jennifer K. Lue, Helen Ma, Renee Lichtenstein, Bijal Shah, Serge Cremers, Simon Jones, e Ahmed Sawas. 2021. «First-in-Class Selective HDAC6 Inhibitor (ACY-1215) Has a Highly Favorable Safety Profile in Patients with Relapsed and Refractory Lymphoma». *The Oncologist* 26(3):184-e366. doi:10.1002/onco.13673.

American Cancer Society. s.d.

An, Sanghyun, e Sungjin Park. 2022. «Association of Physical Activity and Sedentary Behavior With the Risk of Colorectal Cancer». *Journal of Korean Medical Science* 37(19):e158. doi:10.3346/jkms.2022.37.e158.

Aran, Veronica, Ana Paula Victorino, Luiz Claudio Thuler, e Carlos Gil Ferreira. 2016. «Colorectal Cancer: Epidemiology, Disease Mechanisms and Interventions to Reduce Onset and Mortality». *Clinical Colorectal Cancer* 15(3):195–203. doi:10.1016/j.clcc.2016.02.008.

Argilés, G., J. Tabernero, R. Labianca, D. Hochhauser, R. Salazar, T. Iveson, P. Laurent-Puig, P. Quirke, T. Yoshino, J. Taieb, E. Martinelli, e D. Arnold. 2020. «Localised Colon Cancer: ESMO Clinical Practice Guidelines for Diagnosis, Treatment and Follow-Up». *Annals of Oncology* 31(10):1291–1305. doi:10.1016/j.annonc.2020.06.022.

Barna, Robert, Alis Dema, Aura Jurescu, Adrian Ovidiu Văduva, Dorela-Codruța Lăzureanu, Octavia Vița, Bianca Natarâș, Ioana Hurmuz, Adelina Vidac, Sorina Tăban, e Sorin Dema. 2025. «The Relevance of Sex and Age as Non-Modifiable Risk Factors in Relation to Clinical-Pathological Parameters in Colorectal Cancer». *Life* 15(2):156. doi:10.3390/life15020156.

Baxter, Nancy N., e Jose G. Guillem. 2007. «Colorectal Cancer: Epidemiology, Etiology, and Molecular Basis». Pp. 335–52 in *The ASCRS Textbook of Colon and Rectal Surgery*, a cura di B. G. Wolff, J. W. Fleshman, D. E. Beck, J. H. Pemberton, S. D. Wexner, J. M. Church, J. Garcia-Aguilar, P. L. Roberts, T. J. Saclarides, e M. J. Stamos. New York, NY: Springer New York.

Behnisch-Cornwell, Steven, Christoph W. Grathwol, Lukas Schulig, Anika Voigt, Daniel Baecker, Andreas Link, e Patrick J. Bednarski. 2021. «Correlation Analysis of Protein Expression of 10 HDAC/Sirtuin Isoenzymes with Sensitivities of 23 Anticancer Drugs in 17 Cancer Cell Lines and Potentiation of Drug Activity by Co-Treatment with HDAC Inhibitors». *Cancers* 14(1):187. doi:10.3390/cancers14010187.

Bray, Freddie, Jacques Ferlay, Isabelle Soerjomataram, Rebecca L. Siegel, Lindsey A. Torre, e Ahmedin Jemal. 2018. «Global Cancer Statistics 2018: GLOBOCAN Estimates of Incidence and Mortality Worldwide for 36 Cancers in 185 Countries». *CA: A Cancer Journal for Clinicians* 68(6):394–424. doi:10.3322/caac.21492.

Caldiran, Feyzanur, Caglar Berkel, Esra Yilmaz, Burak Kucuk, Aslihan Hatun Cacan, Senol Citli, Emel Canpolat, e Ercan Cacan. 2023. «Combination Treatment of Bortezomib and Epirubicin Increases the Expression of TNFRSF10 A/B, and Induces TRAIL-Mediated Cell Death in Colorectal Cancer Cells». *Biochemical and Biophysical Research Communications* 675:33–40. doi:10.1016/j.bbrc.2023.06.015.

Celesia, Adriana, Marzia Franzò, Diana Di Liberto, Marianna Lauricella, Daniela Carlisi, Antonella D'Anneo, Antonietta Notaro, Mario Allegra, Michela Giuliano, e Sonia Emanuele. 2023.

«Oncogenic BRAF and P53 Interplay in Melanoma Cells and the Effects of the HDAC Inhibitor ITF2357 (Givinostat)». *International Journal of Molecular Sciences* 24(11):9148. doi:10.3390/ijms24119148.

Chen, Jiandong. 2016. «The Cell-Cycle Arrest and Apoptotic Functions of P53 in Tumor Initiation and Progression». *Cold Spring Harbor Perspectives in Medicine* 6(3):a026104. doi:10.1101/cshperspect.a026104.

Chen, Kabytto, Geoffrey Collins, Henry Wang, e James Wei Tatt Toh. 2021. «Pathological Features and Prognostication in Colorectal Cancer». *Current Oncology (Toronto, Ont.)* 28(6):5356–83. doi:10.3390/curroncol28060447.

Cheng, Chunming, Feng Geng, Xiang Cheng, e Deliang Guo. 2018. «Lipid Metabolism Reprogramming and Its Potential Targets in Cancer». *Cancer Communications (London, England)* 38(1):27. doi:10.1186/s40880-018-0301-4.

Cheng, Xiang, Jianying Li, e Deliang Guo. 2018. «SCAP/SREBPs Are Central Players in Lipid Metabolism and Novel Metabolic Targets in Cancer Therapy». *Current Topics in Medicinal Chemistry* 18(6):484–93. doi:10.2174/1568026618666180523104541.

Chou, Ting-Chao. 2010. «Drug Combination Studies and Their Synergy Quantification Using the Chou-Talalay Method». *Cancer Research* 70(2):440–46. doi:10.1158/0008-5472.CAN-09-1947.

Chung, Samantha S., Sara I. Ali, e Brooks D. Cash. 2022. «The Present and Future of Colorectal Cancer Screening». *Gastroenterology & Hepatology* 18(11):646–53.

Colon and Rectal Polyps, University of Michigan Health, 2025. s.d.

Cremolini, C., F. Loupakis, G. Masi, S. Lonardi, C. Granetto, M. L. Mancini, S. Chiara, R. Moretto, D. Rossini, S. Vitello, G. Allegrini, G. Tonini, F. Bergamo, G. Tomasello, M. Ronzoni, A. Buonadonna, S. Bustreo, C. Barbara, L. Boni, e A. Falcone. 2016. «FOLFOXIRI or FOLFOXIRI plus Bevacizumab as First-Line Treatment of Metastatic Colorectal Cancer: A Propensity Score-Adjusted Analysis from Two Randomized Clinical Trials». *Annals of Oncology: Official Journal of the European Society for Medical Oncology* 27(5):843–49. doi:10.1093/annonc/mdw052.

Dávalos-Salas, Mercedes, Magdalene K. Montgomery, Camilla M. Reehorst, Rebecca Nightingale, Irvin Ng, Holly Anderton, Sheren Al-Obaidi, Analia Lesmana, Cameron M. Scott, Paul Ioannidis, Hina Kalra, Shivakumar Keerthikumar, Lars Tögel, Angela Rigopoulos, Sylvia J. Gong, David S. Williams, Prusoth Yoganantharaja, Kim Bell-Anderson, Suresh Mathivanan, Yann Gibert, Scott Hiebert, Andrew M. Scott, Matthew J. Watt, e John M. Mariadason. 2019. «Deletion of Intestinal Hdac3 Remodels the Lipidome of Enterocytes and Protects Mice from Diet-Induced Obesity». *Nature Communications* 10(1):5291. doi:10.1038/s41467-019-13180-8.

De Rosa, Marina, Ugo Pace, Daniela Rega, Valeria Costabile, Francesca Duraturo, Paola Izzo, e Paolo Delrio. 2015. «Genetics, Diagnosis and Management of Colorectal Cancer (Review)». *Oncology Reports* 34(3):1087–96. doi:10.3892/or.2015.4108.

Del Bufalo, Donatella, Marianna Desideri, Teresa De Luca, Marta Di Martile, Chiara Gabellini, Valentina Monica, Simone Busso, Adriana Eramo, Ruggero De Maria, Michele Milella, e Daniela Trisciuoglio. 2014. «Histone Deacetylase Inhibition Synergistically Enhances Pemetrexed Cytotoxicity through Induction of Apoptosis and Autophagy in Non-Small Cell Lung Cancer». *Molecular Cancer* 13:230. doi:10.1186/1476-4598-13-230.

Deng, Boer, Weimin Kong, Xiaochang Shen, Chao Han, Ziyi Zhao, Shuning Chen, Chunxiao Zhou, e Victoria Bae-Jump. 2024. «The Role of DGAT1 and DGAT2 in Regulating Tumor Cell Growth and

Their Potential Clinical Implications». *Journal of Translational Medicine* 22(1):290. doi:10.1186/s12967-024-05084-z.

Depetter, Yves, Silke Geurs, Rob De Vreese, Sophie Goethals, Elien Vandoorn, Alien Laevens, Jonas Steenbrugge, Evelyne Meyer, Pascal de Tullio, Marc Bracke, Matthias D'hooghe, e Olivier De Wever. 2019. «Selective Pharmacological Inhibitors of HDAC6 Reveal Biochemical Activity but Functional Tolerance in Cancer Models». *International Journal of Cancer* 145(3):735–47. doi:10.1002/ijc.32169.

Di Martile, Marta, Marianna Desideri, Maria Grazia Tupone, Simonetta Buglioni, Barbara Antoniani, Carlotta Mastroiorio, Rita Falcioni, Virginia Ferraresi, Nicola Baldini, Roberto Biagini, Michele Milella, Daniela Trisciuoglio, e Donatella Del Bufalo. 2018. «Histone Deacetylase Inhibitor ITF2357 Leads to Apoptosis and Enhances Doxorubicin Cytotoxicity in Preclinical Models of Human Sarcoma». *Oncogenesis* 7(2):20. doi:10.1038/s41389-018-0026-x.

Dierge, Emeline, Elena Debock, Céline Guilbaud, Cyril Corbet, Eric Mignolet, Louise Mignard, Estelle Bastien, Chantal Dessy, Yvan Larondelle, e Olivier Feron. 2021. «Peroxidation of N-3 and n-6 Polyunsaturated Fatty Acids in the Acidic Tumor Environment Leads to Ferroptosis-Mediated Anticancer Effects». *Cell Metabolism* 33(8):1701-1715.e5. doi:10.1016/j.cmet.2021.05.016.

Doncheva, Atanaska I., Yuchuan Li, Prabhat Khanal, Marit Hjorth, Svein O. Kolset, Frode A. Norheim, Alan R. Kimmel, e Knut Tomas Dalen. 2023. «Altered Hepatic Lipid Droplet Morphology and Lipid Metabolism in Fasted Plin2-Null Mice». *Journal of Lipid Research* 64(12):100461. doi:10.1016/j.jlr.2023.100461.

Dorotea, Debra, Daisuke Koya, e Hunjoo Ha. 2020. «Recent Insights Into SREBP as a Direct Mediator of Kidney Fibrosis via Lipid-Independent Pathways». *Frontiers in Pharmacology* 11:265. doi:10.3389/fphar.2020.00265.

Drury, James, Piotr G. Rychahou, Daheng He, Naser Jafari, Chi Wang, Eun Y. Lee, Heidi L. Weiss, Bernard Mark Evers, e Yekaterina Y. Zaytseva. 2020. «Inhibition of Fatty Acid Synthase Upregulates Expression of CD36 to Sustain Proliferation of Colorectal Cancer Cells». *Frontiers in Oncology* 10:1185. doi:10.3389/fonc.2020.01185.

Drury, James, Piotr G. Rychahou, Courtney O. Kelson, Mariah E. Geisen, Yuanyuan Wu, Daheng He, Chi Wang, Eun Y. Lee, B. Mark Evers, e Yekaterina Y. Zaytseva. 2022. «Upregulation of CD36, a Fatty Acid Translocase, Promotes Colorectal Cancer Metastasis by Increasing MMP28 and Decreasing E-Cadherin Expression». *Cancers* 14(1):252. doi:10.3390/cancers14010252.

Ecker, Josef, Elisa Benedetti, Alida S. D. Kindt, Marcus Höring, Markus Perl, Andrea Christel Machmüller, Anna Sichler, Johannes Plagge, Yuting Wang, Sebastian Zeissig, Andrej Shevchenko, Ralph Burkhardt, Jan Krumsiek, Gerhard Liebisch, e Klaus-Peter Janssen. 2021. «The Colorectal Cancer Lipidome: Identification of a Robust Tumor-Specific Lipid Species Signature». *Gastroenterology* 161(3):910-923.e19. doi:10.1053/j.gastro.2021.05.009.

Eckschlager, Tomas, Johana Plch, Marie Stiborova, e Jan Hrabeta. 2017. «Histone Deacetylase Inhibitors as Anticancer Drugs». *International Journal of Molecular Sciences* 18(7):1414. doi:10.3390/ijms18071414.

Emanuele, S., M. Lauricella, D. Carlisi, B. Vassallo, A. D'Anneo, P. Di Fazio, R. Vento, e G. Tesoriere. 2007. «SAHA Induces Apoptosis in Hepatoma Cells and Synergistically Interacts with the Proteasome Inhibitor Bortezomib». *Apoptosis* 12(7):1327–38. doi:10.1007/s10495-007-0063-y.

Fang, Minggang, Jianhong Ou, Lloyd Hutchinson, e Michael R. Green. 2014. «The BRAF Oncoprotein Functions through the Transcriptional Repressor MAFG to Mediate the CpG Island Methylator Phenotype». *Molecular Cell* 55(6):904–15. doi:10.1016/j.molcel.2014.08.010.

Feng, Xuejia, Gui Yang, Litian Zhang, Shishi Tao, Joong Sup Shim, Liang Chen, e Qingxia Wu. 2022. «TRIM59 Guards ER Proteostasis and Prevents Bortezomib-Mediated Colorectal Cancer (CRC) Cells' Killing». *Investigational New Drugs* 40(6):1244–53. doi:10.1007/s10637-022-01306-7.

Ferrara, Napoleone, Kenneth J. Hillan, e William Novotny. 2005. «Bevacizumab (Avastin), a Humanized Anti-VEGF Monoclonal Antibody for Cancer Therapy». *Biochemical and Biophysical Research Communications* 333(2):328–35. doi:10.1016/j.bbrc.2005.05.132.

Fujita, Ken-ichi, Yutaro Kubota, Hiroo Ishida, e Yasutsuna Sasaki. 2015. «Irinotecan, a Key Chemotherapeutic Drug for Metastatic Colorectal Cancer». *World Journal of Gastroenterology* 21(43):12234–48. doi:10.3748/wjg.v21.i43.12234.

Gallois, C., P. Laurent-Puig, e J. Taieb. 2016. «Methylator Phenotype in Colorectal Cancer: A Prognostic Factor or Not?» *Critical Reviews in Oncology/Hematology* 99:74–80. doi:10.1016/j.critrevonc.2015.11.001.

Gao, Yuyan, Qi Zhao, Xiaoqin Mu, Huifen Zhu, Binbin Liu, Bingqing Yao, Xinyi Liu, Wenhan Xue, Bo Wang, e Shulin Liu. 2019. «SREBP1 Promotes 5-FU Resistance in Colorectal Cancer Cells by Inhibiting the Expression of Caspase7». *International Journal of Clinical and Experimental Pathology* 12(3):1095–1100.

Gong, Jin, Yiyun Lin, Huaqin Zhang, Chunqi Liu, Zhong Cheng, Xiaowei Yang, Jiamei Zhang, Yuanyuan Xiao, Na Sang, Xinying Qian, Liang Wang, Xiaobo Cen, Xiao Du, e Yinglan Zhao. 2020. «Reprogramming of Lipid Metabolism in Cancer-Associated Fibroblasts Potentiates Migration of Colorectal Cancer Cells». *Cell Death & Disease* 11(4):267. doi:10.1038/s41419-020-2434-z.

Gram, Inger T., Song-Yi Park, Lynne R. Wilkens, Christopher A. Haiman, e Loïc Le Marchand. 2020. «Smoking-Related Risks of Colorectal Cancer by Anatomical Subsite and Sex». *American Journal of Epidemiology* 189(6):543–53. doi:10.1093/aje/kwaa005.

Gude, Sai Sravya, Rithik S. Veeravalli, Bhuvanasai Vejandla, Sai Sreeya Gude, Tejaswi Venigalla, e Venkateswarlu Chintagumpala. 2023. «Colorectal Cancer Diagnostic Methods: The Present and Future». *Cureus* 15(4):e37622. doi:10.7759/cureus.37622.

He, Ying, Shasha Qi, Lu Chen, Jinyu Zhu, Linda Liang, Xudong Chen, Hao Zhang, Lvjia Zhuo, Shujuan Zhao, Shuiping Liu, e Tian Xie. 2024. «The Roles and Mechanisms of SREBP1 in Cancer Development and Drug Response». *Genes & Diseases* 11(4):100987. doi:10.1016/j.gendis.2023.04.022.

Hossain, Md Sanower, Hidayah Karuniawati, Ammar Abdulrahman Jairoun, Zannat Urbi, Der Jiun Ooi, Akbar John, Ya Chee Lim, K. M. Kaderi Kibria, A. K. M. Mohiuddin, Long Chiau Ming, Khang Wen Goh, e Muhammad Abdul Hadi. 2022. «Colorectal Cancer: A Review of Carcinogenesis, Global Epidemiology, Current Challenges, Risk Factors, Preventive and Treatment Strategies». *Cancers* 14(7):1732. doi:10.3390/cancers14071732.

Huang, Fang-I., Yi-Wen Wu, Ting-Yi Sung, Jing-Ping Liou, Mei-Hsiang Lin, Shiow-Lin Pan, e Chia-Ron Yang. 2019. «MPT0G413, A Novel HDAC6-Selective Inhibitor, and Bortezomib Synergistically Exert Anti-Tumor Activity in Multiple Myeloma Cells». *Frontiers in Oncology* 9:249. doi:10.3389/fonc.2019.00249.

Ionescu, Vlad Alexandru, Gina Gheorghe, Nicolae Bacalbasa, Alexandru Laurentiu Chiotoroiu, e Camelia Diaconu. 2023. «Colorectal Cancer: From Risk Factors to Oncogenesis». *Medicina (Kaunas, Lithuania)* 59(9):1646. doi:10.3390/medicina59091646.

Janani, Balakarthikeyan, Mayakrishnan Vijayakumar, Kannappan Priya, Jin Hee Kim, D. S. Prabakaran, Mohammad Shahid, Sameer Al-Ghamdi, Mohammed Alsaidan, Nasraddin Othman Bahakim, Mohammad Hassan Abdelzaher, e Thiyagarajan Ramesh. 2022. «EGFR-Based Targeted Therapy for Colorectal Cancer—Promises and Challenges». *Vaccines* 10(4):499. doi:10.3390/vaccines10040499.

Jing, Bo, Jin Jin, Rufang Xiang, Meng Liu, Li Yang, Yin Tong, Xinhua Xiao, Hu Lei, Wei Liu, Hanzhang Xu, Jiong Deng, Li Zhou, e Yingli Wu. 2018. «Vorinostat and Quinacrine Have Synergistic Effects in T-Cell Acute Lymphoblastic Leukemia through Reactive Oxygen Species Increase and Mitophagy Inhibition». *Cell Death & Disease* 9(6):589. doi:10.1038/s41419-018-0679-6.

Karagiannis, Dimitris, e Theodoros Rampias. 2021. «HDAC Inhibitors: Dissecting Mechanisms of Action to Counter Tumor Heterogeneity». *Cancers* 13(14):3575. doi:10.3390/cancers13143575.

Kasi, Anup, Shivani Handa, Sajjad Bhatti, Shahid Umar, Ajay Bansal, e Weijing Sun. 2020. «Molecular Pathogenesis and Classification of Colorectal Carcinoma». *Current Colorectal Cancer Reports* 16(5):97–106. doi:10.1007/s11888-020-00458-z.

Kerr, E., C. Holohan, K. M. McLaughlin, J. Majkut, S. Dolan, K. Redmond, J. Riley, K. McLaughlin, I. Stasik, M. Crudden, S. Van Schaeybroeck, C. Fenning, R. O'Connor, P. Kiely, M. Sgobba, D. Haigh, P. G. Johnston, e D. B. Longley. 2012. «Identification of an Acetylation-Dependant Ku70/FLIP Complex That Regulates FLIP Expression and HDAC Inhibitor-Induced Apoptosis». *Cell Death and Differentiation* 19(8):1317–27. doi:10.1038/cdd.2012.8.

Khan, Fahad, Deena Elsori, Meenakshi Verma, Shivam Pandey, Safia Obaidur Rab, Samra Siddiqui, Nadiyah M. Alabdallah, Mohd Saeed, e Pratibha Pandey. 2024. «Unraveling the Intricate Relationship between Lipid Metabolism and Oncogenic Signaling Pathways». *Frontiers in Cell and Developmental Biology* 12:1399065. doi:10.3389/fcell.2024.1399065.

King, Jacob, Maya Patel, e Sriram Chandrasekaran. 2021. «Metabolism, HDACs, and HDAC Inhibitors: A Systems Biology Perspective». *Metabolites* 11(11):792. doi:10.3390/metabo11110792.

Knight, Walter E., Yingqiong Cao, Phoebe Dillon, e Kunhua Song. 2021. «A Simple Protocol to Produce Mature Human-Induced Pluripotent Stem Cell-Derived Cardiomyocytes». *STAR Protocols* 2(4):100912. doi:10.1016/j.xpro.2021.100912.

Knutson, Sarah K., Brenda J. Chyla, Joseph M. Amann, Srividya Bhaskara, Stacey S. Huppert, e Scott W. Hiebert. 2008. «Liver-specific deletion of histone deacetylase 3 disrupts metabolic transcriptional networks». *The EMBO Journal* 27(7):1017–28. doi:10.1038/emboj.2008.51.

Kotula, Anna E., Yash V. Korde, Hayden J. Oyler, Mark R. Wakefield, e Yujiang Fang. 2025. «Colorectal Polyps: Pathophysiology, Malignant Potential, and Advancements in Therapeutic Strategies». *Medical Oncology* 42(8):287. doi:10.1007/s12032-025-02861-8.

Koveitypour, Zahra, Farnoush Panahi, Mehrdad Vakilian, Maryam Peymani, Farzad Seyed Forootan, Mohammad Hossein Nasr Esfahani, e Kamran Ghaedi. 2019. «Signaling Pathways Involved in Colorectal Cancer Progression». *Cell & Bioscience* 9:97. doi:10.1186/s13578-019-0361-4.

Krauß, Dana, Ourania Fari, e Maria Sibilia. 2022. «Lipid Metabolism Interplay in CRC-An Update». *Metabolites* 12(3):213. doi:10.3390/metabo12030213.

Kumar, Anil, Vipasha Gautam, Arushi Sandhu, Kajal Rawat, Antika Sharma, e Lekha Saha. 2023. «Current and Emerging Therapeutic Approaches for Colorectal Cancer: A Comprehensive Review». *World Journal of Gastrointestinal Surgery* 15(4):495–519. doi:10.4240/wjgs.v15.i4.495.

Le, Dung T., Jennifer N. Durham, Kellie N. Smith, Hao Wang, Bjarne R. Bartlett, Laveet K. Aulakh, Steve Lu, Holly Kemberling, Cara Wilt, Brandon S. Luber, Fay Wong, Nilofer S. Azad, Agnieszka A. Rucki, Dan Laheru, Ross Donehower, Atif Zaheer, George A. Fisher, Todd S. Crocenzi, James J. Lee, Tim F. Greten, Austin G. Duffy, Kristen K. Ciombor, Aleksandra D. Eyring, Bao H. Lam, Andrew Joe, S. Peter Kang, Matthias Holdhoff, Ludmila Danilova, Leslie Cope, Christian Meyer, Shibin Zhou, Richard M. Goldberg, Deborah K. Armstrong, Katherine M. Bever, Amanda N. Fader, Janis Taube, Franck Housseau, David Spetzler, Nianqing Xiao, Drew M. Pardoll, Nickolas Papadopoulos, Kenneth W. Kinzler, James R. Eshleman, Bert Vogelstein, Robert A. Anders, e Luis A. Diaz. 2017. «Mismatch Repair Deficiency Predicts Response of Solid Tumors to PD-1 Blockade». *Science* 357(6349):409–13. doi:10.1126/science.aan6733.

Leon Arellano, Miguel, Mariano García-Arranz, Héctor Guadalajara, Rocío Olivera-Salazar, Teresa Valdes-Sanchez, e Damián García-Olmo. 2022. «Analysis of Septin 9 Gene Hypermethylation as Follow-Up Biomarker of Colorectal Cancer Patients after Curative Surgery». *Diagnostics* 12(4):993. doi:10.3390/diagnostics12040993.

Li, J. N., M. A. Mahmoud, W. F. Han, M. Ripple, e E. S. Pizer. 2000. «Sterol Regulatory Element-Binding Protein-1 Participates in the Regulation of Fatty Acid Synthase Expression in Colorectal Neoplasia». *Experimental Cell Research* 261(1):159–65. doi:10.1006/excr.2000.5054.

Li, Jingyuan, Jiashu Pan, Lisheng Wang, Guang Ji, e Yanqi Dang. 2025. «Colorectal Cancer: Pathogenesis and Targeted Therapy». *MedComm* 6(3):e70127. doi:10.1002/mco2.70127.

Li, Qing, Shan Geng, Hao Luo, Wei Wang, Ya-Qi Mo, Qing Luo, Lu Wang, Guan-Bin Song, Jian-Peng Sheng, e Bo Xu. 2024. «Signaling Pathways Involved in Colorectal Cancer: Pathogenesis and Targeted Therapy». *Signal Transduction and Targeted Therapy* 9(1):266. doi:10.1038/s41392-024-01953-7.

Li, Wenjie, Yiming Fu, e Wei Wang. 2024. «A Real-World Pharmacovigilance Study Investigating the Toxicities of Histone Deacetylase Inhibitors». *Annals of Hematology* 103(8):3207–17. doi:10.1007/s00277-024-05691-2.

Li, Yunxia, Qi Han, Yuxin Liu, Jie Yin, e Jie Ma. 2024. «Role of the Histone Deacetylase Family in Lipid Metabolism: Structural Specificity and Functional Diversity». *Pharmacological Research* 210:107493. doi:10.1016/j.phrs.2024.107493.

Liu, Yuan-Ling, Pei-Ming Yang, Chia-Tung Shun, Ming-Shiang Wu, Jing-Ru Weng, e Ching-Chow Chen. 2010. «Autophagy Potentiates the Anti-Cancer Effects of the Histone Deacetylase Inhibitors in Hepatocellular Carcinoma». *Autophagy* 6(8):1057–65. doi:10.4161/auto.6.8.13365.

Mao, Yunuo, Wei Wang, Jingwei Yang, Xin Zhou, Yongqu Lu, Junpeng Gao, Xiao Wang, Lu Wen, Wei Fu, e Fuchou Tang. 2024. «Drug Repurposing Screening and Mechanism Analysis Based on Human Colorectal Cancer Organoids». *Protein & Cell* 15(4):285–304. doi:10.1093/procel/pwad038.

Matsuda, Takahisa, Ai Fujimoto, e Yoshinori Igarashi. 2025. «Colorectal Cancer: Epidemiology, Risk Factors, and Public Health Strategies». *Digestion* 106(2):91–99. doi:10.1159/000543921.

Mounier, Catherine, Lamia Bouraoui, e Eric Rassart. 2014. «Lipogenesis in Cancer Progression (Review)». *International Journal of Oncology* 45(2):485–92. doi:10.3892/ijo.2014.2441.

Mousavinezhad, Maryam, Reza Majdzadeh, Ali Akbari Sari, Alireza Delavari, e Farideh Mohtasham. 2016. «The Effectiveness of FOBT vs. FIT: A Meta-Analysis on Colorectal Cancer Screening Test». *Medical Journal of the Islamic Republic of Iran* 30:366.

Mukhopadhyay, Subhadip, Isabel R. Schlaepfer, Bryan C. Bergman, Prashanta Kumar Panda, Prakash Priyadarshi Praharaj, Prajna Paramita Naik, Rajesh Agarwal, e Sujit Kumar Bhutia. 2017.

«ATG14 Facilitated Lipophagy in Cancer Cells Induce ER Stress Mediated Mitoptosis through a ROS Dependent Pathway». *Free Radical Biology & Medicine* 104:199–213. doi:10.1016/j.freeradbiomed.2017.01.007.

Mukhtar Yusif, Mohammed. 2024. «Histone Deacetylases (HDACs) as Key Targets in Metabolic Disorders». in *Metabolic Syndrome - Lifestyle and Biological Risk Factors*, a cura di K. Daniel Monyeki, H. C. G. Kemper, e P. Modjadji. IntechOpen.

Natarajan, Umamaheswari, Thiagarajan Venkatesan, Vijayaraghavan Radhakrishnan, Shila Samuel, e Appu Rathinavelu. 2018. «Differential Mechanisms of Cell Death Induced by HDAC Inhibitor SAHA and MDM2 Inhibitor RG7388 in MCF-7 Cells». *Cells* 8(1):8. doi:10.3390/cells8010008.

Nguyen, Long H., Ajay Goel, e Daniel C. Chung. 2020. «Pathways of Colorectal Carcinogenesis». *Gastroenterology* 158(2):291–302. doi:10.1053/j.gastro.2019.08.059.

Nouri Nojadeh, Jafar, Shahin Behrouz Sharif, e Ebrahim Sakhinia. 2018. «Microsatellite Instability in Colorectal Cancer». *EXCLI Journal; 17:Doc159; ISSN 1611-2156*. doi:10.17179/EXCLI2017-948.

Ntellas, Panagiotis, Leonidas Mavroeidis, Stefania Gkoura, Ioanna Gazouli, Anna-Lea Amylidi, Alexandra Papadaki, George Zarkavelis, Davide Mauri, Georgia Karpathiou, Evangelos Kolettas, Anna Batistatou, e George Pentheroudakis. 2020. «Old Player-New Tricks: Non Angiogenic Effects of the VEGF/VEGFR Pathway in Cancer». *Cancers* 12(11):3145. doi:10.3390/cancers12113145.

Oliveira-Silva, João Marcos, Leilane Sales de Oliveira, João Vitor Marangoni Tagliéri, Laís Bernardo Lopes, Carlos Vinicius Expedito de Souza, Hanna Karolina de Araújo Batistão, e Angel Mauricio Castro-Gamero. 2025. «HDAC6: Tumor Progression and Beyond». *Current Cancer Drug Targets*. doi:10.2174/0115680096332732241113053459.

Pakiet, Alicja, Jarosław Kobiela, Piotr Stepnowski, Tomasz Sledzinski, e Adriana Mika. 2019. «Changes in Lipids Composition and Metabolism in Colorectal Cancer: A Review». *Lipids in Health and Disease* 18(1):29. doi:10.1186/s12944-019-0977-8.

Park, Jinyoung, Jinhong Cho, e Eun Joo Song. 2020. «Ubiquitin-Proteasome System (UPS) as a Target for Anticancer Treatment». *Archives of Pharmacal Research* 43(11):1144–61. doi:10.1007/s12272-020-01281-8.

Perspectives on the Aetiology and Pathogenesis of Colorectal Cancer. s.d.

Pickhardt, Perry J., Loredana Correale, Silvia Delsanto, Daniele Regge, e Cesare Hassan. 2018. «CT Colonography Performance for the Detection of Polyps and Cancer in Adults ≥ 65 Years Old: Systematic Review and Meta-Analysis». *American Journal of Roentgenology* 211(1):40–51. doi:10.2214/AJR.18.19515.

Qian, Hui, Yuanying Chen, Zongqian Nian, Lu Su, Haoyong Yu, Feng-Jung Chen, Xiuqin Zhang, Wenyi Xu, Linkang Zhou, Jiaming Liu, Jinhai Yu, Luxin Yu, Yan Gao, Hongchao Zhang, Haihong Zhang, Shimin Zhao, Li Yu, Rui-Ping Xiao, Yuqian Bao, Shaocong Hou, Pingping Li, Jiada Li, Haiteng Deng, Weiping Jia, e Peng Li. 2017a. «HDAC6-Mediated Acetylation of Lipid Droplet-Binding Protein CIDEC Regulates Fat-Induced Lipid Storage». *The Journal of Clinical Investigation* 127(4):1353–69. doi:10.1172/JCI85963.

Qian, Hui, Yuanying Chen, Zongqian Nian, Lu Su, Haoyong Yu, Feng-Jung Chen, Xiuqin Zhang, Wenyi Xu, Linkang Zhou, Jiaming Liu, Jinhai Yu, Luxin Yu, Yan Gao, Hongchao Zhang, Haihong Zhang, Shimin Zhao, Li Yu, Rui-Ping Xiao, Yuqian Bao, Shaocong Hou, Pingping Li, Jiada Li, Haiteng Deng, Weiping Jia, e Peng Li. 2017b. «HDAC6-Mediated Acetylation of Lipid Droplet–

Binding Protein CIDEC Regulates Fat-Induced Lipid Storage». *Journal of Clinical Investigation* 127(4):1353–69. doi:10.1172/JCI85963.

Qing, Weixia, Xiaoyi Xing, Dengfeng Feng, Ruilian Chen, e Zhonghua Liu. 2021. «Indocyanine Green Loaded pH-Responsive Bortezomib Supramolecular Hydrogel for Synergistic Chemo-Photothermal/Photodynamic Colorectal Cancer Therapy». *Photodiagnosis and Photodynamic Therapy* 36:102521. doi:10.1016/j.pdpdt.2021.102521.

Raccomandazioni AIOM 2022. s.d.

Raedler, Lisa A. 2016. «Lonsurf (Trifluridine plus Tipiracil): A New Oral Treatment Approved for Patients with Metastatic Colorectal Cancer». *American Health & Drug Benefits* 9(Spec Feature):97–100.

Romero-Zoghbi, Sigfredo E., Evita Krumina, Fernando López-Campos, e Felipe Couñago. 2025. «Current and Future Perspectives in the Management and Treatment of Colorectal Cancer». *World Journal of Clinical Oncology* 16(2):100807. doi:10.5306/wjco.v16.i2.100807.

Roshandel, Gholamreza, Fatemeh Ghasemi-Kebria, e Reza Malekzadeh. 2024. «Colorectal Cancer: Epidemiology, Risk Factors, and Prevention». *Cancers* 16(8):1530. doi:10.3390/cancers16081530.

Salita, Timothy, Yepy H. Rustam, Dmitri Mouradov, Oliver M. Sieber, e Gavin E. Reid. 2022. «Reprogrammed Lipid Metabolism and the Lipid-Associated Hallmarks of Colorectal Cancer». *Cancers* 14(15):3714. doi:10.3390/cancers14153714.

Sano, Wataru, Daizen Hirata, Akira Teramoto, Mineo Iwatate, Santa Hattori, Mikio Fujita, e Yasushi Sano. 2020. «Serrated Polyps of the Colon and Rectum: Remove or Not?» *World Journal of Gastroenterology* 26(19):2276–85. doi:10.3748/wjg.v26.i19.2276.

Santo, Loredana, Teru Hideshima, Andrew L. Kung, Jen-Chieh Tseng, David Tamang, Min Yang, Matthew Jarpe, John H. van Duzer, Ralph Mazitschek, Walter C. Ogier, Diana Cirstea, Scott Rodig, Homare Eda, Tyler Scullen, Miriam Canavese, James Bradner, Kenneth C. Anderson, Simon S. Jones, e Noopur Raje. 2012. «Preclinical Activity, Pharmacodynamic, and Pharmacokinetic Properties of a Selective HDAC6 Inhibitor, ACY-1215, in Combination with Bortezomib in Multiple Myeloma». *Blood* 119(11):2579–89. doi:10.1182/blood-2011-10-387365.

Shaham, Salique H., Puneet Vij, e Manish K. Tripathi. 2025. «Advances in Targeted and Chemotherapeutic Strategies for Colorectal Cancer: Current Insights and Future Directions». *Biomedicines* 13(3):642. doi:10.3390/biomedicines13030642.

Shaw, Eileen, Megan S. Farris, Chelsea R. Stone, Jeroen W. G. Derksen, Rhys Johnson, Robert J. Hilsden, Christine M. Friedenreich, e Darren R. Brenner. 2018. «Effects of Physical Activity on Colorectal Cancer Risk among Family History and Body Mass Index Subgroups: A Systematic Review and Meta-Analysis». *BMC Cancer* 18(1):71. doi:10.1186/s12885-017-3970-5.

Shek, Dmitrii, Liia Akhuba, Matteo S. Carlino, Adnan Nagrial, Tania Moujaber, Scott A. Read, Bo Gao, e Golo Ahlenstiel. 2021. «Immune-Checkpoint Inhibitors for Metastatic Colorectal Cancer: A Systematic Review of Clinical Outcomes». *Cancers* 13(17):4345. doi:10.3390/cancers13174345.

Shen, Wenlong, Ting Xu, Dong Chen, e Xiaojie Tan. 2019. «Targeting SREBP1 Chemosensitizes Colorectal Cancer Cells to Gemcitabine by Caspase-7 Upregulation». *Bioengineered* 10(1):459–68. doi:10.1080/21655979.2019.1676485.

Shi, Mu-Qi, Ying Xu, Xin Fu, De-Si Pan, Xian-Ping Lu, Yi Xiao, e Yi-Zhou Jiang. 2024. «Advances in Targeting Histone Deacetylase for Treatment of Solid Tumors». *Journal of Hematology & Oncology* 17(1):37. doi:10.1186/s13045-024-01551-8.

Siegel, Rebecca L., Nikita Sandeep Wagle, Andrea Cercek, Robert A. Smith, e Ahmedin Jemal. 2023. «Colorectal Cancer Statistics, 2023». *CA: A Cancer Journal for Clinicians* 73(3):233–54. doi:10.3322/caac.21772.

Sogbein, Olusola, Pradipta Paul, Meenakshi Umar, Ali Chaari, Vecihi Batuman, e Rohit Upadhyay. 2024. «Bortezomib in Cancer Therapy: Mechanisms, Side Effects, and Future Proteasome Inhibitors». *Life Sciences* 358:123125. doi:10.1016/j.lfs.2024.123125.

Soltani, Ghodratollah, Arash Poursheikhani, Maryam Yassi, Abdorasool Hayatbakhsh, Matin Kerachian, e Mohammad Amin Kerachian. 2019. «Obesity, Diabetes and the Risk of Colorectal Adenoma and Cancer». *BMC Endocrine Disorders* 19(1):113. doi:10.1186/s12902-019-0444-6.

Söreide, K., E. A. M. Janssen, H. Söiland, H. Körner, e J. P. A. Baak. 2006. «Microsatellite Instability in Colorectal Cancer». *British Journal of Surgery* 93(4):395–406. doi:10.1002/bjs.5328.

Spada, Cristiano, Cesare Hassan, Davide Bellini, David Burling, Giovanni Cappello, Cristina Carretero, Evelien Dekker, Rami Eliakim, Margriet De Haan, Michal F. Kaminski, Anastasios Koulaouzidis, Andrea Laghi, Philippe Lefere, Thomas Mang, Sebastian Manuel Milluzzo, Martina Morrin, Deirdre McNamara, Emanuele Neri, Silvia Pecere, Mathieu Pioche, Andrew Plumb, Emanuele Rondonotti, Manon Cw Spaander, Stuart Taylor, Ignacio Fernandez-Urien, Jeanin E. Van Hooft, Jaap Stoker, e Daniele Regge. 2021. «Imaging Alternatives to Colonoscopy: CT Colonography and Colon Capsule. European Society of Gastrointestinal Endoscopy (ESGE) and European Society of Gastrointestinal and Abdominal Radiology (ESGAR) Guideline – Update 2020». *European Radiology* 31(5):2967–82. doi:10.1007/s00330-020-07413-4.

Subramanian, Srividya, Susan E. Bates, John J. Wright, Igor Espinoza-Delgado, e Richard L. Piekarz. 2010. «Clinical Toxicities of Histone Deacetylase Inhibitors». *Pharmaceuticals (Basel, Switzerland)* 3(9):2751–67. doi:10.3390/ph3092751.

Tahghighi, Azar, Effat Seyedhashemi, Javad Mohammadi, Arash Moradi, Aria Esmaeili, Majid Pornour, Kimia Jafarifar, e Shahla Mohammad Ganji. 2025. «Epigenetic Marvels: Exploring the Landscape of Colorectal Cancer Treatment through Cutting-Edge Epigenetic-Based Drug Strategies». *Clinical Epigenetics* 17(1):34. doi:10.1186/s13148-025-01844-w.

Testa, Ugo, Elvira Pelosi, e Germana Castelli. 2018. «Colorectal Cancer: Genetic Abnormalities, Tumor Progression, Tumor Heterogeneity, Clonal Evolution and Tumor-Initiating Cells». *Medical Sciences (Basel, Switzerland)* 6(2):31. doi:10.3390/medsci6020031.

Tew, William P., Michael Gordon, John Murren, Jakob Dupont, Sandra Pezzulli, Carol Aghajanian, Paul Sabbatini, David Mendelson, Lawrence Schwartz, Scott Gettinger, Amanda Psyrri, Jesse M. Cedarbaum, e David R. Spriggs. 2010. «Phase 1 Study of Aflibercept Administered Subcutaneously to Patients with Advanced Solid Tumors». *Clinical Cancer Research* 16(1):358–66. doi:10.1158/1078-0432.CCR-09-2103.

Tiong, Tung-Yu, Pei-Wei Weng, Chun-Hua Wang, Syahru Agung Setiawan, Vijesh Kumar Yadav, Narpati Wesa Pikatan, Iat-Hang Fong, Chi-Tai Yeh, Chia-Hung Hsu, e Kuang-Tai Kuo. 2022. «Targeting the SREBP-1/Hsa-Mir-497/SCAP/FASN Oncometabolic Axis Inhibits the Cancer Stem-like and Chemoresistant Phenotype of Non-Small Cell Lung Carcinoma Cells». *International Journal of Molecular Sciences* 23(13):7283. doi:10.3390/ijms23137283.

Tirinato, Luca, Carlo Liberale, Simone Di Franco, Patrizio Candeloro, Antonina Benfante, Rosanna La Rocca, Lisette Potze, Roberto Marotta, Roberta Ruffilli, Vijayakumar P. Rajamanickam, Mario Malerba, Francesco De Angelis, Andrea Falqui, Ennio Carbone, Matilde Todaro, Jan Paul Medema, Giorgio Stassi, e Enzo Di Fabrizio. 2015. «Lipid Droplets: A New Player in Colorectal Cancer Stem Cells Unveiled by Spectroscopic Imaging». *Stem Cells (Dayton, Ohio)* 33(1):35–44. doi:10.1002/stem.1837.

Tsai, Tsung-Huang, Elaine Chen, Lan Li, Pradip Saha, Hsiao-Ju Lee, Li-Shin Huang, Gregory S. Shelness, Lawrence Chan, e Benny Hung-Junn Chang. 2017. «The Constitutive Lipid Droplet Protein PLIN2 Regulates Autophagy in Liver». *Autophagy* 13(7):1130–44. doi:10.1080/15548627.2017.1319544.

Vallis, Jillian, e Peizhong Peter Wang. 2022. «The Role of Diet and Lifestyle in Colorectal Cancer Incidence and Survival». in *Gastrointestinal Cancers*, a cura di J. A. Morgado-Diaz. Brisbane (AU): Exon Publications.

Verdaguer, Helena, Josep Tabernero, e Teresa Macarulla. 2016. «Ramucirumab in Metastatic Colorectal Cancer: Evidence to Date and Place in Therapy». *Therapeutic Advances in Medical Oncology* 8(3):230–42. doi:10.1177/1758834016635888.

Vuik, Fanny E. R., Stella A. V. Nieuwenburg, Sarah Moen, Cristiano Spada, Carlo Senore, Cesare Hassan, Marco Pennazio, Emanuele Rondonotti, Silvia Pecere, Ernst J. Kuipers, e Manon C. W. Spaander. 2021. «Colon Capsule Endoscopy in Colorectal Cancer Screening: A Systematic Review». *Endoscopy* 53(08):815–24. doi:10.1055/a-1308-1297.

Walther, Tobias C., Jeeyun Chung, e Robert V. Farese. 2017. «Lipid Droplet Biogenesis». *Annual Review of Cell and Developmental Biology* 33:491–510. doi:10.1146/annurev-cellbio-100616-060608.

Wang, Jin-Dong, Guo-Shuai Xu, Xin-Long Hu, Wen-Qiang Li, Nan Yao, Fu-Zhou Han, Yin Zhang, e Jun Qu. 2024. «The histologic features, molecular features, detection and management of serrated polyps: a review». *Frontiers in Oncology* 14:1356250. doi:10.3389/fonc.2024.1356250.

Wang, Jingzhi, Rui Ling, Yuepeng Zhou, Xingyu Gao, Yun Yang, Chaoming Mao, e Deyu Chen. 2020. «SREBP1 Silencing Inhibits the Proliferation and Motility of Human Esophageal Squamous Carcinoma Cells via the Wnt/β-Catenin Signaling Pathway». *Oncology Letters* 20(3):2855–69. doi:10.3892/ol.2020.11853.

Wang, Leisheng, Shiwei Xu, Mengzhen Zhou, Hao Hu, e Jinyou Li. 2024. «The Role of DGAT1 and DGAT2 in Tumor Progression via Fatty Acid Metabolism: A Comprehensive Review». *International Journal of Biological Macromolecules* 278:134835. doi:10.1016/j.ijbiomac.2024.134835.

Weledji EP 2024. s.d.

White, Alan, Lucy Ironmonger, Robert J. C. Steele, Nick Ormiston-Smith, Carina Crawford, e Amanda Seims. 2018. «A Review of Sex-Related Differences in Colorectal Cancer Incidence, Screening Uptake, Routes to Diagnosis, Cancer Stage and Survival in the UK». *BMC Cancer* 18(1):906. doi:10.1186/s12885-018-4786-7.

Wilhelm, Scott M., Jacques Dumas, Lila Adnane, Mark Lynch, Christopher A. Carter, Gunnar Schütz, Karl-Heinz Thierauch, e Dieter Zopf. 2011. «Regorafenib (BAY 73-4506): A New Oral Multikinase Inhibitor of Angiogenic, Stromal and Oncogenic Receptor Tyrosine Kinases with Potent Preclinical Antitumor Activity». *International Journal of Cancer* 129(1):245–55. doi:10.1002/ijc.25864.

Winkels, Renate M., Akke Botma, Fränzel J. B. Van Duijnhoven, Fokko M. Nagengast, Jan H. Kleibeuker, Hans F. A. Vasen, e Ellen Kampman. 2012. «Smoking Increases the Risk for Colorectal Adenomas in Patients With Lynch Syndrome». *Gastroenterology* 142(2):241–47. doi:10.1053/j.gastro.2011.10.033.

Xu, Guibin, Yaodong Jiang, Yuansong Xiao, Xian D. Liu, Fei Yue, Wenjiao Li, Xun Li, Yongzhong He, Xianhan Jiang, Hai Huang, Qi Chen, Eric Jonasch, e Leyuan Liu. 2016. «Fast Clearance of Lipid

Droplets through MAP1S-Activated Autophagy Suppresses Clear Cell Renal Cell Carcinomas and Promotes Patient Survival». *Oncotarget* 7(5):6255–65. doi:10.18632/oncotarget.6669.

Yamada, Takeshi, Akihisa Matsuda, Michihiro Koizumi, Seiichi Shinji, Goro Takahashi, Takuma Iwai, Kohki Takeda, Kohji Ueda, Yasuyuki Yokoyama, Keisuke Hara, Masahiro Hotta, Satoshi Matsumoto, e Hiroshi Yoshida. 2019. «Liquid Biopsy for the Management of Patients with Colorectal Cancer». *Digestion* 99(1):39–45. doi:10.1159/000494411.

Yan, Yan, Hao Wang, Chuanxian Wei, Yuanhang Xiang, Xuehong Liang, Chung-Weng Phang, e Renjie Jiao. 2019. «HDAC6 Regulates Lipid Droplet Turnover in Response to Nutrient Deprivation via P62-Mediated Selective Autophagy». *Journal of Genetics and Genomics* 46(4):221–29. doi:10.1016/j.jgg.2019.03.008.

Yang, Fan, Ying Li, Xue Shang, Yun Zhu, Wenting Hou, Yi Liu, Qing Hua, e Zhirong Sun. 2025. «PLIN2 Promotes Colorectal Cancer Progression through CD36-Mediated Epithelial-Mesenchymal Transition». *Cell Death & Disease* 16(1):510. doi:10.1038/s41419-025-07836-1.

Yang, Feifei, Na Zhao, Di Ge, e Yihua Chen. 2019. «Next-Generation of Selective Histone Deacetylase Inhibitors». *RSC Advances* 9(34):19571–83. doi:10.1039/c9ra02985k.

Yang, Jing, Xin Jin, Yuqian Yan, Yingjie Shao, Yunqian Pan, Lewis R. Roberts, Jun Zhang, Haojie Huang, e Jingting Jiang. 2017. «Inhibiting Histone Deacetylases Suppresses Glucose Metabolism and Hepatocellular Carcinoma Growth by Restoring FBP1 Expression». *Scientific Reports* 7(1):43864. doi:10.1038/srep43864.

Yano, Mitsutake, Mariko Miyazawa, Naoki Ogane, Aiko Ogasawara, Kosei Hasegawa, Hisashi Narahara, e Masanori Yasuda. 2021. «Up-Regulation of HDAC6 Results in Poor Prognosis and Chemoresistance in Patients With Advanced Ovarian High-Grade Serous Carcinoma». *Anticancer Research* 41(3):1647–54. doi:10.21873/anticanres.14927.

Zhang, Jianbin, Shukie Ng, Jigang Wang, Jing Zhou, Shi-Hao Tan, Naidi Yang, Qingsong Lin, Dajing Xia, e Han-Ming Shen. 2015. «Histone Deacetylase Inhibitors Induce Autophagy through FOXO1-Dependent Pathways». *Autophagy* 11(4):629–42. doi:10.1080/15548627.2015.1023981.

Zhang, Qian-Qian, Wei-Jie Zhang, e Sheng Chang. 2023. «HDAC6 Inhibition: A Significant Potential Regulator and Therapeutic Option to Translate into Clinical Practice in Renal Transplantation». *Frontiers in Immunology* 14:1168848. doi:10.3389/fimmu.2023.1168848.

Zhang, Shi-Lan, Hong-Yi Zhu, Bing-Yi Zhou, Yi Chu, Ji-Rong Huo, Yu-Yong Tan, e De-Liang Liu. 2019a. «Histone Deacetylase 6 Is Overexpressed and Promotes Tumor Growth of Colon Cancer through Regulation of the MAPK/ERK Signal Pathway». *OncoTargets and Therapy* Volume 12:2409–19. doi:10.2147/OTT.S194986.

Zhang, Shi-Lan, Hong-Yi Zhu, Bing-Yi Zhou, Yi Chu, Ji-Rong Huo, Yu-Yong Tan, e De-Liang Liu. 2019b. «Histone Deacetylase 6 Is Overexpressed and Promotes Tumor Growth of Colon Cancer through Regulation of the MAPK/ERK Signal Pathway». *OncoTargets and Therapy* Volume 12:2409–19. doi:10.2147/OTT.S194986.

Zhang, Zhiyong, Xin Zhang, e Aimin Huang. 2021. «Aggresome–Autophagy Associated Gene HDAC6 Is a Potential Biomarker in Pan-Cancer, Especially in Colon Adenocarcinoma». *Frontiers in Oncology* 11:718589. doi:10.3389/fonc.2021.718589.

Zhang, Zhongyang, Zhenghang Yu, Dianyuan Liang, Ke Song, Xiangxin Kong, Ming He, Xinxin Liao, Ziyan Huang, Aijia Kang, Rubing Bai, e Yixing Ren. 2024. «Roles of Lipid Droplets and Related Proteins in Metabolic Diseases». *Lipids in Health and Disease* 23(1):218. doi:10.1186/s12944-024-02212-y.

Zhao, Qiushi, Xingyu Lin, e Guan Wang. 2022. «Targeting SREBP-1-Mediated Lipogenesis as Potential Strategies for Cancer». *Frontiers in Oncology* 12:952371. doi:10.3389/fonc.2022.952371.

Zheng, Yi-Chao, Hui-Qin Kang, Bo Wang, Yuan-Zai Zhu, M. a. A. Mamun, Long-Fei Zhao, Hai-Qian Nie, Ying Liu, Li-Juan Zhao, Xiao-Nan Zhang, Mei-Mei Gao, Dan-Dan Jiang, Hong-Min Liu, e Ya Gao. 2023. «Curriculum Vitae of HDAC6 in Solid Tumors». *International Journal of Biological Macromolecules* 230:123219. doi:10.1016/j.ijbiomac.2023.123219.

Zheng, Ying, Lingnan Meng, Hao Liu, Lijuan Sun, Yongzhan Nie, Qiong Wu, Daiming Fan, e Mengbin Li. 2022. «Let Food Be Thy Medicine: The Role of Diet in Colorectal Cancer: A Narrative Review». *Journal of Gastrointestinal Oncology* 13(4):2020–32. doi:10.21037/jgo-22-32.